

Rating Optimization of Three Phase Series Hybrid Power Filter for Power Quality Compensation and Renewable Energy Integration

by

Muftah ABUZIED

THESIS PRESENTED TO ÉCOLE DE TECHNOLOGIE SUPÉRIEURE
IN PARTIAL FULFILLMENT FOR A MASTER'S DEGREE WITH THESIS
IN ELECTRICAL ENGINEERING
M.A.Sc

MONTREAL, June 07, 2018

ÉCOLE DE TECHNOLOGIE SUPÉRIEURE
UNIVERSITÉ DU QUÉBEC



Muftah Abuzied, 2018



This Creative Commons licence allows readers to download this work and share it with others as long as the author is credited. The content of this work can't be modified in any way or used commercially.

BOARD OF EXAMINERS
THIS THESIS HAS BEEN EVALUATED
BY THE FOLLOWING BOARD OF EXAMINERS

Mr. Kamal Al-Haddad, Thesis Supervisor
Department of Electrical Engineering, École de technologie supérieure

Mr. Abdelhamid Hamadi, Thesis Co-supervisor
Department of Electrical Engineering, École de technologie supérieure

Mme Lyne Woodward, President of the Board of Examiners
Department of Electrical Engineering, École de technologie supérieure

Mr. Pierre Jean Lagacé, Member of the jury
Department of Electrical Engineering, École de technologie supérieure

THIS THESIS WAS PRESENTED AND DEFENDED
IN THE PRESENCE OF A BOARD OF EXAMINERS AND PUBLIC
MONTREAL, MAY 14, 2018
AT ÉCOLE DE TECHNOLOGIE SUPÉRIEURE

ACKNOWLEDGMENT

I would like to express my sincere gratitude to my thesis supervisor, Professor Kamal Al-Haddad, for the opportunity he has given me to carry out my work in this field. Without his thrust, excellent technical guidance, patience, and moral support, my research would not have been successful.

I would also like to express my profound thanks to my thesis Co-supervisor, Mr. Abdelhamid Hamadi, for his continuous advice, technical supervision and all his support. Undoubtedly, he was the most influential persons during my master studies and I hope the tie that we established during the time that this research project has being carried out will continue for many years to come.

I would like to acknowledge the Higher Institute for Comprehensive Professions-Tarhounah and Libyan Ministry of Education for providing me the opportunity to pursue my Master study and recommending me for scholarships offered.

Special thanks go to my parents, and friends that my success in carrying out and completion of this project would certainly not have been possible without their generous support, the best thanks go to all my friends at ETS.

Thanks to my lovely sons who give me the will and power to go beyond difficulties and without them this work would not have been completed easily, I dedicate this thesis to my sweet sons Mohamed and Ilyas.

Finally, I wish to give my wholehearted thanks to my beloved wife for her support, encouragements, and patience while lifting much of the burden of life during the final stages of this thesis.

ÉVALUATION DE L'OPTIMISATION DU FILTRE À ÉNERGIE HYBRIDE SÉRIE TRIPHASÉE POUR LA COMPENSATION DE LA QUALITÉ DE L'ÉNERGIE ET L'INTÉGRATION DE L'ÉNERGIE RENOUVELABLE

Muftah ABUZIED

RÉSUMÉ

Les filtres séries hybrides et les filtres passifs shunt améliorent considérablement la qualité de l'énergie et assurent une alimentation en tension fiable en atténuant ou en éliminant les problèmes tels que les distorsions de tension, les creux, les surtensions et les déséquilibres. Ils peuvent également compenser les problèmes de courant liés aux charges linéaires et non linéaires, telles que, les courants harmoniques et la puissance réactive. Dans cette étude de thèse, un filtre de puissance série hybride triphasé fut conçu pour la compensation de la qualité de l'énergie.

Une recherche majeure dans cette thèse concerne une approche permettant de compenser simultanément la puissance réactive en supprimant un convertisseur TCR proposé dans l'article publié qui a un impact sur la réduction du coût du filtre série hybride triphasé. Une comparaison de deux approches de la conception du filtre passif pour évaluer l'impact sur le dimensionnement du filtre est étudiée et des résultats ont été validés par simulation.

Le filtre série hybride (HSeAF) est très utilisé en tant que compensateur de puissance basé sur l'électronique de puissance car il s'est avéré très efficace. Sans la partie active du HSeAF, le filtre passif shunt est incapable de résoudre seul les problèmes de tension en tant que restaurateur de tension dynamique. Un système à trois phases HSeAF conventionnel comprend trois transformateurs d'isolement en série connectés à un convertisseur triphasé partageant un bus de liaison CC commun. Il est contrôlé comme une source de tension variable similaire à un filtre de puissance actif shunt, ce dernier étant réglé pour les fréquences harmoniques et installé pour créer un chemin alternatif pour les harmoniques de courant de charge. La littérature existante se concentre sur l'utilisation de filtres de puissance actifs hybrides pour compenser uniquement les problèmes de courant de charge, en raison de la complexité et du coût des dispositifs. La présente recherche cherche plutôt à optimiser les ressources disponibles afin d'améliorer l'efficacité du produit et de réduire les coûts globaux.

Une approche permet également une utilisation plus intelligente du filtre passif shunt en vue de réduire le dimensionnement du filtre actif série et une réduction globale des coûts. Les simulations MATLAB montrent que le SHPF triphasé est capable de résoudre simultanément les problèmes de tension et de charger les problèmes de courant.

Mots-clés: Filtre actif de puissance, Compensation d'harmoniques de courant, Filtre série Hybride, Qualité d'énergie, Energie renouvelable.

RATING OPTIMIZATION OF THREE PHASE SERIES HYBRID POWER FILTER FOR POWER QUALITY COMPENSATION AND RENEWABLE ENERGY INTEGRATION

Muftah ABUZIED

ABSTRACT

Hybrid series active filters and shunt passive filter can significantly improve power quality and ensure a reliable voltage supply to the load through mitigating or eliminating issues such as voltage distortions, sags, swells, and unbalances. They can also compensate current problems related to linear and non-linear loads, such as load reactive power, current harmonics

In this thesis study, a 3-phase hybrid series power filter for power quality compensation is used for current harmonic, reactive power compensation, unbalance/sag/swell grid voltage compensation. A major research in this thesis concerns an approach to compensate simultaneously a reactive power by removing a TCR converter proposed in the paper published which has an impact on the reduction of the cost of the three phases series hybrid filter. Other research concerns the comparison of two approaches of the design of the passive filter to evaluate the impact on the series active filter rating.

The hybrid series active filter (HSeAF) has gained in popularity as a highly efficient power electronics-based active power compensator. Without the active portion of the HSeAF, a shunt passive filter is unable to resolve voltage problems on its own as a dynamic voltage restorer. A conventional HSeAF 3-phase system comprises three series isolation transformers connected to a 3-phase converter sharing a common DC link bus. It is controlled as a variable voltage source similar to a shunt active power filter, the latter which is tuned for harmonic frequencies and installed to create an alternative path for load current harmonics. The existing literature focuses on using hybrid active power filters to compensate for load current issues only, due to the complexity and expense of the devices. The present research looks instead at optimizing available resources in order to enhance product efficiency and reduce overall costs.

Also an approach provides smarter use of the shunt passive filter; along with a reduced series active filter rating and an overall reduction in cost. MATLAB simulations show that the 3-phase SHPF is able to simultaneously resolve voltage problems and load current issues.

Keywords: Active power filter, Current harmonic compensation, Series Hybrid filter, Power quality compensation and Renewable energy

TABLE OF CONTENTS

	Page
INTRODUCTION	1
CHAPTER 1 LITERATURE REVIEW	5
1.1 Introduction.....	5
1.2 Types of Loads.....	6
1.2.1 Balanced Loads.....	6
1.2.2 Unbalanced Loads.....	6
1.2.3 Linear Loads	6
1.2.4 Non-linear Loads	7
1.3 Power Quality Solution.....	7
1.3.1 Passive Filter (PF).....	8
1.3.2 Active Filter (AF)	9
1.4 Series Active Filter (SeAF).....	9
1.4.1.1 Hybrid Filter (Series Active and Passive Filter).....	13
1.4.1.2 Unified Power Quality Conditioner.....	14
1.5 Modeling of Series Hybrid Power Filter (SHPF)	15
1.5.1 Configuration of Series Hybrid Power Filters (SHPFs)	16
1.5.2 Novel HSAF for Power Quality Compensation.....	17
1.5.3 New HSAF Configuration to Offset Reactive Power, Current/Voltage Harmonics, and Voltage Swell/Sag	19
1.5.4 SHAPF for Mitigating Voltage Unbalance and Harmonics under Unbalanced Non-Sinusoidal Supply Conditions	21
1.5.5 Improving Power Quality Through a Photovoltaic-based 3-Phase 4-Wire SHAPF	23
1.5.6 Enhancing Power Quality Through the Use of Hybrid Series Active Power Compensator	26
1.5.7 Enhanced Strategy to Offset Unbalanced Loads in HSAFs.....	28
1.6 Research Objectives.....	30
1.7 Conclusion	30
CHAPTER 2 SLIDING MODE CONTROL WITH SERIES HYBRID POWER FILTER AND REDUCING SIZE WITH DIFFERENT PASSIVE FILTER DESIGN.....	33
2.1 Introduction.....	33
2.2 System Configurations.....	34
2.2.1 Modeling of 3-Phase HSPF with Bridge Diode.....	34
2.2.2 Control Strategy of 3-Phase SHAF.....	35
2.2.3 Passive filter design	40
2.3 First method of passive filter design.....	42
2.4 Simulation Results	43

2.4.1.1	Second method to design passive filter by minimum cost of resonant filter	62
2.4.2	Simulation Results	66
2.5	Conclusion	73
CHAPTER 3 THREE-PHASE HYBRID SERIES ACTIVE FILTER WITHOUT BRIDGE DIODE		
		75
3.1	Introduction.....	75
3.2	System Configurations.....	76
3.2.1	Modeling of 3-Phase HSAF without Bridge Diode.....	76
3.2.2	Control Strategy of 3-Phase HSAF.....	77
3.2.2.1	Control of HSAF Active Part.....	77
3.2.2.2	Series APF Reference Voltage Signal Generation.....	80
3.2.3	Simulation Results	81
3.2.3.1	Current harmonic compensation	81
3.2.3.2	Load variation	85
3.2.3.3	Unbalanced voltage.....	86
3.2.3.4	Sag and swell voltage.....	87
3.3	Conclusion	88
CHAPTER 4 THREE-PHASE HYBRID SERIES ACTIVE FILTER INTEGRATING RENEWABLE ENERGY CONNECTED TO THE GRID.....		
		91
4.1	Introduction.....	91
4.2	Solar Photovoltaic (PV) System	92
4.2.1	Boost converter modeling.....	93
4.2.2	PV solar design	95
4.2.3	Solar panels arrangement.....	96
4.2.4	Energy storage system design.....	96
4.2.5	Maximum Power Point Tracking (MPPT) Algorithm	98
4.3	System Configurations.....	100
4.3.1	Modeling of 3-Phase HSAF with PV solar.....	100
4.3.2	Control Strategy of 3-Phase HSAF.....	101
4.3.3	Simulation results.....	102
4.3.3.1	Current harmonic compensation	102
4.3.3.2	Grid ON/OFF	106
4.4	Conclusion	107
CONCLUSION.....		109
RECOMMENDATIONS		111
LIST OF BIBLIOGRAPHICAL REFERENCES.....		113

LIST OF TABLES

		Page
Table 2.1	System Configuration parameters.....	41
Table 2.2	System parameters with minimum cost of design passive filter.....	43
Table 2.3	Power parameters and THD's during steady state.....	48
Table 2.4	Power parameters and THDs during load variation.....	54
Table 2.5	Power parameters used during sag and swell voltage compensation	56
Table 2.6	Power parameters and THDs during unbalanced voltage.....	60
Table 2.7	Parameters of the passive filter in the second method.....	66
Table 2.8	Power parameters and THDs during current harmonic compensation	70
Table 3.1	Power parameters and THD's during steady state.....	85
Table 4.1	Solar panel characteristics.....	97
Table 4.2	Power parameters and THD's during steady state.....	106

LIST OF FIGURES

		Page
Figure 1.1	Passive filter	9
Figure 1.2	Functionality schematics of series compensation	11
Figure 1.3	Hybrid filter	14
Figure 1.4	A typical unified Power quality conditioner resolving power quality issues.	15
Figure 1.5	Hybrid series power filter configuration.....	16
Figure 1.6	Hybrid series active filter with non-linear loads.....	17
Figure 1.7	Control scheme of active power filter.....	19
Figure 1.8	Proposed series hybrid power filter configuration.....	20
Figure 1.9	Circuit configuration of the SHAPF	22
Figure 1.10	TCR control scheme for SHAPF	22
Figure 1.11	PV-based SeAF with ShAF topology	24
Figure 1.12	Proposed controller of PV-based SeAF	25
Figure 1.13	THSeAF connected to the single-phase system.....	27
Figure 1.14	Control scheme of Hybrid Series Active Power Compensator.....	28
Figure 1.15	Diagram for simulation.....	29
Figure 1.16	Proposed control for series active filter	30
Figure 2.1	Series hybrid active filter with nonlinear load and linear load	35
Figure 2.2	Control scheme for the active filter	40
Figure 2.3	a) Equivalent Passive filter, b) Impedance representation versus frequency.....	41
Figure 2.4	Simulation results during steady state.....	45

Figure 2.5	THDs during steady state.....	46
Figure 2.6	Three-phase powers flow with steady state	47
Figure 2.7	Leading voltage.....	49
Figure 2.8	Lagging voltage	50
Figure 2.9	Phasor diagram (a) leading voltage (b) lagging voltage	51
Figure 2.10	Simulation results during load variation.....	52
Figure 2.11	Results of the THD during Load Variation.....	53
Figure 2.12	System behavior during sag and swell voltage compensation.....	55
Figure 2.13	Power flow with sag and swell voltage.....	56
Figure 2.14	System behavior during unbalanced compensation.....	58
Figure 2.15	Power flow with unbalanced voltage.....	59
Figure 2.16	Power flow with passive filter variation	61
Figure 2.17	Single-phase diagram of a simplified network with filters.....	64
Figure 2.18	Results of the current harmonics compensation during the steady state....	68
Figure 2.19	THD during current harmonics compensation.....	69
Figure 2.20	Leading voltage.....	71
Figure 2.21	Lagging voltage	72
Figure 2.22	Phasor diagram (a) lagging voltage (b) leading voltage	72
Figure 3.1	Hybrid series active filter with non-linear loads.....	77
Figure 3.2	Control scheme of the active power filter.....	80
Figure 3.3	Steady state simulation results of the active power filter control scheme.....	82
Figure 3.4	Power flow with the steady state	83
Figure 3.5	THD during current harmonics compensation.....	84
Figure 3.6	Simulation results of the system during the load variation.....	86

Figure 3.7	Results of the system during a source voltage unbalance.....	87
Figure 3.8	Results of the system during sag/swell source voltage.....	88
Figure 4.1	Scheme of the PV solar panels based energy supply system.....	92
Figure 4.2	Post regulator boost converter	93
Figure 4.3	(a) Current control loop of the boost converter, (b) Control scheme of the boost converter.....	94
Figure 4.4	Characteristics of the PV solar.....	99
Figure 4.5	Perturb and observe MPPT algorithm.....	99
Figure 4.6	Hybrid series active filter with PV solar.....	101
Figure 4.7	Control scheme of the active power filter.....	102
Figure 4.8	Simulation results of the system in steady state.....	103
Figure 4.9	Power flow with the steady state	104
Figure 4.10	THD during current harmonics compensation.....	105
Figure 4.11	Shows the simulation results during grid ON/OFF.....	107

LIST OF ABBREVIATIONS

3P4W	Three-phase four-wire system
3P3W	Three-phase three-wire system
AC	Alternating current
AFs	Active Filters
APFs	Active power filters
DC	Direct current
DVR	Dynamic voltage restorer
ESs	Energy Sources
FACTS	Flexible AC transmission systems
FLC	Fuzzy logical controller
HPF	High Pass Filter
HSAF	Hybrid Series Active Filter
HSAPF	Hybrid Series Active Power Filter
HSPF	Hybrid Series Power Filter
LPF	Low Pass Filter
MPPT	Maximum Power Point Tracking
PCC	Point of common coupling
PF	Passive Filter
PLL	Phase Locked Loop
PMSG	Permanent Magnetic Synchronous Generator
PQ	Power Quality

XX

PV	Solar Photovoltaics Panel
SAPF	Series Active Power Filter
SCIG	Squirrel Cage Induction Generator
SeAF	Series Active Filter
SeAPF	Series Active Power Filter
SFR	Synchronous Reference Frame
SG	Synchronous Generator
SHAPF	Series Hybrid Active Power Filter
SHPF	Series Hybrid Power Filter
SPF	Series Power Filter
TCR	Thyristor Control Reactor
UPS	Uninterruptible Power Supply
UPQC	Unified Power Quality Conditioner
VSI	Voltage Source Inverter

LIST OF SYMBOLS

ω	Angular frequency
δ	Power angle between source and load voltages
φ	Phase angle between source current w.r.t. to source voltage
C_{dc}	DC link capacitor
C_f	Ripple filter capacitor
D	Distortion power
f	System frequency
F_h	Respective harmonic's order shunt passive filter
G	Gain proportional to current harmonics
h	Harmonic order
Hz	Hertz
HP	Horse power
i_s	Source current
i_L	Load current
I_{sh}	Source harmonic current
K_p	Proportional gain
K_i	Integral gain
L	Inductance
Ω	Ohm
P	Active power
Q	Reactive power

XXII

r or R	Resistance
s	Second
S	Apparent power
T_s	Discrete sampling time
V	Voltage
W	Watt
Z	Impedance

Multiple and sub-multiple of SI unities

M:	$10^6 = 1\,000\,000$	mega
k:	$10^3 = 1\,000$	kilo
m:	$10^{-3} = 0.001$	mili
μ :	$10^{-6} = 0.000\,001$	micro

Mathematical symbols

Bold (V or v)	Matrix
Asterisk (V*)	Reference signal
Hat (\hat{v})	Measured value
V	rms value
v	Instantaneous value

INTRODUCTION

Just prior to the start of the twentieth century, electrical power underwent a series of dramatic changes. In 1882, customers received the first transmission of electric power with direct current (DC). However, maintaining a steady voltage over long-distance transmissions proved challenging to the emerging industry, so engineers devised the alternating current (AC) along with 3-phase power systems. Then, to better improve power quality, a hybrid series filter was introduced because of its low rating and ease of control.

The twentieth century saw an expansion of the electrical industry, in large part due to massive government investment. At the same time, there was a substantial rise in the generation of power from renewable sources. The turn towards sustainable energy was prompted by a widespread desire by consumers and governments to scale back exploitation of natural resources as well as to decrease harmful emissions. These renewable energies were dubbed 'green' and refer to natural processes that can be harnessed for energy but with few to no adverse environmental impacts (Javadi, 2016).

However, the industry experienced a broad range of challenges in attempting to harvest electrical power from alternative resources. For instance, most of the sources cannot generate constant power because of their natural characteristics (e.g., solar energy only being able to be harvested during sunny days) and unpredictable behaviour (e.g., the wind). Hence, they have reduced commercial efficiency. Moreover, most alternative sources need highly advanced and costly components and controllers, again making them unattractive to users. Despite these challenges, governments have continued to support alternative suppliers with the aim of making a 'greener' future. Sensing the trend, some commercial entities are slowly coming on board and shifting their focus to generating electricity from resources that are less harmful than oil and gas.

Against this backdrop, the ideal power system should be flexible, have the ability to control energy management, and be able to manage power flow from several sources at once. Current power systems have not yet achieved this ideal, but they could come closer with the adoption

of the smart grid concept. Under such a concept, the power system's infrastructures would have to be updated or modified to handle greater power supplies from the system's distributed sources. Meanwhile, the components and smart devices would also have to be updated or modified to recognize different scenarios and function on an instinctive level.

Current Harmonics: This type of harmonics comprises components that include frequencies other than the system's nominal frequency (e.g., 50 or 60 Hz). Such components with different amplitudes can become sources of several types of disorders in electrical systems, such as voltage distortions when passing through an inductance or transformer, decreased efficiency, extreme losses in lines and electrical components, acoustic noises in electro-magnetic devices, and the production of a neutral current (Javadi, 2016). Thus, the increase in harmonic pollution originating in non-linear loads can have a negative impact on the power system and equipment. To curtail current levels of disturbance, IEEE standards 519 and 1459 were introduced (IEEE Recommended Practices and Requirements for Harmonic Control in Electrical Power Systems, 1993; IEEE Standard Definitions for the Measurement of Electric Power Quantities Under Sinusoidal, Nonsinusoidal, Balanced, or Unbalanced Conditions, 2010). As well, the International Electro-technical Commission (IEC) released some technical reports to gauge the connection between non-linear loads and power plants (International Electro technical Commission [IEC], 2009-04).

Reactive Power: Voltages and currents are sinusoidal waveforms in the AC systems. However, power calculation is difficult if the waveforms do not align. The outcome of such misalignments is apparent power (S), designated as the cross-operation of the two waves. It has two distinct components: one moves from the source to the load and works at the load, while the other component cannot perform useful work at the load because of delays between voltage and current (phase angle). This section is referred to as reactive power. It essentially lowers power flow efficiency in terms of power consumed vs. installed capacity.

Voltage Unbalance: An unbalance occurs when the three phases of a 3P3W or 3P4W system do not share the same voltage magnitude and phase shift precisely. Because voltage unbalance can damage motors and transformers, the IEEE std 1159 (IEEE Recommended Practice for

Monitoring Electric Power Quality, 1995) has instituted strict rules for power operators (Javadi, 2016).

Voltage Sags: The IEEE's Standard Recommended Practice for Monitoring Electric Power Quality (1995), states that voltage sag is a decrease in voltage of a relatively short duration, or specifically "a decrease between 0.1 and 0.9 p.u in rms voltage for duration of 0.5 cycles to 1 min." Voltage sags can occur as a result of load changes or motor start-up, as induction motors can consume up to ten times their nominal rated current at the start-up phase.

Voltage Swells: These are short duration increases in rms voltage from 0.5 cycles to 1 min. The magnitude usually ranges between 1.1 and 1.8 p.u. Swells occur less frequently than sags and are often associated with system fault conditions. Cases during which swells can occur include switching on a large capacitor bank or switching off a sizeable load.

In this section of the thesis, we briefly discussed the significance of compensating for various phenomena that impact power quality. We concluded the chapter by highlighting the contribution of this project regarding the improvement of power quality enhancement. The first main contribution is the integration in the control technique of the compensation of the reactive power which helps to remove the TCR converter used in the published research.

The second contribution is the design of passive filters by two different techniques with the objectives to analyse the performances and to reduce the rating of the active filter.

The third one concerns the modification of the configuration by removing the bridge, testing the regulation of the dc bus voltage by the active filter and the different perturbations.

The configuration of the HSPF proposed integrate a PV solar and the battery in the DC side of the active filter to be acted during grid OFF operation in order to maintain uninterruptible power supply to the load.

In the first chapter, the literature review for different harmonics mitigation techniques, series active filter topologies and control is presented. The latest advanced configurations and their respective control are included.

The second chapter analyzes the modeling of a three phase series hybrid power filter with bridge diode to regulate dc bus voltage, using sliding mode control design to improve power quality (sag/swell/unbalance voltage, current harmonics, and reactive power compensation). In addition, this chapter covers a passive filter design, and studies the stability of the control system.

The third chapter contains a modeling of a three phase series hybrid power filter with dc bus voltage regulated with itself using nonlinear control design for compensating current harmonics, reactive power and unbalance voltage.

The final and fourth chapter covers the application of the PV solar through three phase series hybrid power filter method, and presentation the simulation results, which allows the validation of the proposed grid on/off operation scheme.

CHAPTER 1

LITERATURE REVIEW

1.1 Introduction

This chapter describes hybrid series power filters (HSPFs) and provides some relevant background information on their control as well as on synchronized passive filters. In addition, the chapter provides an overview of the most recent advances in power quality enhancer devices. After defining HSPF and the filtering application for power quality improvement, the chapter discusses the advantages of an intelligently controlled power system that uses renewable energy sources. To overcome any issues related to this advancement in technology, alternating current (AC) transmission systems along with 3-phase power systems were developed. The following power compensation approaches were later developed to boost power quality:

- Harmonic voltage compensation;
- Harmonic current compensation;
- Sag and swell voltage compensation;
- Neutral current compensation;
- Reactive power compensation;
- Unbalanced voltage compensation.

A variety of HSAF approaches have been developed over the years, each with its own particular advantages and disadvantages. For instance, a few of the approaches are meant to resolve power quality issues, such as voltage and current harmonics, load reactive power, and voltage sag and swell. An additional parameter that is based on HSAF is the level of reactive power required. Another factor is the price of the materials and equipment needed for reactive power. These parameters and factors help to determine which approach is best suited for which projects. The methods can also differ in relation to the sizing of the HSAF elements.

There has been a recent surge in the use of renewable energy sources for power generation. Therefore, integrating an HSPF could help to reduce the usage of traditional resources, which

will consequently reduce pollution emissions. Renewable energy sources are popularly referred to as 'green' energy and include natural (i.e., non-processed) sources that can generate energy with little to no residual pollution. Despite their benefits to the environment, however, green energies bring with them a whole host of new problems, chief among which is their lack of constancy due to their unique characteristics (e.g., solar energy being reliant on sunny days) and oftentimes unexpected behaviour (wind energy being reliant on windy weather). Green sources also have generally low commercial efficiency. Thus, a hybrid series could be applied as an uninterruptible power supply (UPS) to resolve these issues.

1.2 Types of Loads

Based on the network system(s) being utilized, there is a wide variety of load types, such as linear and non-linear loads. Each type of load likewise has subtypes, such as balanced and unbalanced loads.

1.2.1 Balanced Loads

Load balancing is intended to store the load information of peer nodes in several directories, which then can schedule reassignments of virtual servers to achieve better balance, if needed. The distributed load balancing problem can then be reduced to a centralized problem at each directory.

1.2.2 Unbalanced Loads

An unbalanced 3-phase load can be defined as a load which is unequally distributed across three phases. To rate as a 3-phase load, the highest single phase load must be multiplied by 3. An unbalanced load can lead to unequal phase-to-phase and phase-to-neutral voltages.

1.2.3 Linear Loads

A linear load is the one which exhibits steady impedance to the supply voltage, causing the current wave shape to change directly proportional to the supply voltage. Constant impedance shows a sinusoidal current waveform if the supply voltage waveform is sinusoidal. Examples of linear loads include motors, incandescent lighting, and resistance heating (Debasish and Rakesh, 2013).

1.2.4 Non-linear Loads

In contrast to a linear load, a non-linear load exhibits changing impedance to the applied voltage, which means that the current waveform can not alter based on voltage waveform. The result is a non-sinusoidal current waveform. Furthermore, non-linear loads offer large impedance at some sections of the voltage waveform. This impedance is reduced when the voltage reaches peak value. When low impedance occurs, the current experiences a sharp rise, whereas when the impedance value increases, the current drops. Thus, as the voltage and the current waveform are not in synch, they are considered non-linear. Examples include drives with altering speeds, loads with diode-capacitor power supplies, and uninterruptible power supply. These types of loads draw short pulse currents during the crest of the line voltage. Moreover, the non-sinusoidal current pulses inject unpredictable reflective currents into the power distribution system, which leads to the current functioning at frequencies different from the primal frequency (Debasish and Rakesh, 2013).

1.3 Power Quality Solution

Recent advances in power electronics have seen active filters (AFs) gaining in popularity. On a commercial basis, shunt active filters have been available for small and medium voltage applications. Shunt AFs have several advantages compared to traditional passive filters. For instance, they are independent of the system parameter state, do not require tuning, and respond well to load variations. Additionally, the compensation efficiency of shunt AFs is not dependent on external parameters. They have near total control and can carry out every type of modification without the need to change the hardware (Javadi, 2016).

Given the recent technological improvements in the industry, along with the decrease in the output cost of power electronic converters, the use of active compensators is inevitable.

Furthermore, the increasing popularity of ‘smart’ grids has confirmed the application of compensators to improve power quality compared to more traditional passive filters. Furthermore, as they have topologies similar to FACTS devices, the industry is satisfied that they will be reliable in critical operating states. The following section presents an overview of the various categories of filters (Javadi, 2016).

1.3.1 Passive Filter (PF)

Passive filters (PFs) can be generated easily and at a low cost from basic electrical components (e.g., resistors, capacitors, and inductors), making them attractive to industry. At the same time, traditional filters comprised of passive components can significantly improve the current and voltage harmonics of power systems. However, they can have considerable drawbacks; they require load and system parameters (e.g., impedances) to be meshed properly. Therefore, when installed, they operate through defined system specifications and are not readily adaptable to load differences or changes in those specifications. This means that although under special conditions they might initially improve power quality, they could also worsen it later by not operating as predicted. Hence, they need to be re-tuned occasionally to maintain efficiency, as there are no controls on their process state (Javadi, 2016).

PFs have been utilized since the introduction of the AC supply system. Their main purpose is to improve the power quality of the system. Typical characteristics of PFs include lossless reactive elements (capacitors and inductors) and dependence on the source’s impedance value. Furthermore, PFs can be applied to improve the voltage, dynamics, steady-state, transit, and angle stabilities. The source impedance at the network frequency should be relatively low to prevent the fundamental voltage from crossing the limits. Figure.1.1 shows a passive filter. Its advantages are: improving grid stability, improving load balancing in instances of several parallel circuits, correcting the power factor, regulating voltage, reducing losses and voltage drops and reducing neutral current in the grid. Also its disadvantages are: Reducing line impedance (which coordinates increase in harmonics from the load to the source) and potentially producing subharmonic-type resonance between line impedance and series capacitor.

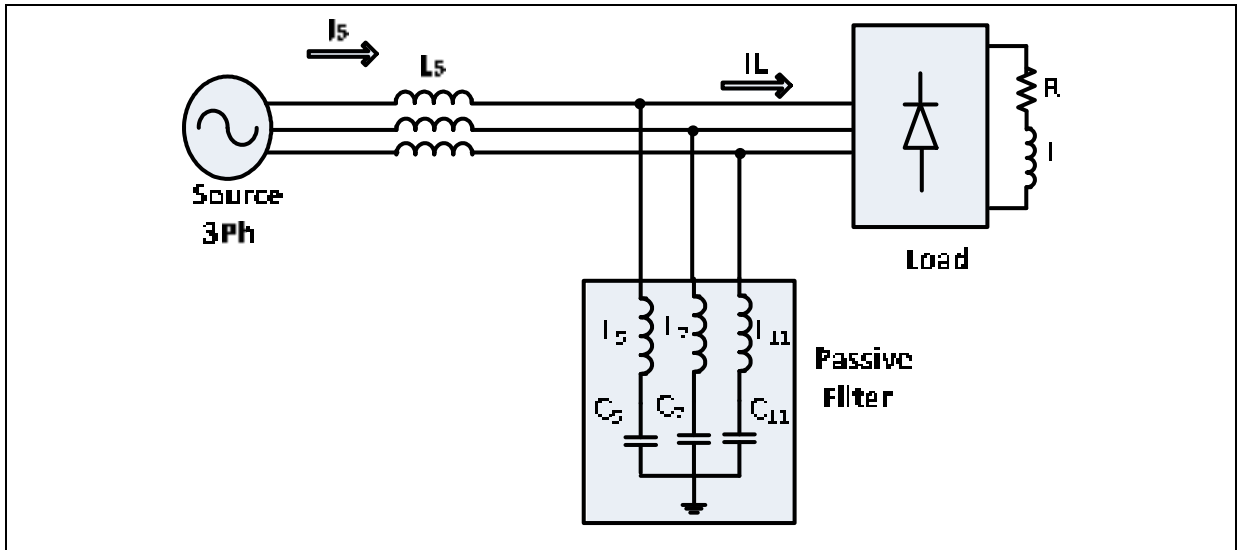


Figure 1.1 Passive filter

1.3.2 Active Filter (AF)

Active filters (AFs) are derived from the notion of compensating reactive power as well as the harmonic currents created by non-linear loads, which are caused by semi-conductor switches such as converters, diode bridges and thyristors bridges. They are compensated by being injected with the same magnitude and amplitude in the opposite direction. Harmonic components of non-linear loads are usually used as references to AF currents. Thus, AFs have emerged as a viable solution in harmonics and reactive power compensation (Javadi, 2016).

Active filters are created from a range of semiconductors operating as switches. The main element of an AF is its converter, which, in case of the control side, may depend on the voltage or current source. A continuous voltage source type capacitor is one which opposes the voltage variations, whereas a current source type converter is an inductance which opposes current variations. Different kinds of active filters include series AFs, shunt AFs, and hybrid AFs (Javadi, 2016).

1.4 Series Active Filter (SeAF)

Series active filters (SeAFs) were developed to introduce a voltage in series with the circuit, with the intention of isolating the source from the load. In particular, they were developed to

offset the disadvantages of passive filters, which are quite costly and overall inadequate. At the same time, PFs are difficult to install, as a precise estimate of system parameters is necessary prior to installation, and such an estimate can take immense time and effort. Furthermore, parameters change as the power grid develops, so PFs likewise need to be altered to reflect these changes. This serves to decrease the efficiency of PFs while increasing related costs.

Shunt AFs are often used instead of passive filters, but they are typically restricted to correcting the power factor and compensating current harmonic pollution produced by non-linear loads. To resolve issues around power, line conditioning systems can be used for repressing and/or counteracting power system disturbances. Series active filters and dynamic voltage restorers (DVRs) can be utilized to compensate current issues and reduce voltage distortions. However, given the complexity of series active compensators compared to conventional shunt AFs, the use of these devices is generally confined to applications where PQ requirements are relatively strict (Javadi, 2016).

Along with issues related to current to compensate current, it is important to safeguard critical loads and PCCs from voltage distortions, sags, and swells. To accomplish this, a dynamic voltage restorer can be used. DVRs and SAFs divide similar topologies that are comparatively complex in parts because of the isolation transformer needed to couple to the grid. Although providing reasonably good isolation for the compensating system, the transformer is costly and can cause a range of undesirable performance issues, such as hysteresis phenomena and electrical losses (Javadi, 2016). The SeAF model is shown in Figure 1.2.

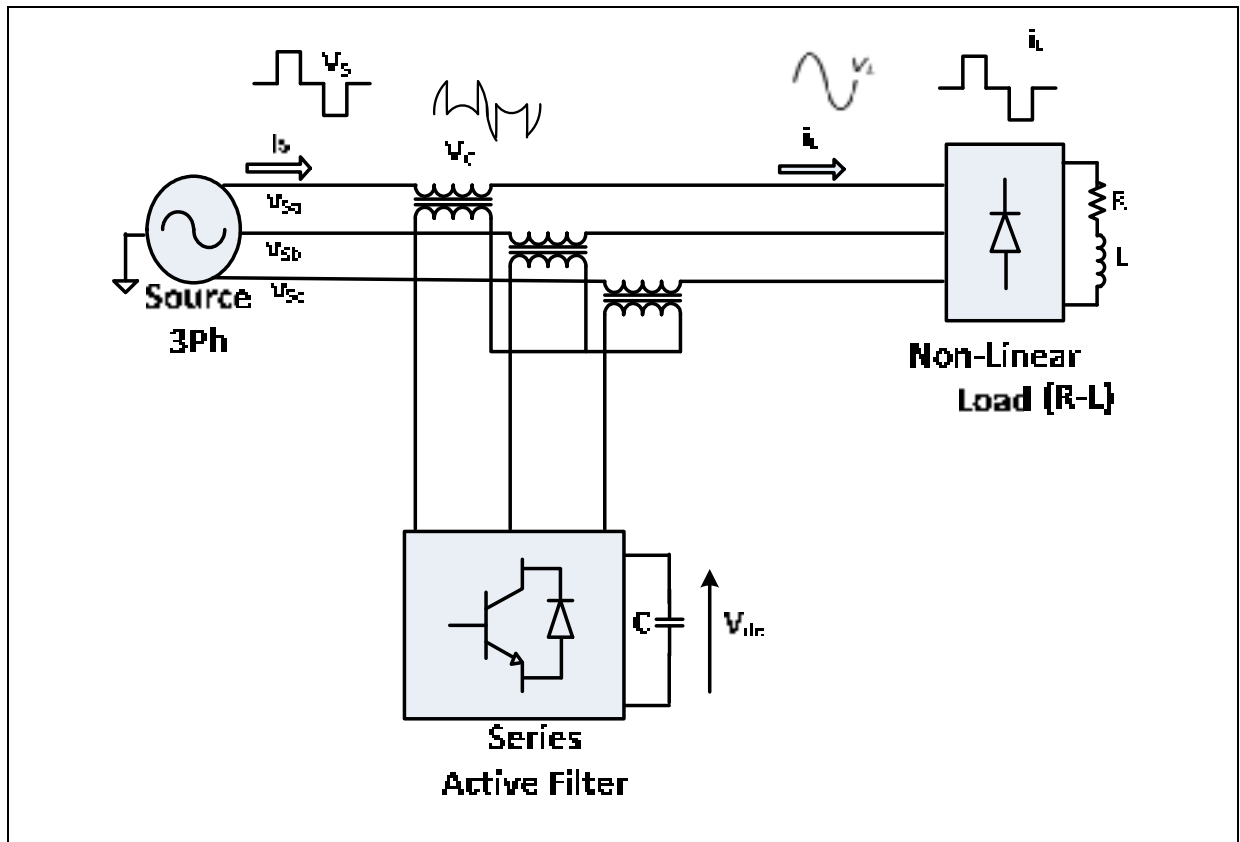


Figure 1.2 Functionality schematics of series compensation

The idea of series active compensation was introduced near the end of the 1980s to enable voltage regulators to operate in sensitive loads (Gyugyi, 1979). Series-connected filters protect users from insufficient supply-voltage quality, and they should also ensure a sinusoidal balanced voltage on the load side, even with perturbations in the source voltage. Typical perturbations include harmonic distortion, sags and swells, and unbalance; they can also include disturbances in the current load, such as distortion by harmonics, step changes, unbalance, and distortion by harmonics. Through increasing usage of this method, it was found to have the ability to isolate current harmonics of a voltage-fed type of non-linear load (VSC) from the power system. In most instances, and in order to compensate load current harmonics, series active power filters (which are a controllable voltage source) must function together with shunt passive filters. However, if passive (L-C) filters are connected in parallel, the series active power filter functions as a harmonic isolator, enabling the load current harmonics to

circulate primarily through the passive filter instead of the power system (Javadi et Al-Haddad, 2011).

This method is extremely useful for compensating voltage unbalances as well as sags and swells from the AC supply; it is also useful for low-power applications. As equally important, it is a cost-effective alternative to UPS, as no energy storage on the DC bus is needed, so the overall sizing of the components is relatively small.

Furthermore, since the efficiency of active compensators makes them attractive for industrial smart grids application, the compensators could potentially help to increase the amount of renewable energy that enters the grid (Singh, Al-Haddad and Chandra, 1999). The recent wave of novel low-cost power electronics has made active filters desirable to the industry. As an affordable solution, active filters could prove to be indispensable in the future for boosting and streamlining the power quality of grids with smart and adaptive devices. Currently, shunt active filters (SAF) are being used at the distribution level in instances where passive filters have proven inefficient, unsafe, and imprecise.

For resolving current and voltage issues simultaneously, there is a relatively efficient but expensive solution known as the unified power quality conditioner (UPQC) (Brenna, Faranda and Tironi, 2009; Khadkikar and Chandra, 2008). For regulating problems around voltages and currents as well as to improve the quality of the energy produced, the UPQC uses a series active filter in combination with a shunt. The shunt active portion compensates current harmonics and adjusts the power factor of a non-linear load, whereas the series active portion gets rid of voltage distortions and monitors the 3-phase voltage at the PCC (Khadkikar and Chandra, 2009; 2011). This approach has been shown to be a viable solution for enhancing power quality, with several different topologies being developed (e.g., the shunt active filter connected in the right - or left- side of the series active part). However, the overall complexity of the system's components makes it relatively unaffordable for most commercial and residential users (Javadi, 2016). Despite its success in practice, the core issue with this particular configuration is the non-isolation of the DC bus bar and 3-phase power system.

1.4.1.1 Hybrid Filter (Series Active and Passive Filter)

Today's electrical equipment makes stringent demands on supply voltage stability and quality. However, at the same time, power networks need to be free from harmonics and related electrical issues. Getting rid of unwanted harmonics in the system and avoiding resonance issues are some of the main problems that emerge when boosting power quality. Overcoming these problems can bring numerous benefits, including a higher power factor, greater voltage stability, and decreased network loss. Purging the network of problems also has the added benefit of reducing stress on equipment, which then increases its life-time. Longer equipment life means reduced overall costs related to replacement of worn-out equipment (Javadi, 2016).

To benefit from the advantages of both passive and active filters, several different types of hybrid filters have been developed. Within the context of this present study, a series active filter in parallel with a passive filter bank configuration is most appropriate. This hybrid will be studied in detail, with an aim to resolve current issues while taking into account the restoration of load supply (Javadi, 2016). This type of filter has benefits both in the simplicity of the passive division and the high dynamic provided by the active portion. The combination of benefits thus offers higher VAR compensation than active or passive filters.

A hybrid filter is based on an approach that combines an active and passive filter. As mentioned previously, passive power filters in power system applications can have issues around source impedance that can detrimentally affect the filtering process and system resonance. These issues can, however, be resolved or at least mitigated by adding a combination of active and passive power filters. Harmonics that are generated from non-linear loads constantly change frequency and frequency components. As they consist of passive and active power filters, hybrids can supply ideal harmonic compensation for dynamic non-linear loads as well as repress series and parallel resonances. Hybrid filters can also filter more rows of harmonics. As the hybrid series filter compensation is the subject of the current research work, it will be described in detail for the remainder of this thesis (Javadi, 2016). A hybrid filter model is shown in Figure 1.3.

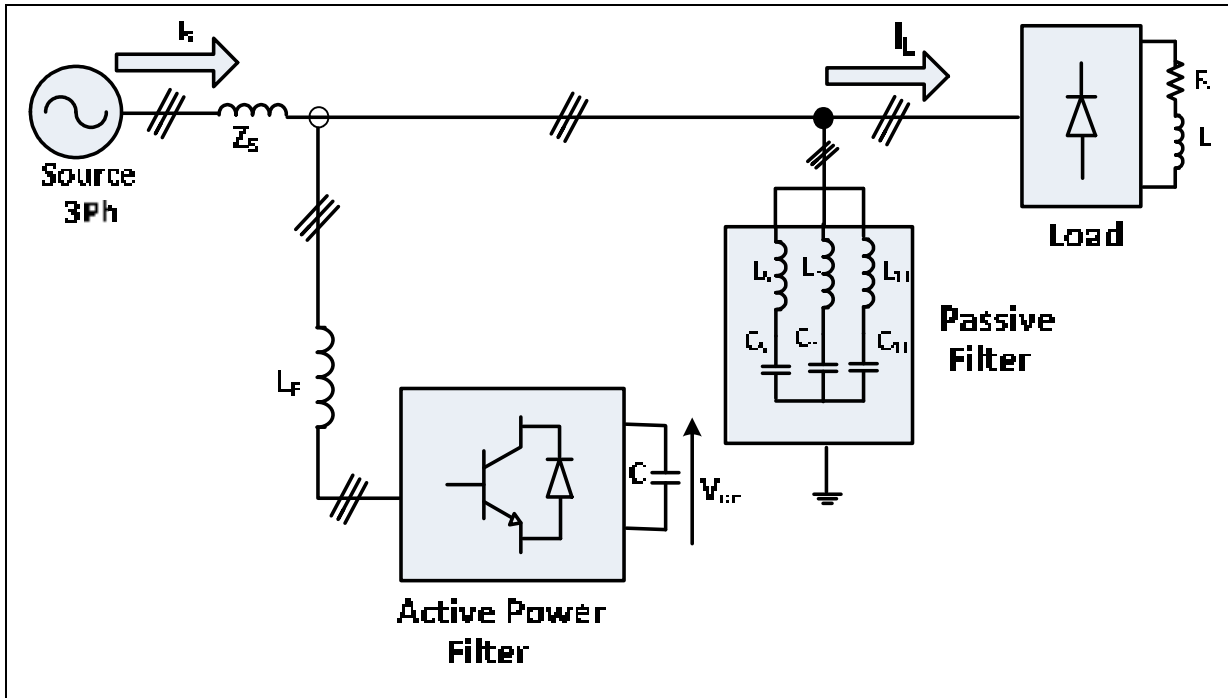


Figure 1.3 Hybrid filter

1.4.1.2 Unified Power Quality Conditioner

The unified power quality conditioner (UPQC) combines series and shunt active filters (Khadkikar, 2012). The series-connected active filter compensates issues around voltage harmonics, and the shunt portion which is connected across the load cuts down on current distortions (Ganguly, 2014). However, although the UPQC provides an efficient response to power quality issues, it is only rarely used commercially due to its complexity and high cost. Figure 1.4 illustrates a typical configuration for a UPQC in a power system.

UPQCs evolved from the line of active filters where series and shunt AF functionalities are used in tandem to achieve enhanced and immediate control over power quality problems (Quoc-Nam and Hong-Hee, 2014). The back-to-back converter configuration emerged when Fujita and Akagi (1998) demonstrated how this system functions using 20 kVA experimental results. They called their device a “unified power quality conditioner”.

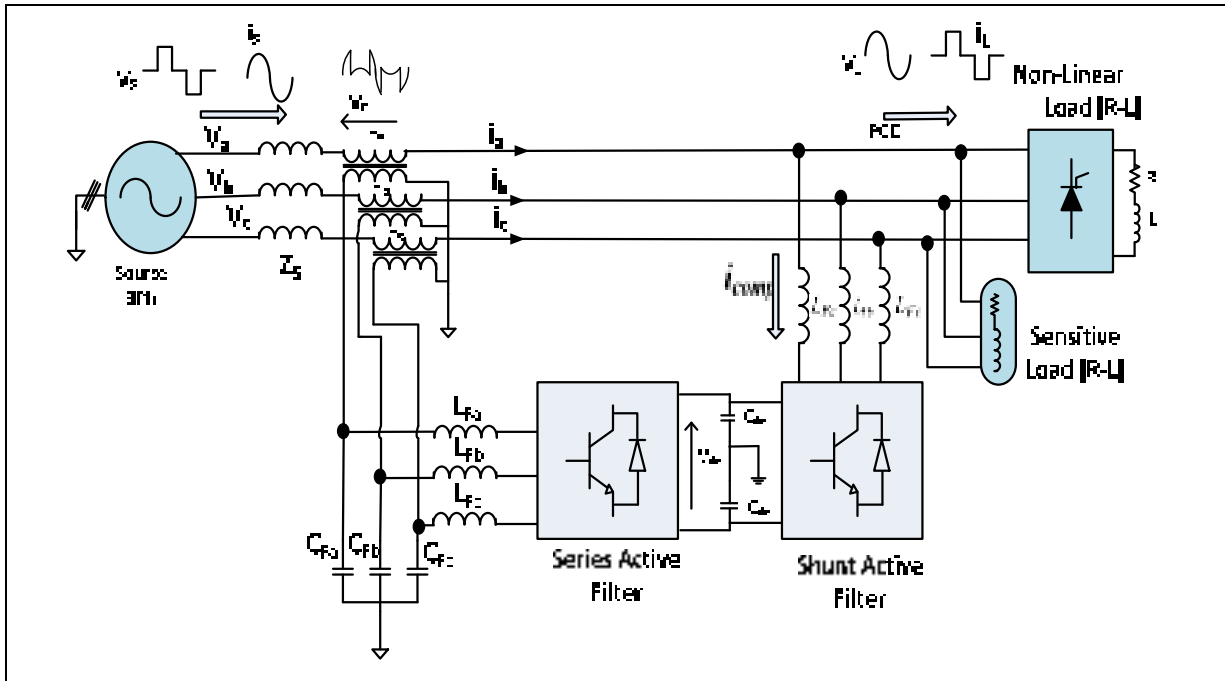


Figure 1.4 A typical unified Power quality conditioner resolving power quality issues.

1.5 Modeling of Series Hybrid Power Filter (SHPF)

A series hybrid power filter (SHPF) system is a type of compensator interfaced between the grid and linear or non-linear loads. Also considered as viable solution for power quality problems, SHPFs function has high impedances at frequency harmonics, thus helping to force current harmonics to move into the passive filter. The main purpose of SHPF systems is to inject voltage at the primary transformer as a mean of compensating for undesirable perturbations. Under normal operating conditions, SHPFs utilize a minimum of two integral technologies.

The role of SHPFs is as follows:

- to ensure uninterrupted, stable, low-cost and high-quality power to local loads;
- to compensate or augment current harmonics, sag and swell voltage, and reactive power.

1.5.1 Configuration of Series Hybrid Power Filters (SHPFs)

Hybrid series power filter (SHPF) systems have a series active filter with a passive filter connected to the network. An SHPF is shown in Figure 1.5. This type of power filter system not only improves power quality, but also decreases current harmonics. To that end, several different solutions have been put forth as options. Of these, series and shunt active power filters are well-positioned as alternative solutions to compensate for problems related to current and voltage power quality in distribution systems. A broad range of shunt APF and series APF topologies have been suggested by a number of researchers. However, series APF systems need to supply active power in order to preserve the requisite level of load voltage throughout voltage sag. Simultaneously, power flow in SeAPF systems can dramatically increase throughout voltage sag. In this case, the energy sources should be inserted into a series APF system (Javadi, 2016).

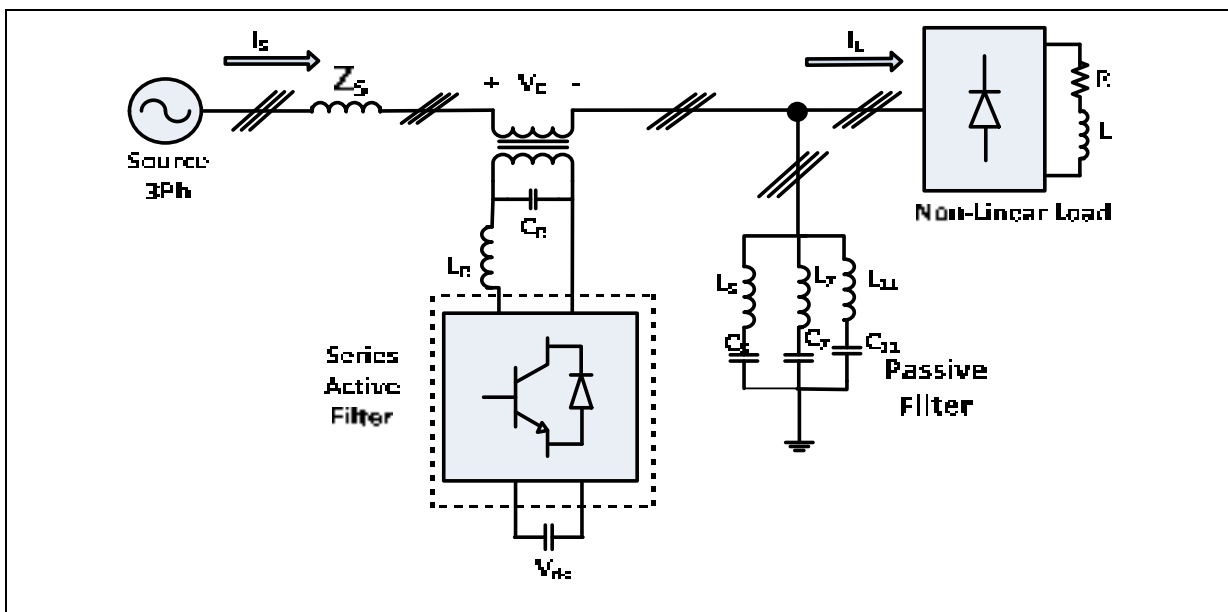


Figure 1.5 Hybrid series power filter configuration

A number of different solutions have been proposed to enhance power quality. These solutions succeed in resolving many issues related to power quality, such as load reactive power, voltage and current harmonics, and voltage swell and sag. The most promising of these solutions are detailed in the following sections.

1.5.2 Novel HSAF for Power Quality Compensation

Hamadi (2007) discussed a series hybrid active filter (SHAF) to compensate voltage/current harmonics, reactive power, load type, and resonance damping. Hamadi's (2007) approach is essentially a collective system of series active filters and shunt passive filters as shown in Figure 1.6. Combining active and passive power filters succeeds in reducing "the power rating of the active section, while the novel SPF uses a minimal component count. The principal of the SPF is to have a high impedance at the standard frequency and a very low impedance for higher harmonics compensates created by the load" (Hamadi, 2007). The power factor is thus improved through the compensation of all reactive power and harmonics. Furthermore, the SAF offers high impedance levels via harmonics compensation, forcing the harmonics to flow over the ShPF and compensating both the reactive power and voltage harmonic. The synchronous reference frame (SFR) approach is used for controlling the SeAF in this application.

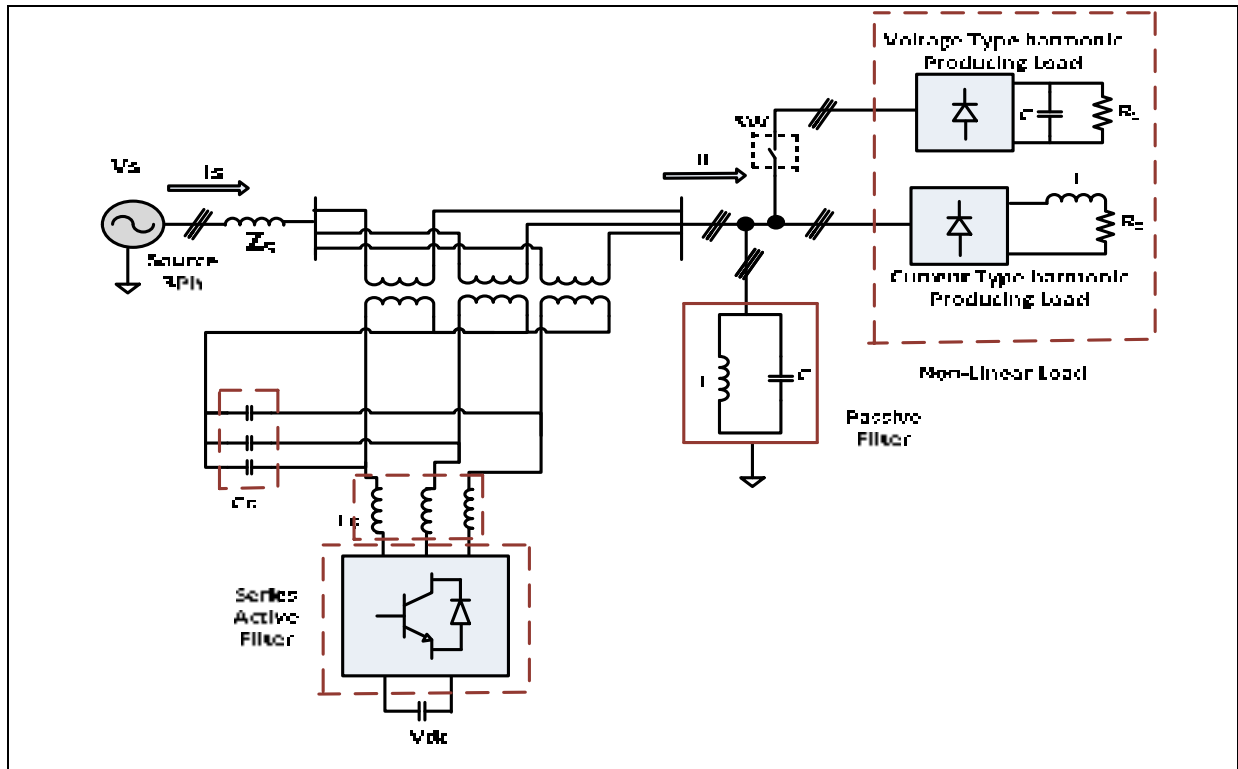


Figure 1.6 Hybrid series active filter with non-linear loads taken from (Hamadi, 2007)

In this section, a configuration for a novel HSAPF for power quality compensation is discussed. This version contains both a SeAPF and ShPF, with a model voltage-type of source and current harmonics. Specifically, the SeAPF is useful for extending the fundamental frequencies of either very low or very high impedances that have been created due to the sensitivity of loads to variations "in the supply voltage. Because it can inject a voltage component in series with the supply voltage, it is considered a controlled voltage source" (Hamadi, 2007).

Hence, by controlling the SeAF, reactive power, the load harmonic voltages and the source voltage distortion can all be compensated. At the same time, there is a contribution to the ShPF. At fundamental frequencies, the ShPF contributes low levels of impedance as well as higher levels of resistance K for harmonic currents that are load-related. In this way, such currents must enter the ShPF. This means that because both the load/source harmonic voltages and the controlled compensation voltages are more or less the same with regard to amplitude, although they are not the same in phases: the one essentially cancels out the other.

The method that applies control as a means to create reference compensating voltages is crucial in the series APF. In generating the appropriate compensating voltages, the source harmonic component must be precisely detected in order to give correct series APF reference voltages. In fact, control algorithms which are utilized for obtaining SeAPF references are derived from parts of synchronous reference frames. In this approach, we can use an active power filter to play the role of both harmonic isolator and current-controlled voltage source, effectively preventing source harmonic voltages from entering loads or load harmonic currents from entering sources. In Figure 1.7, we can see how the control method is applied in series APF reference compensating voltages.

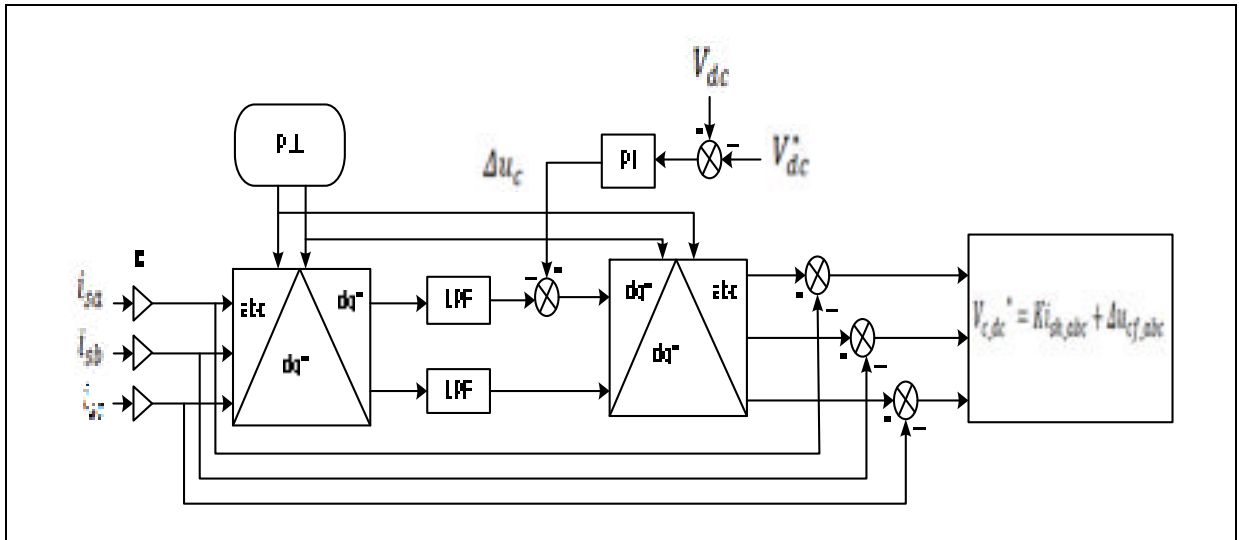


Figure 1.7 Control scheme of active power filter

1.5.3 New HSAF Configuration to Offset Reactive Power, Current/Voltage Harmonics, and Voltage Swell/Sag

Hamadi (2009) introduced a new model of series hybrid power filter (SHPF) configuration adaptable to all harmonic loads. The novel filter comprises a shunt passive filter and a small rated series active power filter (SAPF), with changing inductance that utilizes a thyristor control reactor (TCR). The DC voltage found at the load side of a model voltage harmonics source (e.g., a diode bridge rectifier followed by a capacitor) serves as a source of DC power for the SAPF. Hamadi (2009) used a MATLAB/Simulink simulation to develop the hybrid filter and then was successful in applying it for offsetting voltage sag, swell and harmonics, as well as the current harmonics and load reactive. The configuration is shown in Figure 1.8.

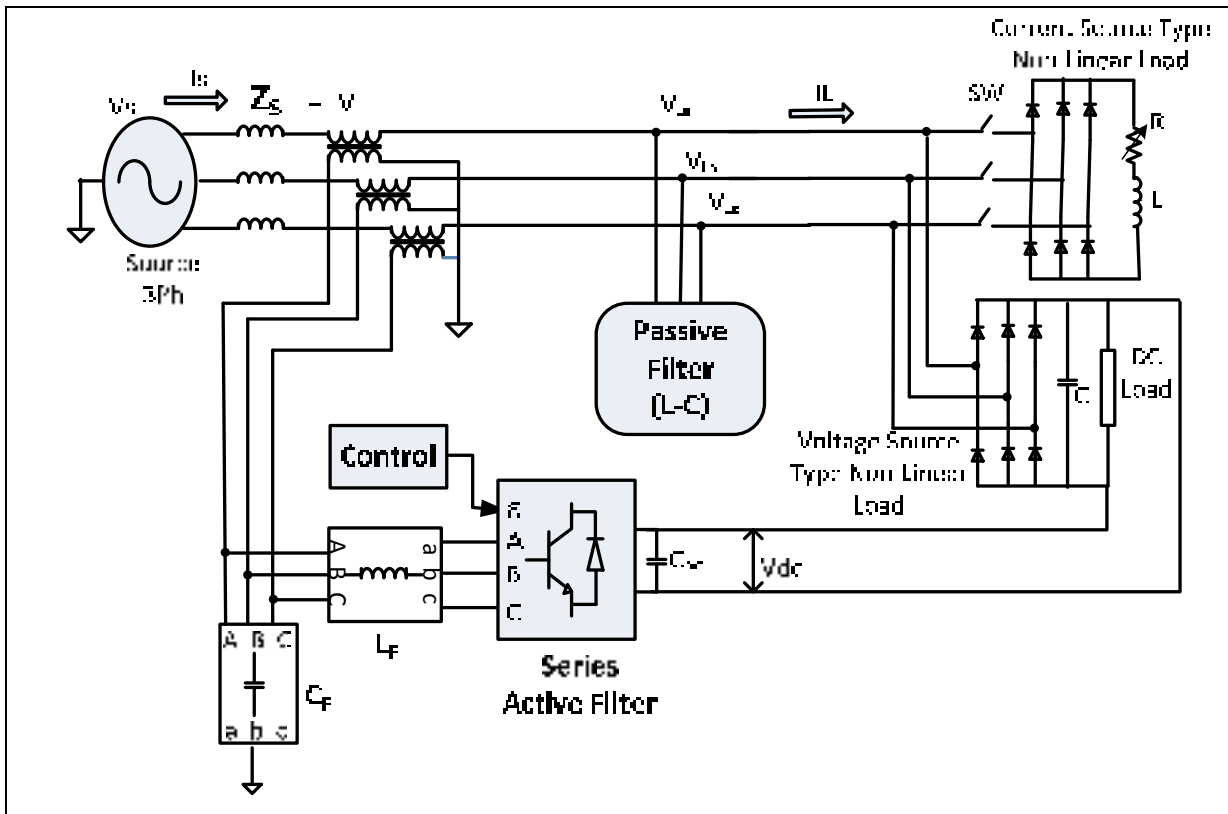


Figure 1.8 Proposed series hybrid power filter configuration

Hamadi (2009) used non-linear-type control in his research. This approach controls the SeAF in order to offset reactive power, voltages related to load harmonics, and distortions in the source voltage. Furthermore, it is intended to support the passive filter that provides ultra-low impedance for higher than normal resistance in currents of load harmonics as well as for standard frequencies. As a result, the load harmonic currents can enter the ShPF. This method of control utilizes hybrid control and simultaneously detects the source current as (abc) and the load voltage V_L (abc) in order to obtain harmonic parts as a means to boost the series transformer impedance levels for harmonic frequencies.

The offset effects are essentially related to the ration of control gain (k), which represents the rations for compensating harmonic voltages created as a result of the SAPF response to harmonic currents moving through it. As can be seen, by reducing k from 5 to 2, there is a subsequent decrease in the harmonics amplitude of the series transformer voltages, which then adversely impacts the filtering effect. When $k = 5$, the reflected impedance of SAPF is quite

high, enabling the load current harmonic to move through the shunt passive branches (Hamadi, 2009).

The main reason for wanting to control the TCR is to enable control of the thyristor's firing in order to control the reactor current. This is done to gain control over TCR-absorbed reactive power. When applying the abc format, we can use the laws of voltages and currents proposed by Kirchhoff, but removing the inductance resistor used in the system. From this, we can obtain 3 differential equations.

1.5.4 SHAPF for Mitigating Voltage Unbalance and Harmonics under Unbalanced Non-Sinusoidal Supply Conditions

Mulla (2012) introduced a novel definition for instantaneous reactive, active and apparent power quantity. The work also discussed the decomposition of a voltage vector for different components of power quantities, as well as reference generation for a series hybrid active power filter (SHAPF) for supply voltage balancing and harmonic elimination as shown in Figure 1.9. Additionally, Mulla (2012) applied the proposed control scheme to SHAPF, recording the simulation results. Along with its primary aim of relieving current and voltage type harmonics, SHAPF helps to resolve problems related to power quality, including unbalance, swell and sag, and voltage (Mulla, 2012).

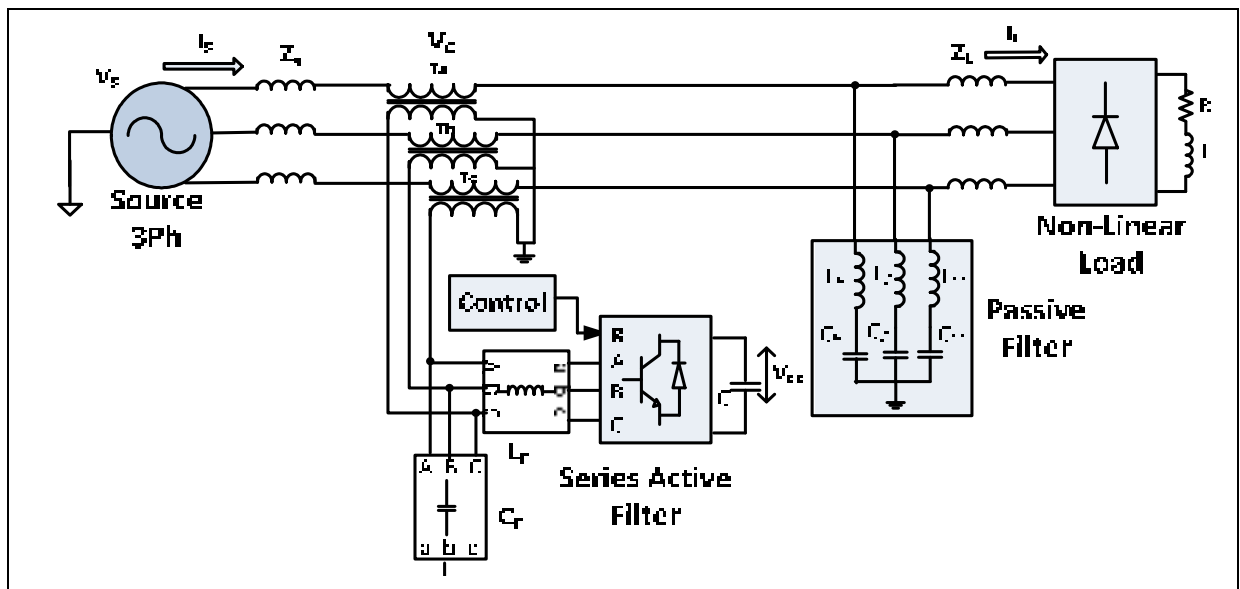


Figure 1.9 Circuit configuration of the SHAPF

Figure 1.10 shows the proposed novel algorithm of SHAPF for generating reference voltage, Mulla (2012) performed the tests under unbalanced non-sinusoidal supply conditions. He also decomposed multiphase vectors of voltages into quantities that represent various power components. Because instantaneous reactive and active power includes an oscillating component as well as an average component, it is possible, using vector algebra, to obtain the voltage vectors corresponding to average and oscillating powers. Moreover, because it is a series arrangement, non-sinusoidal and unbalanced fundamental components of source voltages can be added. This addition can be accomplished by appropriate modification of the reference for harmonic mitigation.

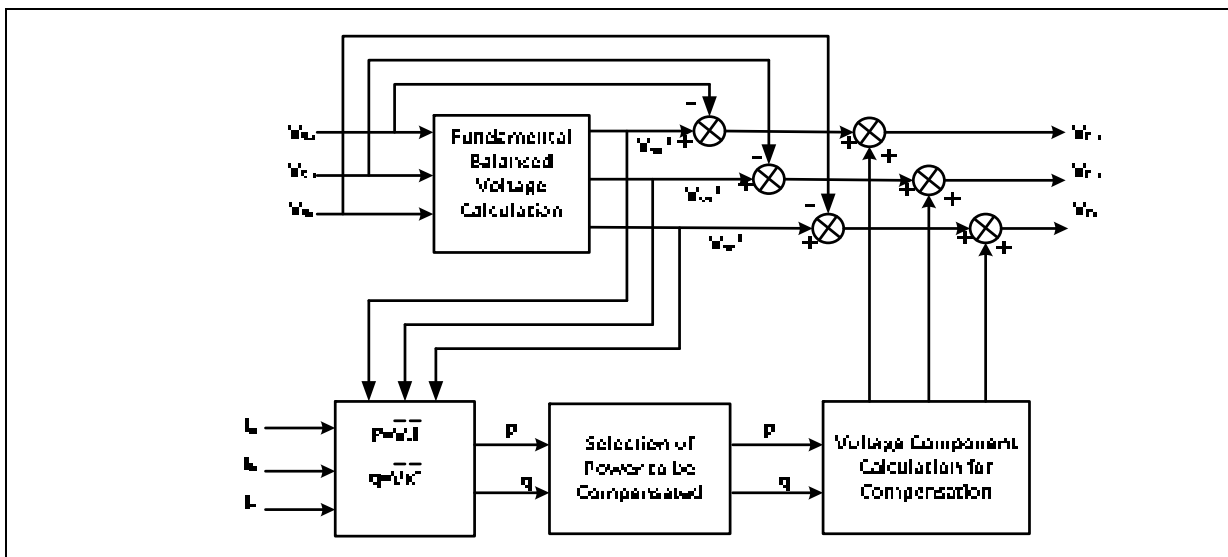


Figure 1.10 TCR control scheme for SHAPF

In this section, the researcher used 3-phase voltage generation as a reference (Mulla, 2012). The existing control strategies for SHAPF depend on decomposing the voltage vector by applying the generalised instantaneous power theory for SHAPF under the non-sinusoidal supply condition. The control scheme not only is valid for unbalanced and balanced, non-sinusoidal and sinusoidal source conditions, but is also able to balance load voltages and deal with voltage or current-type harmonics (Mulla, 2012).

1.5.5 Improving Power Quality Through a Photovoltaic-based 3-Phase 4-Wire SHAPF

In this study, Vijayakumar (2014) presented a photovoltaic panel (PV) and a battery connected to a series hybrid power filter (SHPF) comprised of an LC shunt passive filter and a series active power filter as shown in Figure 1.11. The primary benefit in using this system is its ability to compensate current harmonics, voltage harmonics and voltage interruption throughout an entire day. The SHPF requires an energy source in order to compensate the voltage swell and sag. At the same time, the topology of this system uses a green energy source linked to an energy storage unit to gauge the SHPF DC-link voltage needed. The control strategy here is grounded in the double formulation of the compensation system principles with adaptive fuzzy logic control (FLC). Vijayakumar (2014) also proposed a novel coordinate reason control that can offer ongoing harmonics and outage compensation under various conditions.

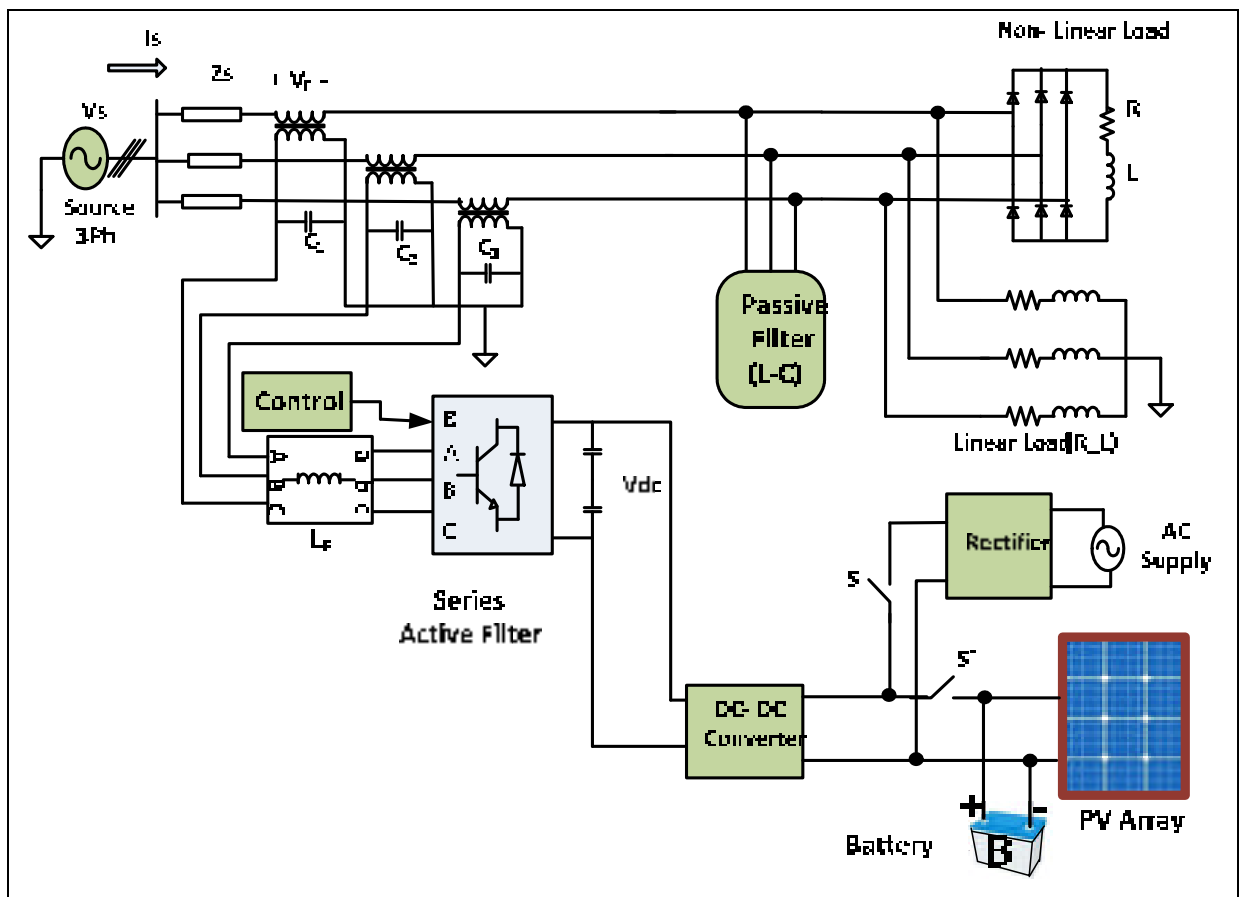


Figure 1.11 PV-based SeAF with ShAF topology

Vijayakumar (2014) studied the PV-interfaced 3P4W series hybrid active power filter as a means for offsetting voltage interruption/unbalance, voltage sag/swell, and harmonic currents. The intended users are either commercial (small industry) or residential. The researcher presented a PV system with battery attached to an SHPF comprised of an LC shunt passive filter and SAPF. The main benefit in using this approach is compensation gains for the voltage interruption, and current and voltage harmonics. The SAPF requires an energy source to compensate the voltage sag and swell, and the topology of this system also employs a low-energy approach that features an energy-storage unit for gauging the SAPF DC-link voltage demand.

Vijayakumar's (2014) control strategy uses adaptive fuzzy logic (FLC) control instituted by doubling the principles of the compensation system. This method is then applied to control the voltage source inverter (VSI), as shown in Figure 1.12. A novel coordinate reason control is also introduced to provide constant outage and harmonics compensation under various conditions. Because the point of common coupling (PCC) must follow linear characteristics, the voltage and current of the 3P4W distribution system can be defined as vectors. Furthermore, the balance resistive load can be seen as an ideal reference load if the system currents are unbalanced and non-sinusoidal (Vijayakumar, 2014).

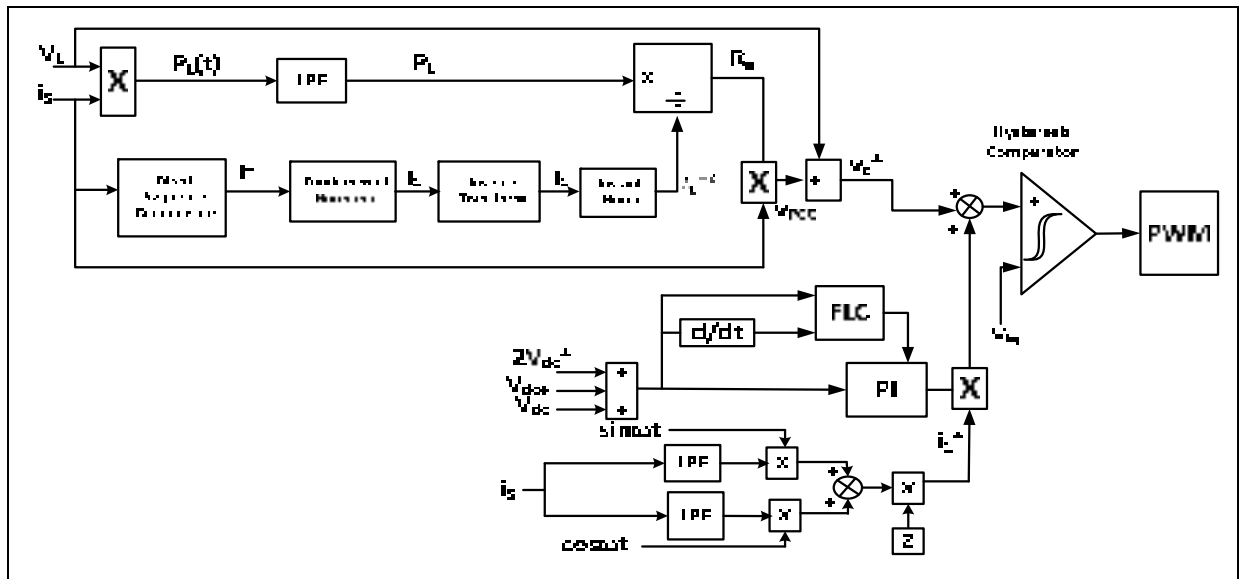


Figure 1.12 Proposed controller of PV-based SeAF

Any system, to be viable, has to offer its users a reliable and cost-effective sinusoidal balanced voltage. Hence, the compensation must be premised on a suitable reference load. This includes, for instance, a resistive load which is balanced and has linear features. As well, the supply voltage and source currents should be in-phase, as this would give the system a unity power factor (Vijayakumar, 2014).

The objective here is to obtain ideal behavior from the PCC though the load and equipment used for the compensation. The controller input signal current and voltage vectors are calculated from the source side and load, respectively. The voltage and current vectors would thus be multiplied to gain instant power, while load active power would be gained from a low pass filter (LPF). In the proposed control scheme, the purpose of the AFLC is to modify the PI controller parameters in order to decrease in-built error characteristics which might occur between the reference and system responses. Hence, the primary objective of this structure is to simplify the control scheme without resorting to mathematical modeling, but all the while maintaining optimal dynamic performance. In this approach, the fuzzy sets were defined for both the input and output variables.

1.5.6 Enhancing Power Quality Through the Use of Hybrid Series Active Power Compensator

Alireza (2016) introduced a novel THSeAF configuration with a sliding mode controller which was proposed and tested to overcome power quality issues of a voltage fed type of nonlinear load. In Figure 1.13 the theoretical modeling has been realized and simulated for further developments. A second-order SMC is developed and adapted for practical real-time implementations. A notch harmonic detection is implemented and tested to extract harmonic components of a polluted signal. It has been demonstrated that the proposed configuration along with the control approach is able to feature reactive power exchange with the utility as well. With regard to the control approach and taking advantage of the proposed robust structure, a harmonic-free voltage is delivered across the residential terminals (Javadi, 2016). The whole system is implemented on a real-time simulator to ensure feasibility of the developed controller. It is worthy to mention that this topology does not make use of a bulky transformer, which is mandatory for series active/hybrid filters topologies; it has a natural feature of limiting short-circuit current during faulty condition. It also replaces the function of UPS/UPQC devices with much less reactive and semiconductor components.

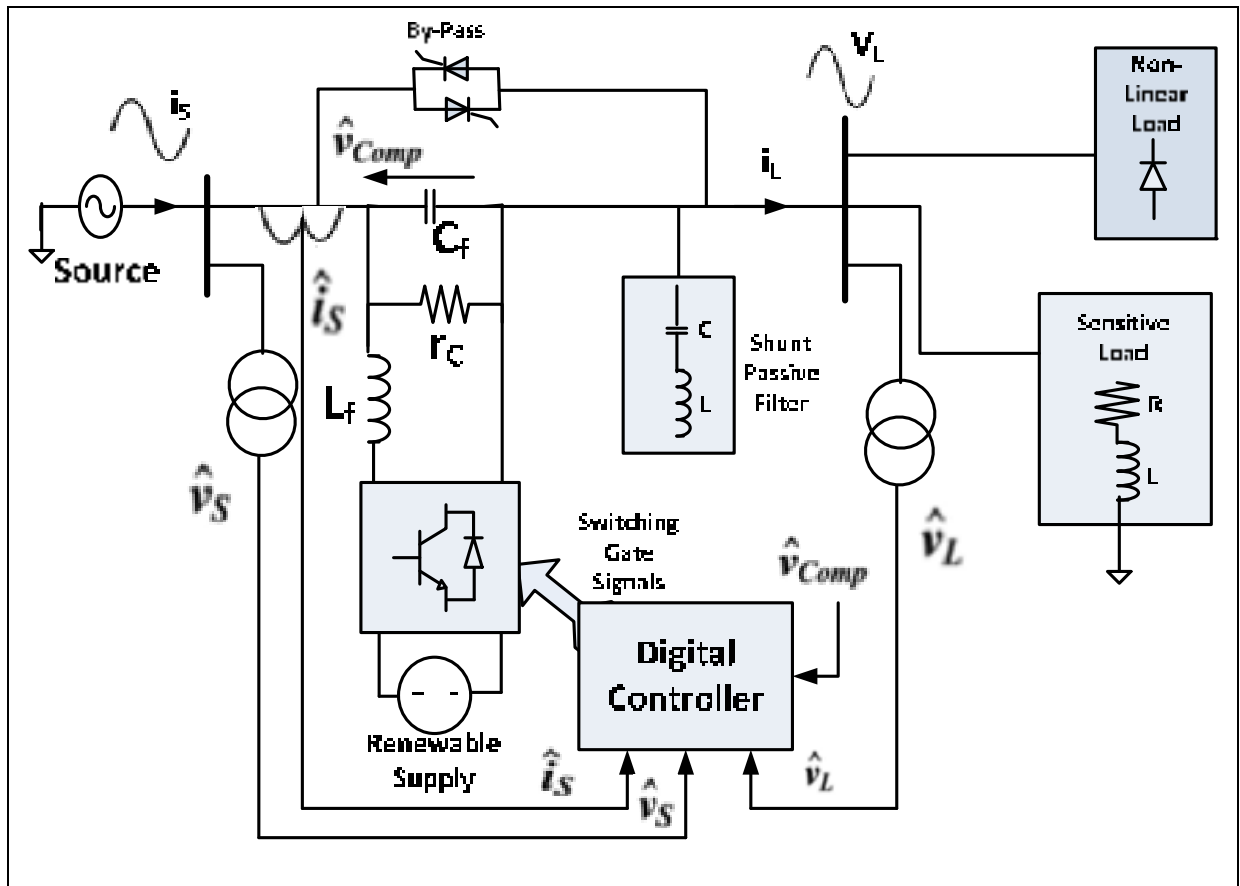


Figure 1.13 THSeAF connected to the single-phase system

The sliding mode control has been proposed in this case, the controller's outer loop is composed of two parallel sections based on a notch filter harmonics extraction technique. The first part is dedicated to compensate for load's voltage regulation and added to a second part, which compensates for source current harmonics. The controller demonstrated in Figure 1.14 restores a stable voltage at the load PCC terminals, while compensating for reactive power and current harmonics. In the source current regulation block, the harmonics and reactive components remain behind after the fundamental (along with its phase degree) are extracted by the notch filter. Hence, the control gain, G , which indicates source impedance in the current harmonics, should be sufficient for ridding the grid of the current harmonics which entered via nonlinear loads. To obtain more exact compensation for the current harmonics, source/load voltage harmonics in the algorithm can also be taken into consideration. Both the source current and the source/load voltages serve as input signals for the system. To determine the

reference angular frequency, a single-phase discrete phase-locked loop (PLL) was employed, synchronized with the source utility voltage (ω_S). Furthermore, the v_{Comp} has a core feature that is synched to the source voltage as a means to offset the reactive power. In this configuration, the gain, G , indicates harmonic convert resistance that is offsetting the currents at relative voltages, while v_{Comp} indicates the generated reference voltage that is needed for removing source currents out of the harmonics (Javadi, 2016).

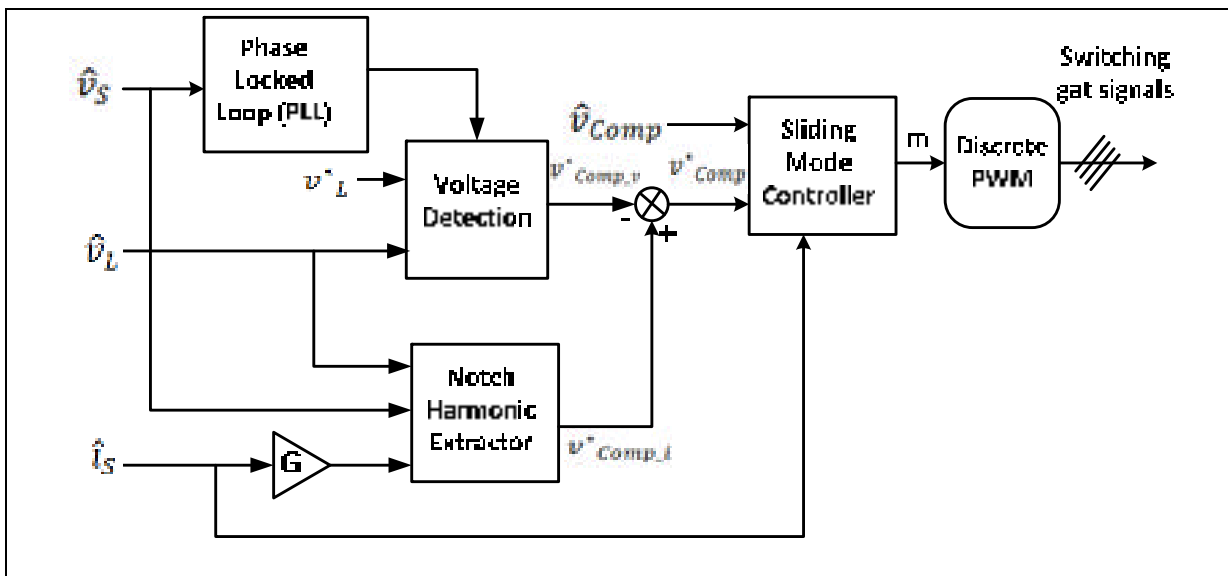


Figure 1.14 Control scheme of Hybrid Series Active Power Compensator

1.5.7 Enhanced Strategy to Offset Unbalanced Loads in HSAFs

As shown in Figure 1.15, Alireza (2015) presented an enhanced strategy for controlling HSAFs (hybrid series active power filters) featuring unbalanced nonlinear 3-phase 3-wire loadings. The researcher proposed an algorithm which used the instantaneous power theory as a means for removing harmonic components out of the supply current. The approach could also be applied in unbalanced loadings situations that have been contaminated by negative sequence components. A control strategy that relies on the sequence extraction algorithm was presented and tested by simulations, showing enhanced outcomes in harmonics reduction, particularly in unbalances and nonlinear loadings (Javadi, 2015).

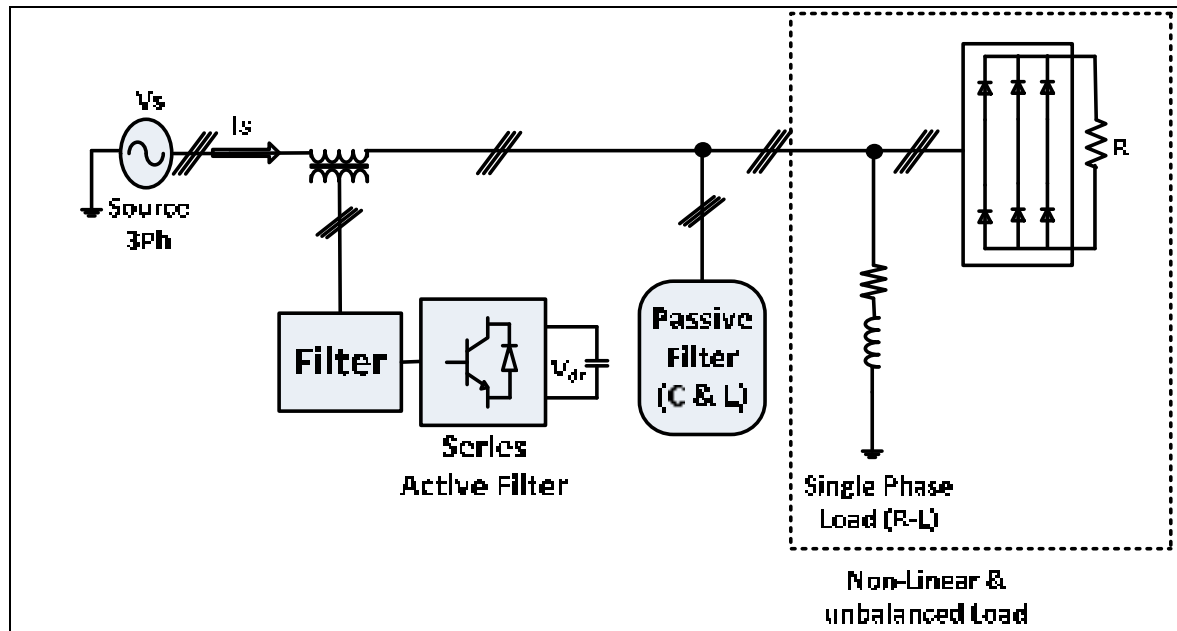


Figure 1.15 Diagram for simulation

Figure 1.16 illustrates a control circuit with a 3-phase load current. As can be seen, the current has been changed to a stationary α - β frame, and the auxiliary positive/negative sequence voltages are created by the PLL circuit. Auxiliary voltages and currents from the α - β frame are then fed into sequence extraction blocks (positive/negative). From this, the α - β frame's output sequence currents (positive/negative) are funneled into an inverse α - β transform, from which are obtained sequence currents (positive/negative) for the 3-phase abc frame. Next, following the extraction of the positive/negative sequence components, the harmonic currents are removed out of supply currents and the individual harmonic currents are funneled into a gain block (using K as the amplification factor) to determine reference voltage v_F (Javadi, 2015). The v_F is then used in every PWM convertor as a gate-control circuit.

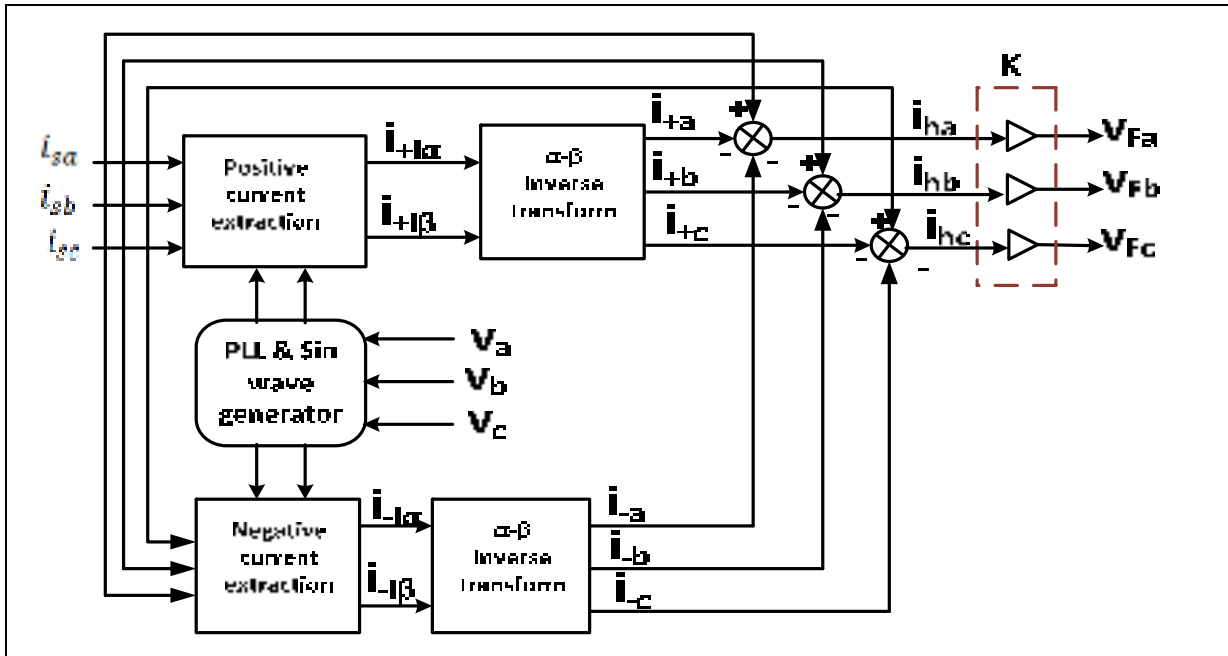


Figure 1.16 Proposed control for series active filter

1.6 Research Objectives

The main objective of this research is to study, improve and test a low-cost 3-phase HSPF for dynamic reactive power and current harmonics compensation in a distribution power system. Furthermore, the 3-phase HSPF topology has been chosen for further investigation because it can provide the lowest initial size, weight, and cost. It could also possibly offer optimal dynamic reactive power compensation capabilities among competing topologies. Another reason is that its coupling LC serves as both a harmonic filter and switching ripple filter. Given the real and potential advantages of this topic, this thesis will therefore focus on HSPF topology in 3-phase distribution power system applications.

1.7 Conclusion

This chapter highlighted some basic characteristics and features of a hybrid series power filter while also providing an overview of harmonic compensation and power quality-related issues. As a technical background, research work centering on recent developments and applications of series hybrid power filter for improving their power quality was presented. As well, various

load types that compromise power quality were analyzed, while the effect of applying traditional passive components to harmonic compensation was looked into. The literature indicates that active filtering is the best approach for overcoming deficiencies in passive filtering, so the present work will pursue this research course.

Additionally, in this chapter, a short review of research dealing with active filtering in active compensation was provided. In order to decrease the costs associated with compensators while still enhancing power quality, issues such as voltage swell and sag, load reactive power, and current and voltage harmonics need to be addressed. The most optimized solution appears to be hybrid series filter configurations. Finally, after presenting a detailed overview of power definitions for multiple types of applications, this chapter discussed the importance of semiconductor switching phenomena and practical modulation techniques for practical implementations.

CHAPTER 2

SLIDING MODE CONTROL WITH SERIES HYBRID POWER FILTER AND REDUCING SIZE WITH DIFFERENT PASSIVE FILTER DESIGN

2.1 Introduction

Following on the proposed system introduced in Chapter 1, this chapter discusses the viability of a series active compensator in a realistic distribution network. Recent research on harmonic pollution indicates that it not only has an impact on equipment in one plant but can also affect equipment in other plants. This alone is sufficient grounds for operators to limit or even restrict the possibility of disturbances by issuing standards for maximum allowable distortions. Two methods can be used to address power quality issues: load conditioning and installation of conditioning systems. Load conditioning ensures that equipment is relatively well protected from power disturbances and that operations can continue even under intense voltage distortion. The other solution to power quality issues installing line conditioning systems, serves as a means to counteract or mitigate power system disturbances (Rudnick, Dixon and Moran, 2003).

Recent developments in power conditioners and active power compensators are resulting in realizable solutions toward power quality improvement. One of the most promising solutions is the series active filter, which is generally less well-known and studied than the shunt configuration. This chapter presents a detailed overview of the series compensator, along with a discussion on its configurations, control strategies, and related involvements in the field. The chapter also looks into the series active hybrid compensator technology investigated by several researchers in their quest to overcome power quality issues. The studies include simulation results and evaluations of the passive components used to compensate for harmonics. Additionally, this chapter introduces a sliding mode control approach aimed at improving the accuracy of series harmonic compensation. A study gauging the system stability is also presented, together with experimental results.

2.2 System Configurations

Although series active compensators are not yet incorporated in power systems, they still have the greatest potential among active compensators for boosting the electric power quality of smart grids. The main problem preventing the application of series compensators are their complexity and high price tag, making them currently the least popular alternative for resolving power quality issues. Despite their inherent problems, series compensators could be repositioned in the future as the technology matures and simplifies.

Series compensators are generally divided into two categories: series active filters (SeAFs) and dynamic voltage restorers (DVRs). Both SeAFs and DVRs are highly complex and are joined to the grid through an isolation transformer. Although offering excellent isolation of the compensating system, the transformer is not only expensive, but brings with it a wide range of performance issues, including the need to be short-circuited if there is a fault in the secondary device, electrical losses, and hysteresis-related phenomena. In acknowledgement of these drawbacks, transformerless DVR technology has been proposed but is still in the development stage. Moreover, they are only able to compensate for voltage issues at the PCC, and as yet are unable to address current perturbations in the power grid.

2.2.1 Modeling of 3-Phase HSPF with Bridge Diode

With the goal of decreasing the power rating, the integration of active and passive power filters is crucial. From Figure 2.1, the SHPF system utilizes a minimal component count, the principle of which is to provide low-impedance higher harmonics generated by the load and high impedance at fundamental frequency. This results in efficient compensation of reactive power and harmonics, thus enhancing and improving the power factor. As the SAF gives high impedance over harmonics compensation, it forces the harmonics to flow during the SPF and thus compensates the reactive power and voltage harmonics. The SAF is controlled via the synchronous reference frame (SFR) method (Hamadi, 2007). In the following section, the topology's performance is evaluated and the simulation results discussed.

In order to gauge its performance level, the proposed SHPF configuration is simulated in a MATLAB-PSB environment. The efficiency of the proposed scheme is studied through

applying a set of loads consisting of current-source types of non-linear loads and voltage-source types of non-linear loads. Furthermore, in order to validate the SHPF performance, the system underwent testing for a variety of operating conditions, including steady-state, transience, voltage sag and swell, and balanced non-sinusoidal utility voltages. The control and results of this model are given in the following figures. They are also discussed in the following sections.

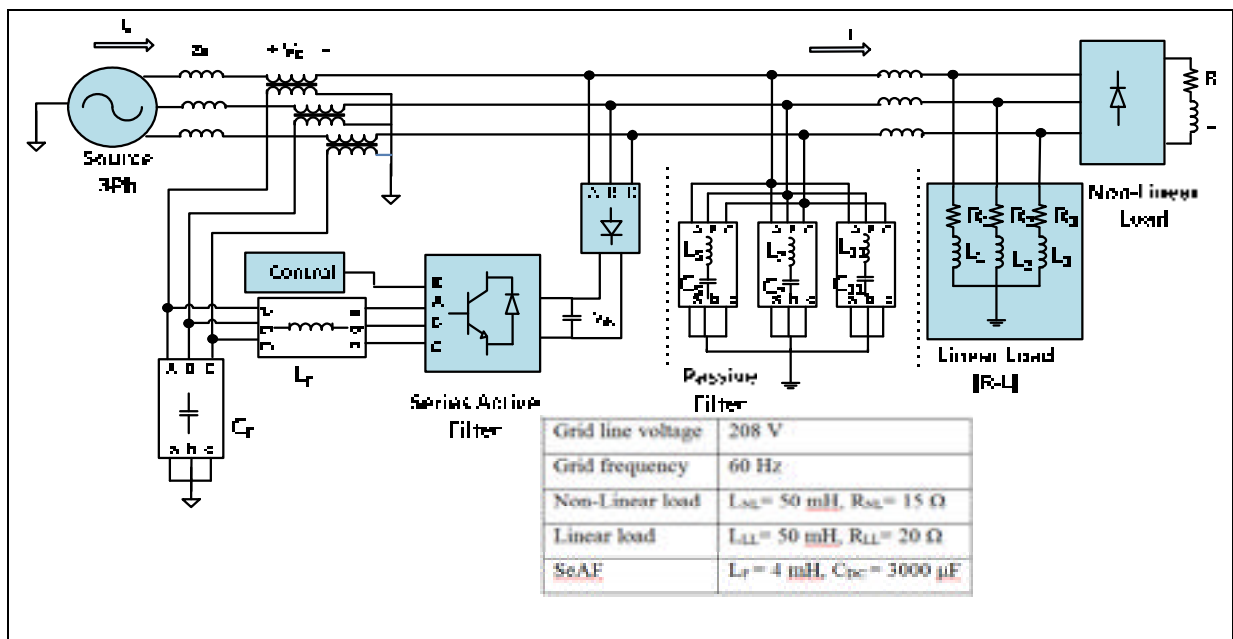


Figure 2.1 Series hybrid active filter with nonlinear load and linear load

2.2.2 Control Strategy of 3-Phase SHAF

A controlled series active filter functions to offset reactive power, source voltage distortion, and load harmonic voltages, and works together with shunt passive filters. These filters provide high resistance, K , against load harmonic currents as well as zero impedance when at fundamental frequencies. As a result, the load harmonic currents are funnelled towards the shunt passive filter. Because these voltages along with the load harmonic voltages (or occasionally source harmonic voltages) represent the same amplitude with opposing phases, each then cancels out the other as a means to enhance the shunt passive filter's filtering capabilities while resolving any dynamic issues. Consequently, the series active filter can be

relatively low in cost, as it represents only a small fraction in overall compensating kVAR energy.

The control method used in the series APF as reference compensating voltages represents a crucial feature, as the load harmonic component needs to be precisely measured in relation to the series APF reference voltage when creating appropriate compensating voltages. In this regard, it was determined that synchronous reference frame (SRF)-based compensators obtain the best outcomes for various load and supply conditions in comparison to more elaborate compensators (e.g., instantaneous reactive power) (Hamadi, 2009). In fact, the control algorithm employed to find voltage references for SeAPF is derived from SRF components.

Here, we use series APF reference compensating voltages as a control method, as follows:

$$V_C^* = Ki_{Sh} - v_{Lh} \quad (2.1)$$

Where i_{Sh} , is the source harmonic current, and v_{Lh} is the load harmonic voltage.

Modeling by using Kirchhoff's law;

$$\begin{cases} i_{ca} = C_f \frac{dv_{ca}}{dt} \\ i_{cb} = C_f \frac{dv_{cb}}{dt} \\ i_{cc} = C_f \frac{dv_{cc}}{dt} \end{cases} \quad (2.2)$$

In dq frame, by using Park transformation the equations of the current are given by:

$$\begin{cases} L_f \frac{di_{fd}}{dt} = -R_f i_{fd} - V_{dc} d_d + V_{cd} + L_f \omega i_{fq} \\ L_f \frac{di_{fq}}{dt} = -R_f i_{fq} - V_{dc} d_q + V_{cq} - L_f \omega i_{fd} \end{cases} \quad (2.3)$$

where i_{fd} and i_{fq} indicate SAPF inductor currents as a synchronous (d-q) frame; v_{cd} and v_{cq} denote voltages on the transformer's main side; d_d , d_q indicate duty cycles for the inverter topology's upper switches; V_{dc} indicates the inverter's DC voltage; and ω is the primary angular frequency (Hamadi, 2009).

In dq frame, the equations of the voltage are given by the following equations:

$$\begin{cases} C_f \frac{dv_{cd}}{dt} = C_f \omega_0 v_{sq} - i_{fd} + i_{sd} \\ C_f \frac{dv_{cq}}{dt} = C_f \omega_0 v_{sd} - i_{fq} + i_{sq} \end{cases} \quad (2.4)$$

Using a PI controller to regulate the voltage of the SAF, it follows that

$$\begin{cases} u_d = k_p v_{cd} + k_i \int v_{cd} dt \\ u_q = k_p v_{cq} + k_i \int v_{cq} dt \end{cases} \quad (2.5)$$

Using a PI controller to estimate the active filter reference current, one gets:

$$\begin{cases} i_{fd}^* = -u_d + C_f \omega_0 v_{sq} + i_{sd} \\ i_{fq}^* = -u_q + C_f \omega_0 v_{sd} + i_{sq} \end{cases} \quad (2.6)$$

Let's define the control law of sliding mode control as follows:

$$\begin{cases} d_d = u_{eq-d} + k_1 \text{sign}(\sigma_d) \\ d_q = u_{eq-q} + k_2 \text{sign}(\sigma_q) \end{cases} \quad (2.7)$$

Along with the following sliding surface:

$$\sigma = \begin{bmatrix} \sigma_d \\ \sigma_q \end{bmatrix} = \begin{bmatrix} k_1(i_{fd} - i_{fd}^*) \\ k_2(i_{fq} - i_{fq}^*) \end{bmatrix} \quad (2.8)$$

Let's make the system as follows:

$$\dot{X} = AX + BU + G \quad (2.9)$$

$$\text{Where, } A = \begin{bmatrix} -\frac{R_f}{L_f} & \omega \\ \omega & -\frac{R_f}{L_f} \end{bmatrix}, \quad B = \begin{bmatrix} -\frac{v_{dc}}{L_f} & 0 \\ 0 & -\frac{v_{dc}}{L_f} \end{bmatrix}, \quad X = \begin{bmatrix} i_{fd} \\ i_{fq} \end{bmatrix}, \quad U = \begin{bmatrix} d_d \\ d_q \end{bmatrix}, \quad G = \begin{bmatrix} \frac{v_{cd}}{L_f} \\ \frac{v_{cq}}{L_f} \\ 0 \end{bmatrix}$$

The control laws are obtained using a derivative of both sliding surface.

As,

$$\dot{\mathbf{x}}^* = \mathbf{A}\mathbf{x} + \mathbf{B}\mathbf{U} + \mathbf{G} \quad (2.10)$$

It follows that:

$$\mathbf{e}^* = k_1(\dot{\mathbf{x}}^* - \dot{\mathbf{x}}^g) = k(\mathbf{A}^*\mathbf{x} + \mathbf{B}^*\mathbf{U} + \mathbf{G} - \dot{\mathbf{x}}^g) = 0 \quad (2.11)$$

When $\mathbf{U} = \mathbf{u}_{eq}$, the equation (2.11) can be rewritten as follows:

$$k(\mathbf{A}^*\mathbf{x} + \mathbf{B}^*\mathbf{u}_{eq} + \mathbf{G} - \dot{\mathbf{x}}^g) = 0$$

and \mathbf{u}_{eq} can be expressed by :

$$\mathbf{u}_{eq} = -(\mathbf{k}^*\mathbf{B})^{-1} * \mathbf{k}(\mathbf{A}^*\mathbf{x} + \mathbf{G} - \dot{\mathbf{x}}^g) \quad (2.12)$$

Derivation of the equivalent control expressions, the development of every term in equation (2.12), gives that:

$$(\mathbf{k}^*\mathbf{B})^{-1} = \begin{bmatrix} -k_1 \frac{v_{dc}}{L_f} & 0 \\ 0 & -k_2 \frac{v_{dc}}{L_f} \end{bmatrix}$$

Then,

$$\mathbf{k}(\mathbf{A}^*\mathbf{x} + \mathbf{G} - \dot{\mathbf{x}}^g) = \begin{bmatrix} -k_1 \frac{R_f}{L_f} x_1 + k_1 \omega x_2 + k_1 \frac{v_{cd}}{L_f} - k_1 \dot{\mathbf{x}}_1^* \\ -k_2 \omega x_1 - k_2 \frac{R_f}{L_f} x_2 - k_2 \dot{\mathbf{x}}_2^* \end{bmatrix}$$

Substituting the above matrices into equation (2.11), the coordinates of the equivalent control are obtained as:

$$\mathbf{u}_{eq-d} = -\frac{L_f}{v_{dc}} \left(\frac{R_f}{L_f} x_1 + \omega x_2 + \frac{v_{cd}}{L_f} - \dot{\mathbf{x}}_1^* \right) \quad (2.13)$$

$$\mathbf{u}_{eq-q} = -\frac{L_f}{v_{dc}} \left(\frac{R_f}{L_f} x_2 + \omega x_1 + \frac{v_{cq}}{L_f} - \dot{\mathbf{x}}_2^* \right) \quad (2.14)$$

In order to prove the stability, one uses a candidate of Lyapunov function chosen such as :

$$\begin{aligned}
\dot{\mathbf{x}} &= k(A^* x + B^*(u_{eq} + \text{sgn}(\sigma)) + G - \dot{\mathbf{x}}) \\
&= k(A^* x + B^* u_{eq} + G - \dot{\mathbf{x}}) + k B \text{sgn}(\sigma) \\
&= k B \text{sgn}(\sigma)
\end{aligned} \tag{2.15}$$

The time derivative gives:

$$\begin{aligned}
\frac{dV}{dt} &= \sigma_d \dot{\mathbf{x}}_d + \sigma_q \dot{\mathbf{x}}_q = \sigma_d k_1 (\dot{\mathbf{x}}_1 - \dot{\mathbf{x}}_1^*) + \sigma_q k_2 (\dot{\mathbf{x}}_2 - \dot{\mathbf{x}}_2^*) \\
&= k_1 \sigma_d \left(-\frac{R_f}{L_f} x_1 + \omega x_2 - \frac{V_{dc}}{L_f} d_d + \frac{V_{cd}}{L_f} - \dot{\mathbf{x}}_1^* \right) \\
&\quad + k_2 \sigma_d \left(\frac{R_f}{L_f} x_2 + \omega x_1 - \frac{V_{dc}}{L_f} d_q + \frac{v_{cq}}{L_f} - \dot{\mathbf{x}}_2^* \right) \\
&= \left(-k_1 \frac{v_{dc}}{L_f} \right) \text{sgn}(\sigma_d) \sigma_d + \left(-k_2 \frac{v_{dc}}{L_f} \right) \text{sgn}(\sigma_q) \sigma_d
\end{aligned} \tag{2.16}$$

By using the inequality $\text{sgn}(\sigma)\sigma \leq \|\sigma\|$, the equation (2.17) can be rearranged in the following form:

$$\left(-k_1 \frac{v_{dc}}{L_f} \right) \text{sgn}(\sigma_d) \sigma_d + \left(-k_2 \frac{v_{dc}}{L_f} \right) \text{sgn}(\sigma_q) \sigma_d \leq -k_1 \frac{v_{dc}}{L_f} \|\sigma_d\| - k_2 \frac{v_{dc}}{L_f} \|\sigma_d\| \tag{2.17}$$

Since the test turn of equation (2.18) should be negative, the stability condition is thus:

$$-k_1 \frac{v_{dc}}{L_f} \|\sigma_d\| - k_2 \frac{v_{dc}}{L_f} \|\sigma_d\| < 0 \tag{2.18}$$

Expanding the above equation, it can be proved that sufficient condition for \dot{V} to be a negative, definite function is will choose $-k_1$ and k_2 are positive.

Figure 2.2 shows the configuration and control scheme for series hybrid filter.

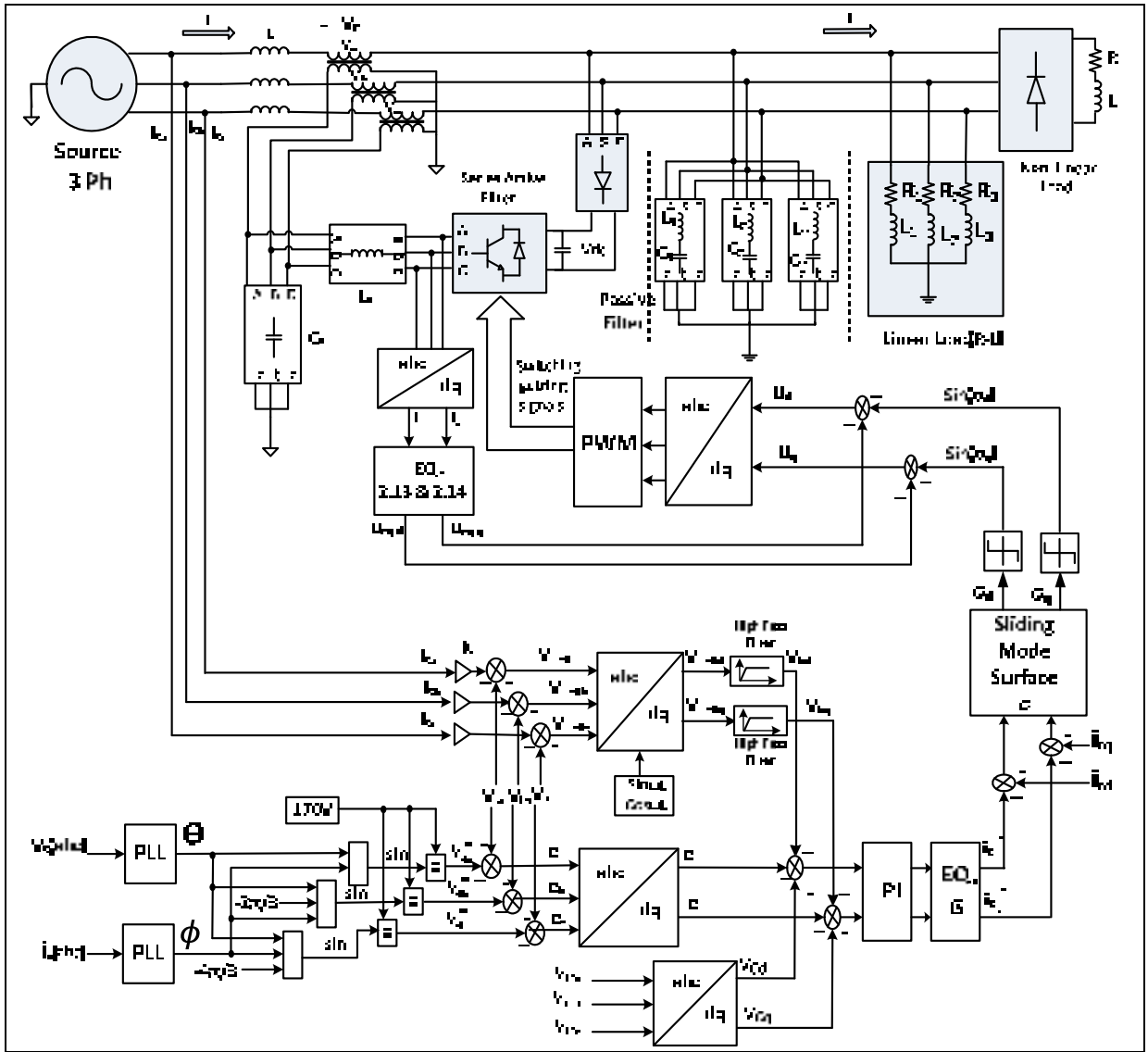


Figure 2.2 Control scheme for the active filter

2.2.3 Passive filter design

A shunt passive filter represents a second-order damped filter that comprises L-C components in parallel combinations. Although the filter forms sizeable impedance in fundamental frequencies, it represents only low impedance for harmonic frequencies. In order to inhibit source-side flow, the filter offers low impedance sinks in current-type harmonic frequencies. Specifically, the impedance of the filter is capacity in higher harmonics and inductive in lower frequencies (i.e., less than fundamental frequency). If employed on its own, the behavior of the

passive filter is strongly impacted by the source inductance. Figure 2.3 (a) and (b) show a parallel passive filter and frequency response, respectively.

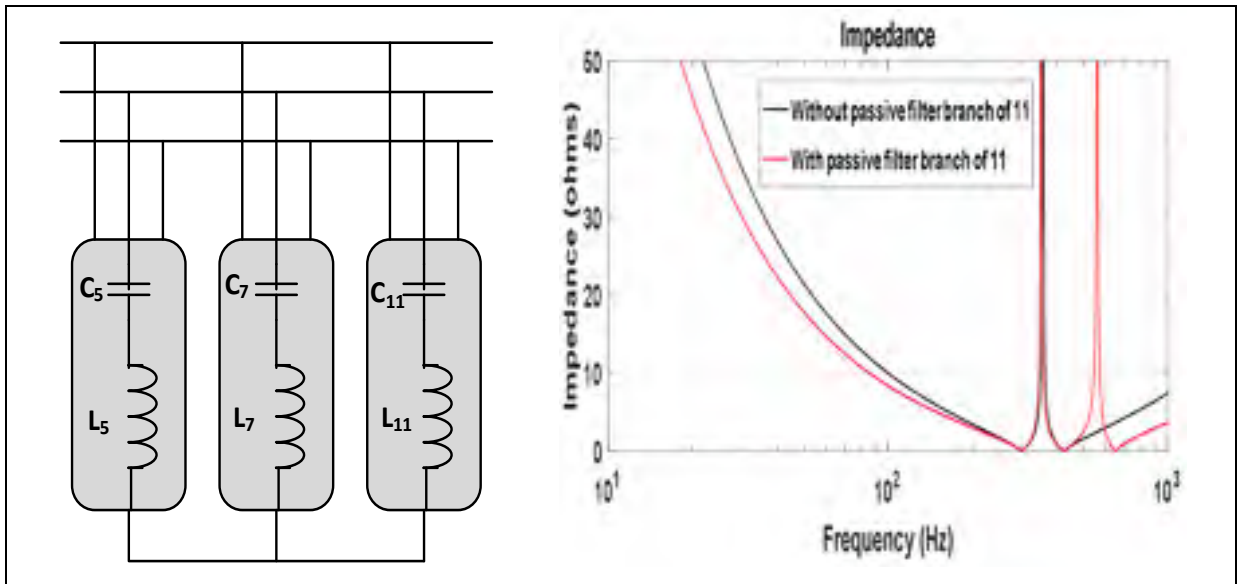


Figure 2.3 a) Equivalent Passive filter, b) Impedance representation versus frequency

In Table 2.1 the parameters of the system configuration during the second method to design passive filter.

Table 2.1 System Configuration parameters

Order harmonic	Value	Capacitor	Inductor
5 th	9.7 mH, 29.08 μ F	7\$/kVAR	50\$/ kVAR
7 th	4.8 mH, 29.62 μ F	7\$/kVAR	45\$/kVAR
11 th and high	1.9 mH, 30 μ F	6\$/kVAR	5\$/kVAR

This part, will present two methods of design passive filter, one of them to minimize the rating of the series active filter, and the other one is minimum cost to minimize the passive filter.

2.3 First method of passive filter design

The filter is tuned to suppress a single frequency and is designed based on three quantities; the harmonic current order that requires to be blocked, the capacitive reactive power that it is going to provide, and its quality factor. The voltage level and the fundamental frequency, which are given by the system, must also be considered during the design process. In summary, the values used to define the input parameters are:

h: tuning point of the filter (harmonic order);

Q_c : reactive power of the filter [Var];

Q: quality factor;

f: system frequency [Hz];

V: system voltage [kV].

The reactive power of the filter is given by the following equation:

$$Q_c = V_c^2 C \omega \left(\frac{h^2}{h^2 - 1} \right) = V_c^2 C \omega \left(1 + \frac{1}{h^2 - 1} \right) = Q_{1c} + \frac{Q_{1c}}{h^2 - 1} \quad (2.19)$$

And as known that;

$$LC(h\omega)^2 = 1 \rightarrow L = \frac{1}{C(h\omega)^2} = \frac{V_c^2}{\omega(h^2 - 1)Q_{1c}}$$

Then the total reactive power generated by the passive filter is then given by:

$$Q_F = \frac{V^2}{\left(LC\omega - \frac{1}{C\omega} \right)} \quad (2.20)$$

In order to minimize the rating of the series active filter, the passive filter (5,7 and 11) should supply the reactive power exchanged by the load with the grid.

$$Q_{F_TOTAL} = Q_{1_5} + Q_{1_7} + Q_{1_11} = Q_L \quad (2.21)$$

$$Q_{1_h} = \frac{Q_L}{3}$$

$$3C_h = \left(\frac{h^2 - 1}{\omega h^2 V_c^2} \right) Q_{1_c} \quad (2.22)$$

$$L_h = \frac{1}{C_h(h\omega)^2} \quad (2.23)$$

It is recommended that the size of the resonant filter be greater than the harmonic current captured. If the resonant filter is less than the harmonic level present in the network, this condition is harmful to the filter when the tolerance threshold is exceeded. The values of the system parameters (in this case) are presented in Table 2.2.

Table 2.2 System parameters with minimum cost of design passive filter

Symbol	Definition	Value
V_S	Line phase-to-neutral voltage	120 V_{rms}
f	System frequency	60 Hz
L_S	Supply equivalent inductance	0.5 mH
L_F	Switching ripple filter inductance	4 mH
C_F	Switching ripple filter capacitance	0.6 μF
R_{NL}, L_{NL}	R-L Non-linear Load	50 mH, 20 Ω
R_{LL}, L_{LL}	R-L Linear Load	150 mH, 20 Ω
R_{LL}, C_{LL}	R-C Linear Load	40 μF , 20 Ω
F_5	Passive filter branch for fifth harmonic	3.25 mH, 87 μF
F_7	Passive filter branch for seventh harmonic	2.4 mH, 55.5 μF
F_{11}	Passive filter branch for eleventh harmonic	2 mH, 30 μF

2.4 Simulation Results

In order to evaluate the performance of the proposed control algorithm, many scenarios are tested such as, sudden variation of different loads as balanced and unbalanced nonlinear load.

The obtained results demonstrate that the proposed control algorithm is able to protect loads from grid-initiated perturbation by monitoring the load voltage and removing compensating components, For this test, configuration shown in Figure 2.2 is implemented using Matlab/SPS by applying a fixed discrete time step of $T_s = 10\mu\text{s}$.

One can see clearly from the obtained simulation results from Figure 2.4 to Figure 2.22 that the power quality is improved and all current harmonics are compensated. Furthermore, the source voltage is perfectly balanced, which leads that the proposed passive filter for this configuration is best solution.

Scenario 1: Current harmonics compensation

The main objective of this test (scenario1) is to demonstrate the capability of the proposed control algorithm to compensate all current harmonics in source side as presented in Figure 2.2. For this test a fixed discrete time equal to $10\mu\text{s}$ is selected.

In figure 2.5, steady state of source current (I_s) and voltage (V_s), load current (I_L) and voltage (V_L), voltage of active filter (V_{AF}), passive filter current (I_{PF}) and DC bus voltage (V_{DC}) are presented.

Passive filters 5, 7 and 11 should supply the reactive power exchanged by the load with the grid as a means to reduce the series active filter's rating. Figure 2.6 shows how the main part in source current harmonics can be immediately compensated when the current's total harmonic distortion (THD) of 1.95% is achieved. The figure also shows that a THD equal to 20.10% renders the current of the load highly polluted. It is observed that the proposed control scheme reacts swiftly, in that the reference is being forced by the PI controller to produce the exact compensating voltage within three cycles. Furthermore, because the DC link voltage is so well-regulated, this assists in drawing a sinusoidal current which is in phase to related source voltages. From this, a unity power factor is obtained.

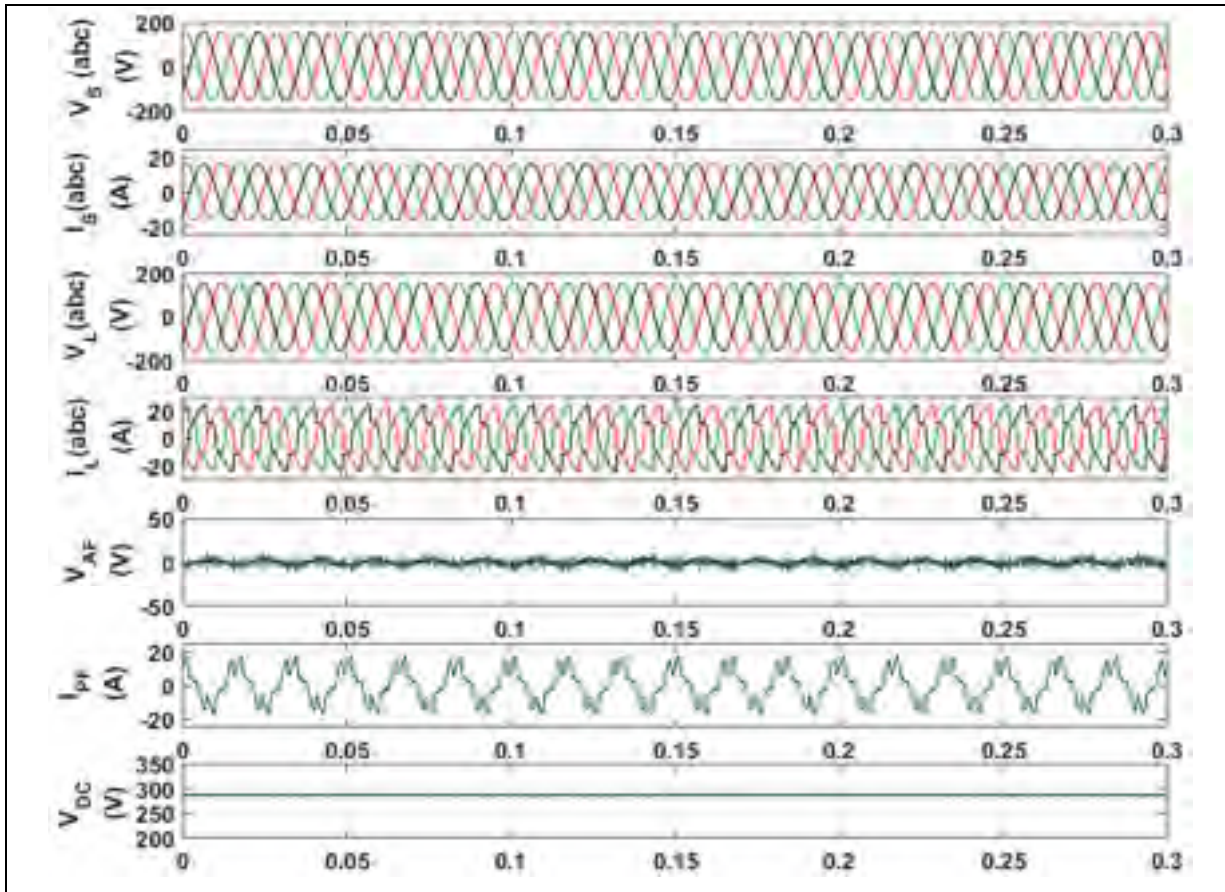


Figure 2.4 Simulation results during steady state

In the voltage pollution phase, compensators keep the suitably regulated and harmonic-free voltage for load terminals. Meanwhile, the proposed compensator adjusts the power factor through compensating current harmonics in the grid. The THD of the load's voltage remains less than 5%, as is required by regulations and standards.

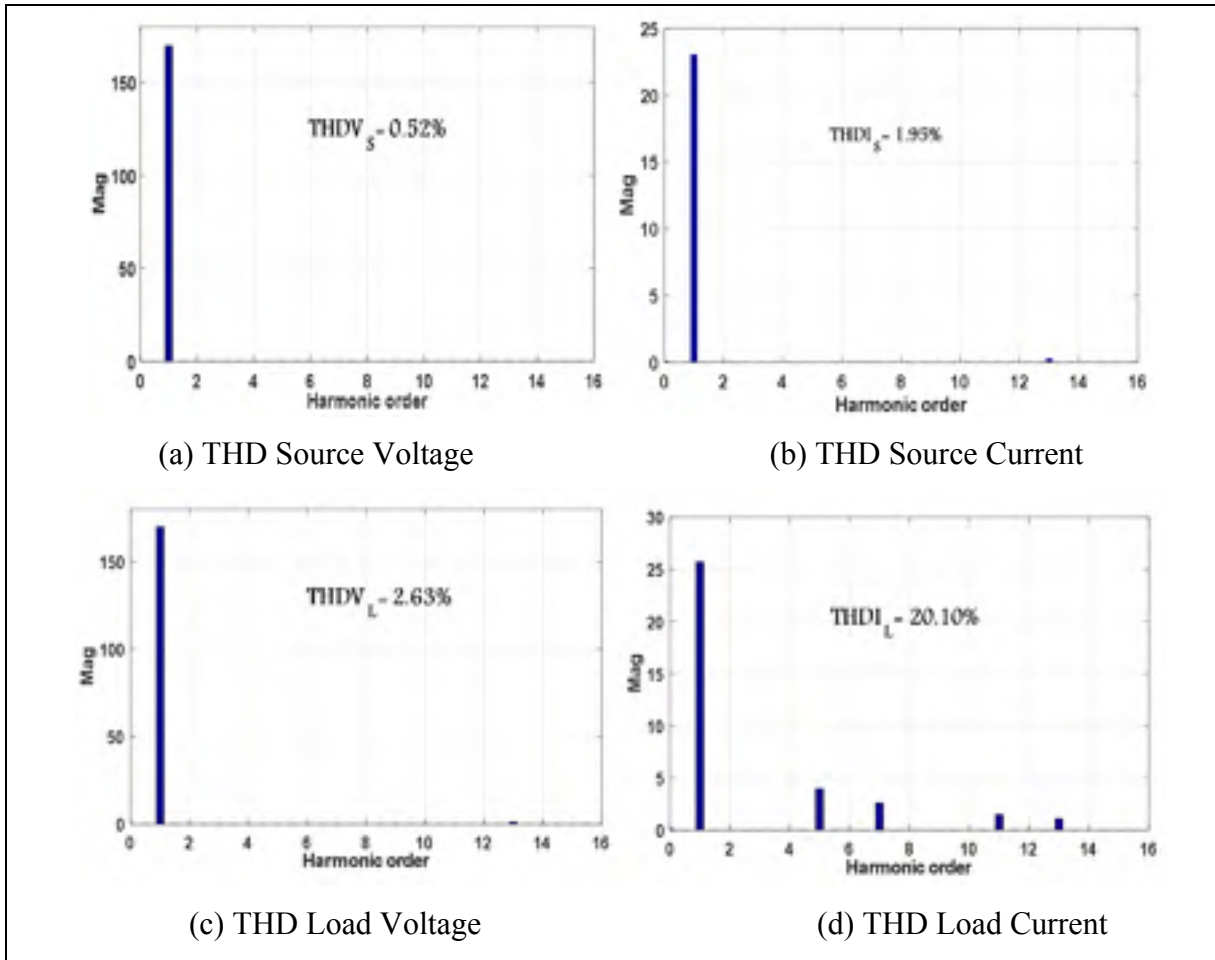


Figure 2.5 THDs during steady state

Figure 2.7 illustrates the load and source's active/reactive powers. As can be seen, because the active part only has been supplied, the compensator can offset any of the load's reactive power that is exiting the source. The figure also shows the measured average 3-phase active power (P) as well as reactive power (Q) related to the 3-phase current and voltage in one or two cycles, causing a lack of interference between the compensator and the active power flow. This position enables it to have control over power flow, either through leading or lagging the current. All the values of power are shown in Table 2.3.

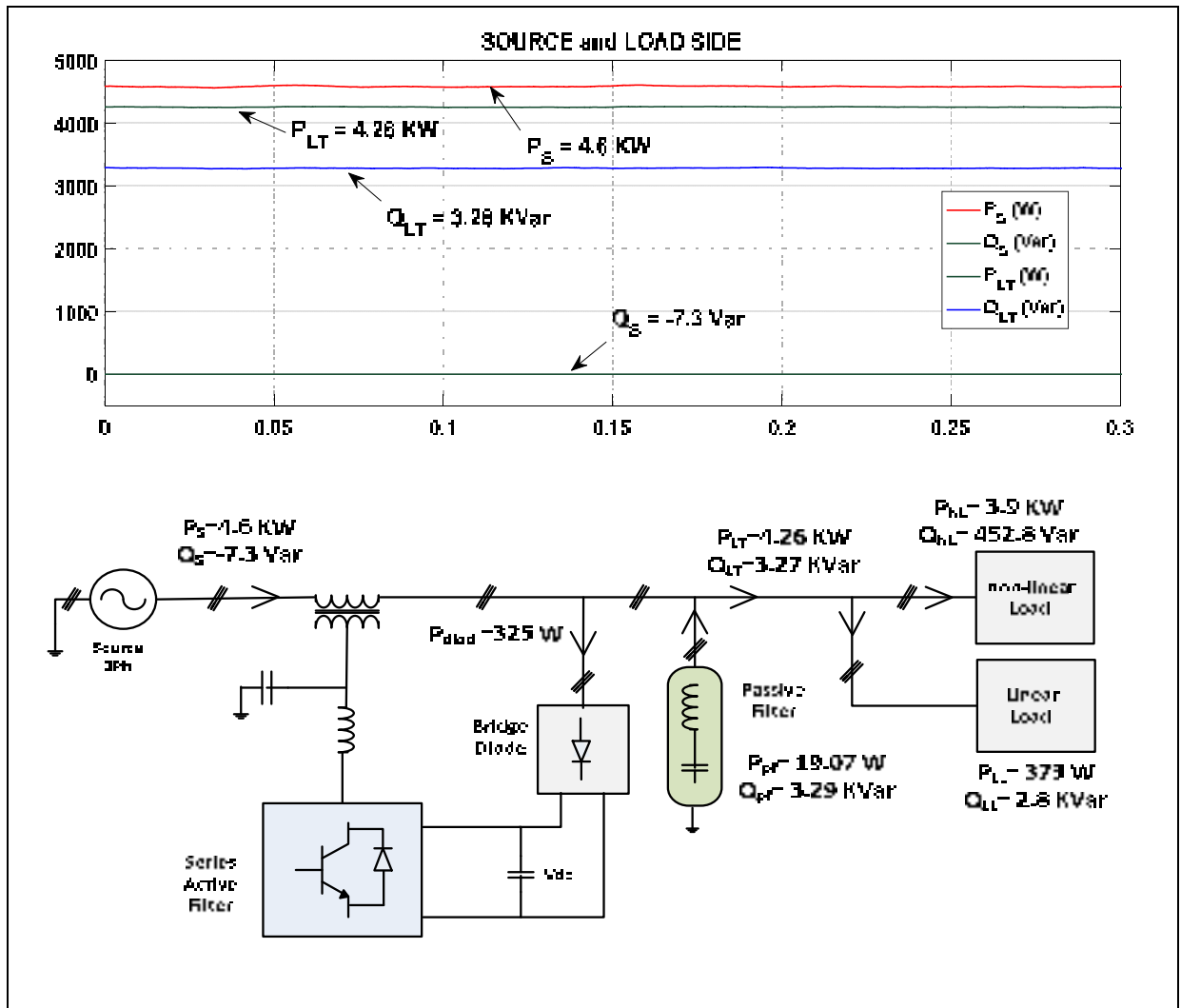


Figure 2.6 Three-phase powers flow with steady state

Table 2.3 Power parameters and THD's during steady state

Parameters	V_S (V rms)	I_S (A rms)	V_L (V rms)	I_L (Arms)
THD (%)	0.52%	1.95%	2.63%	20.10%
Rms	120	23.93	120	25.07
Source power	$P_S = 4.6 \text{ kW}$			
	$Q_S = -7.3 \text{ Var}$			
	$S_S = 4.6 \text{ kVA}$			
Total load power	$P_T = 4.26 \text{ kW}$			
	$Q_T = 3.27 \text{ kVar}$			
	$S_T = 5.38 \text{ kVA}$			
Non-Linear Load Power	$P_{NLL} = 3.9 \text{ kW}$			
	$Q_{NLL} = 452.8 \text{ Var}$			
	$S_{NLL} = 3.92 \text{ kVA}$			
Linear Load Power	$P_{LL} = 373 \text{ W}$			
	$Q_{LL} = 2.8 \text{ kVar}$			
	$S_{LL} = 2.82 \text{ kVA}$			
Apparent power of active filter	4.6 kVA			
Passive Filter	$P_F = 19.07 \text{ W}$			
	$Q_F = 3.29 \text{ kVar}$			
Power of Diode Bridge Losses	$P_{\text{Diode}} = 325 \text{ W}$			

Scenario 2: Reactive power compensation

Figure 2.8 illustrates passive filter performance if the system connects to a linear R-L, R-C load ($R=20\Omega$, $L=40 \text{ mH}$, $C=150\mu\text{F}$). Such a highly inductive load is capable for drawing a load current that forms a leading power factor in regard to supply voltage. Thus, if connected with resistance in series, the inductor satisfies the reactive power needs of the load through the injection of leading quadrature current. As shown in Figure 2.9, there is local compensation by

the passive filter for the loads' reactive power needs. In this way, loads at source present like linear resistive loads, providing the active power needs as a unity power factor. On the other hand, when the capacitor is connected with resistance in series, the loads' reactive power needs are provided through the injection of lagging quadrature currents. As illustrated in Figure 2.9, there is local compensation by the passive filter for the loads' reactive power requirements. This is justified as well by the decrease of source current magnitude when comparing it to the actual load current magnitude.

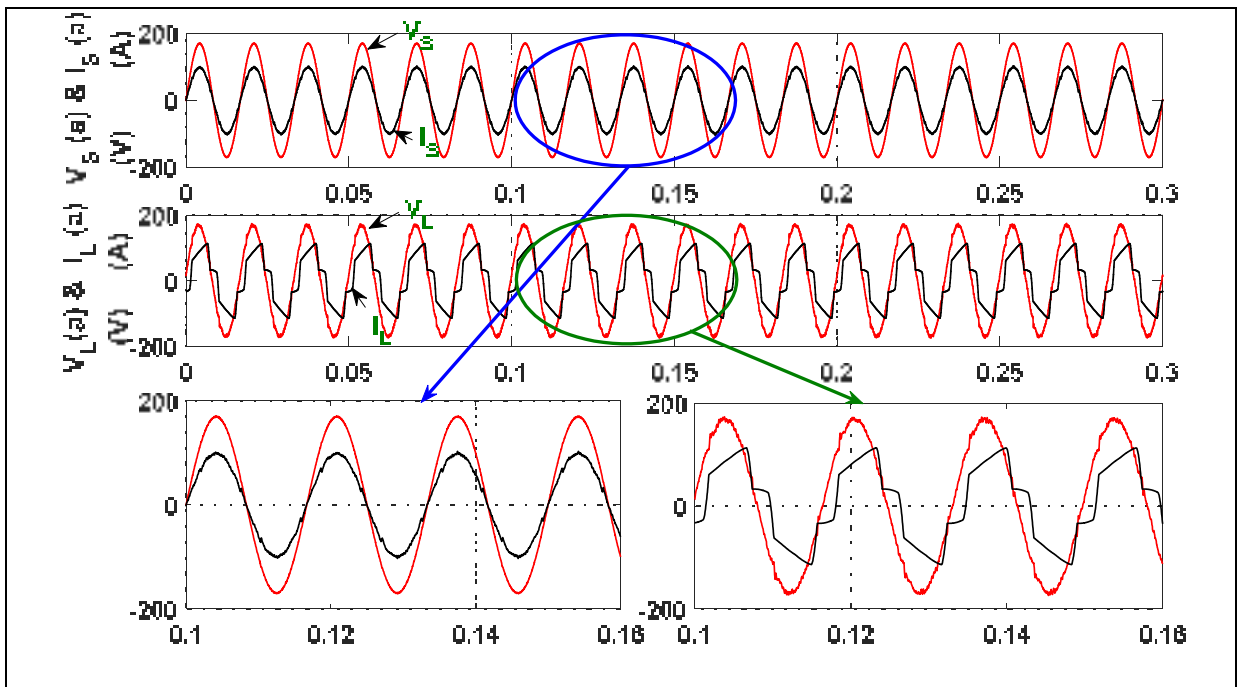


Figure 2.7 Leading voltage

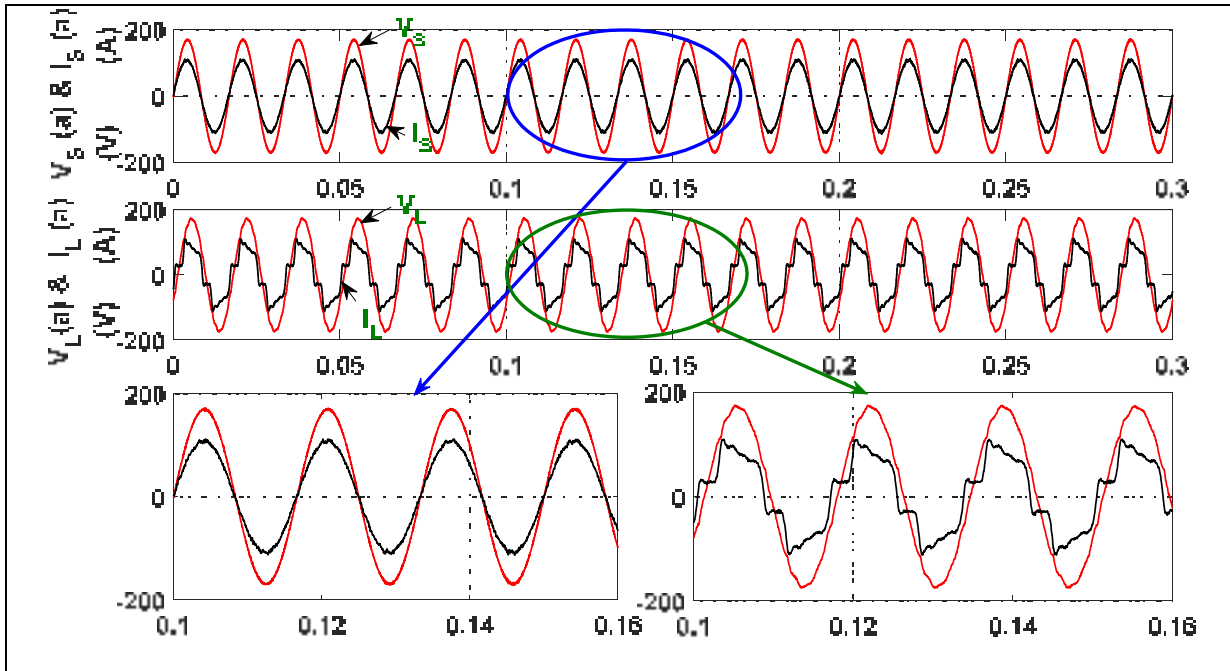


Figure 2.8 Lagging voltage

According to the vector diagrams of Figure 2.10a, the leading compensating voltage has shifted the inductive load's voltage phase angle and the power factor is improved. While, in the diagram of Figure 2.10b a lagging compensation voltage is applied. In this case the load's voltage is still kept constant, but the power factor has been deteriorated as a consequence. For a capacitive load the opposite result are found. As mentioned previously, one can observe that it is impossible to regulate the DC voltage and correcting the PF simultaneously. Both control strategies operate by shifting the V_{Comp} .

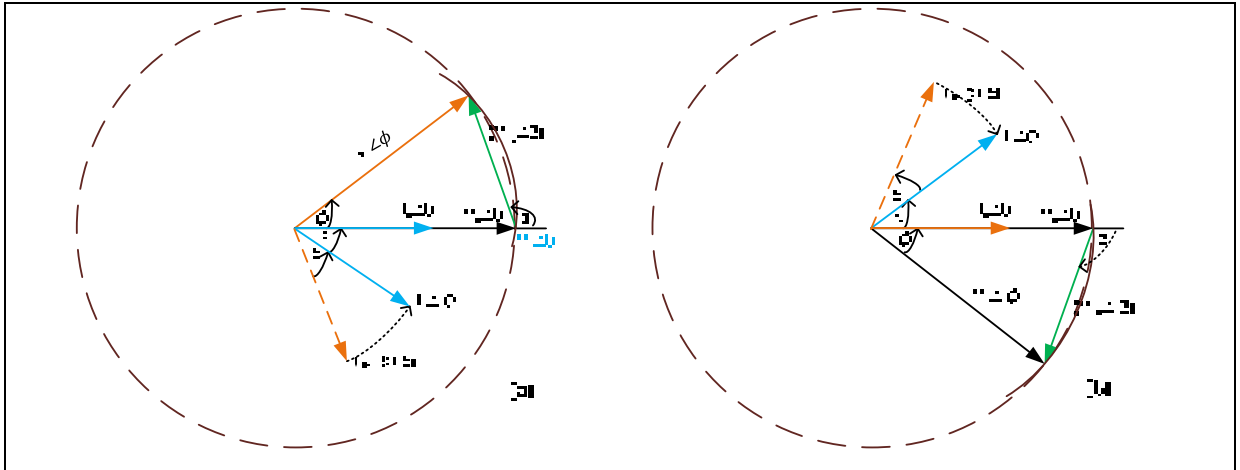


Figure 2.9 Phasor diagram (a) leading voltage (b) lagging voltage

Scenario 3: Load Variation

During the process of power factor adjustment and removal of source current out of the harmonics, the compensator also controls the voltage of the load terminal using the auxiliary source's energy for continuation of the load terminals', even in the case of grid perturbations. Figure 2.11 shows the proposed compensator's behavior in cases of variations of dynamic load where the load is suddenly changed. As can be seen, there is an immediate response from the THSeAF, but the response does not alter the functionality of its operations. Nevertheless, a small change in transient voltage will likely appear, according to the extent of the loads' connections or disengagements. All the values of power are shown in Table 2.4, and the THD spectrums are shown in Figure 2.12.

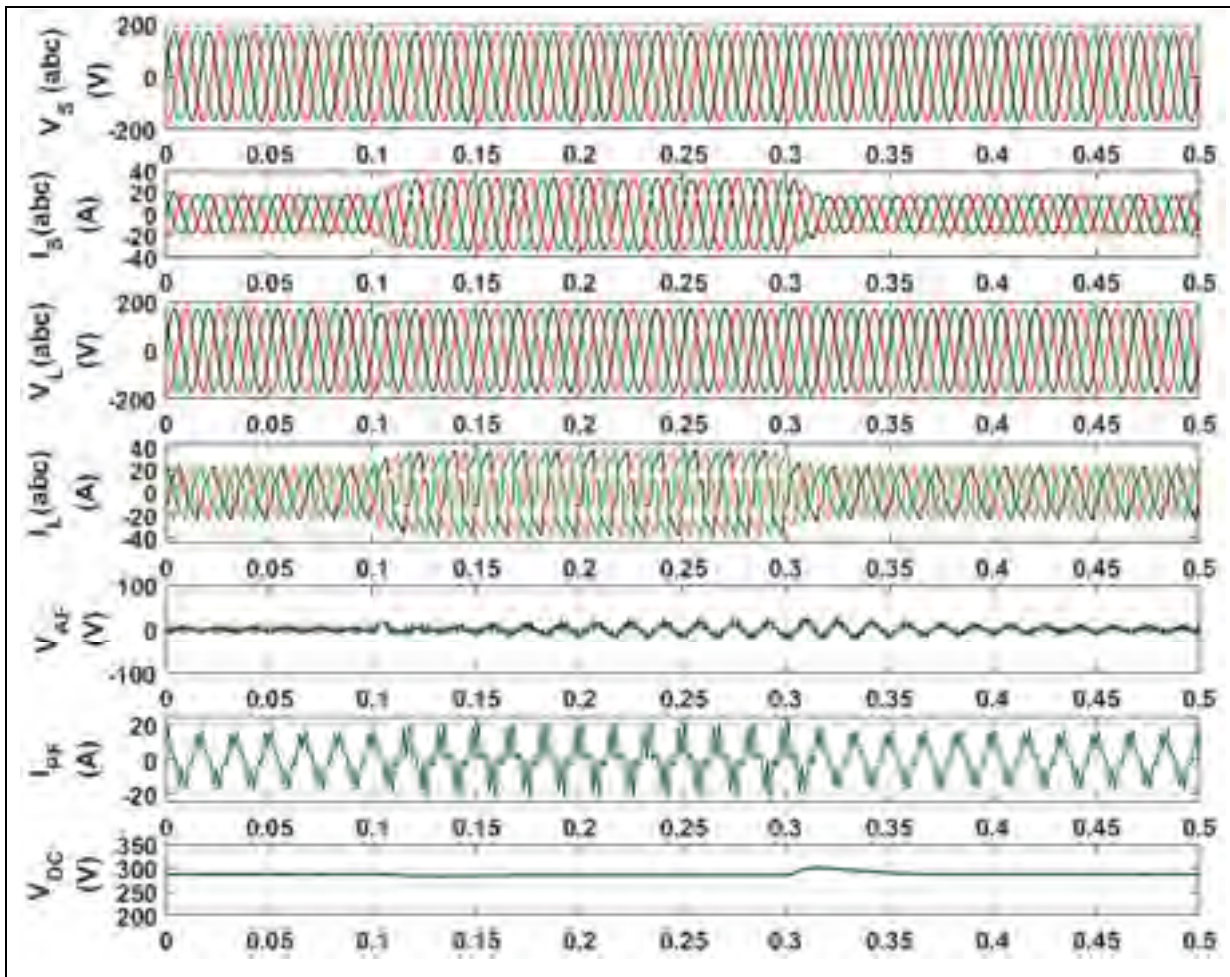


Figure 2.10 Simulation results during load variation

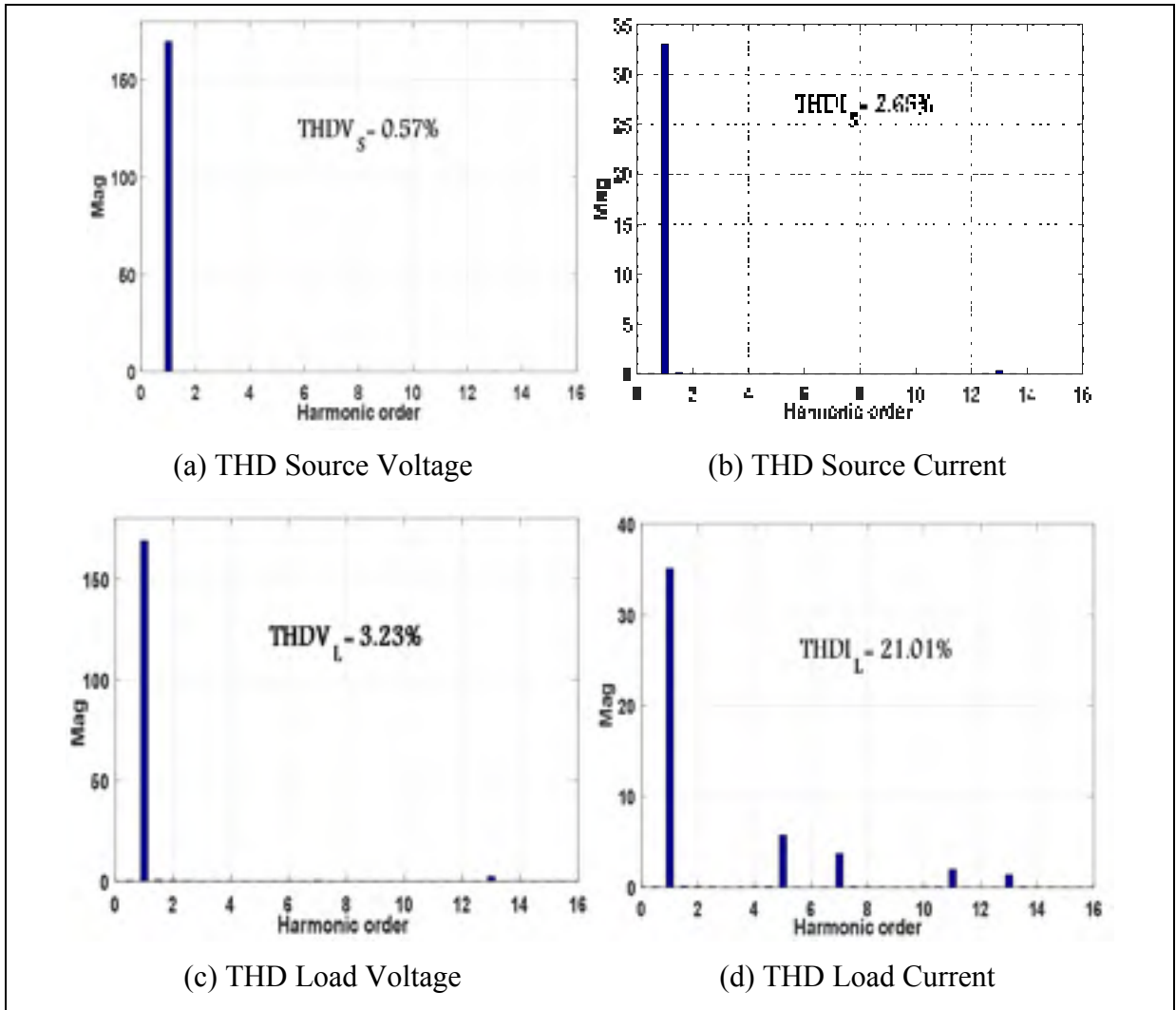


Figure 2.11 Results of the THD during Load Variation.

Table 2.4 Power parameters and THDs during load variation

Parameters	V_S (V rms)	I_S (A rms)	V_L (V rms)	I_L (Arms)
THD (%)	0.57%	2.65%	3.23%	21.01%
Rms	120	23.37	120	24.82
Source power	$P_S = 3.3 \text{ kW}$			
	$Q_S = 0.051 \text{ Var}$			
	$S_S = 3.3 \text{ kVA}$			
Total load Power	$P_T = 2.98 \text{ kW}$			
	$Q_T = 3.1 \text{ kVar}$			
	$S_T = 4.3 \text{ kVA}$			
Non Linear Load Power	$P_{N-L} = 2.61 \text{ kW}$			
	$Q_{N-L} = 248.9 \text{ Var}$			
	$S_{N-L} = 2.62 \text{ kVA}$			
Linear Load Power	$P_{L-L} = 248.9 \text{ Var}$			
	$Q_{N-L} = 2.83 \text{ kVar}$			
	$S_{N-L} = 2.85 \text{ kVA}$			
Apparent power of active filter	3.28 kVA			
Passive Filter	$P_F = 18.31 \text{ W}$			
	$Q_F = 3.26 \text{ kVar}$			
Power of Diode Bridge Losses	$P_{\text{Diode}} = 290 \text{ W}$			

Scenario 4: Sag and Swell voltage compensation

The simulation results for SHPF approach implemented using fixed power angle based concept are given in Figure 2.13. Before time 0.2s, the system is working under steady state condition to compensate the load reactive power using passive filter. At time 0.2s, a swell of 30% is imposed on the system for a time period going from 0.2sec to 0.4sec. Between the time period going from $t=0.4\text{sec}$ to $t=0.6\text{sec}$, the system is again in steady-state. A sag of 30% is introduced

on the system (sag last till time $t=0.6\text{sec}$). The active and reactive power flow through the source and load are given in Figure 2.14, and all the values of the power are shown in Table 2.5.

As depicted in Figure 2.13, in instances of voltage swells and/or sags, the series hybrid active filter can be a better alternative, with the 3-phase source voltage amplitude being decreased across two or three cycles. As can be seen, the necessary active power for continuation of the load voltage amplitude's constant value is absorbed by the compensator.

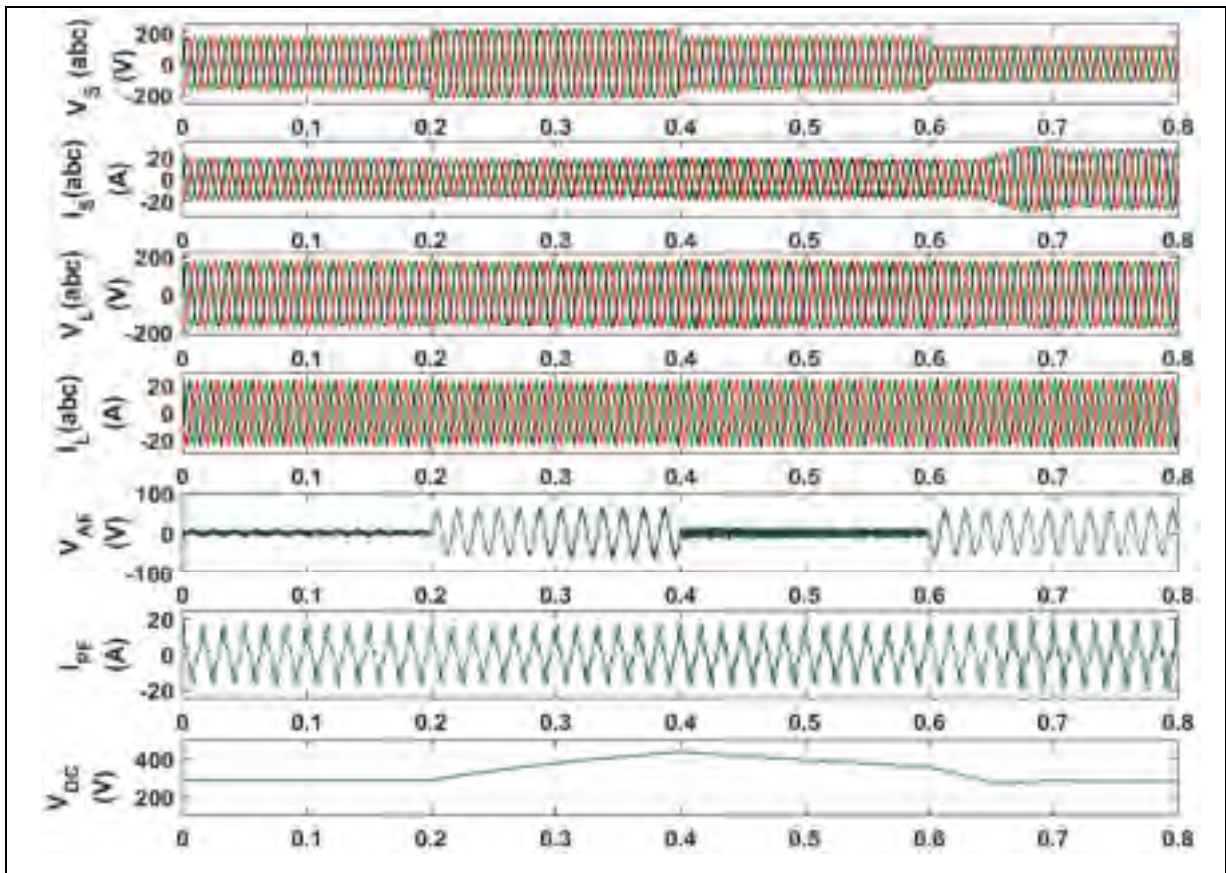


Figure 2.12 System behavior during sag and swell voltage compensation

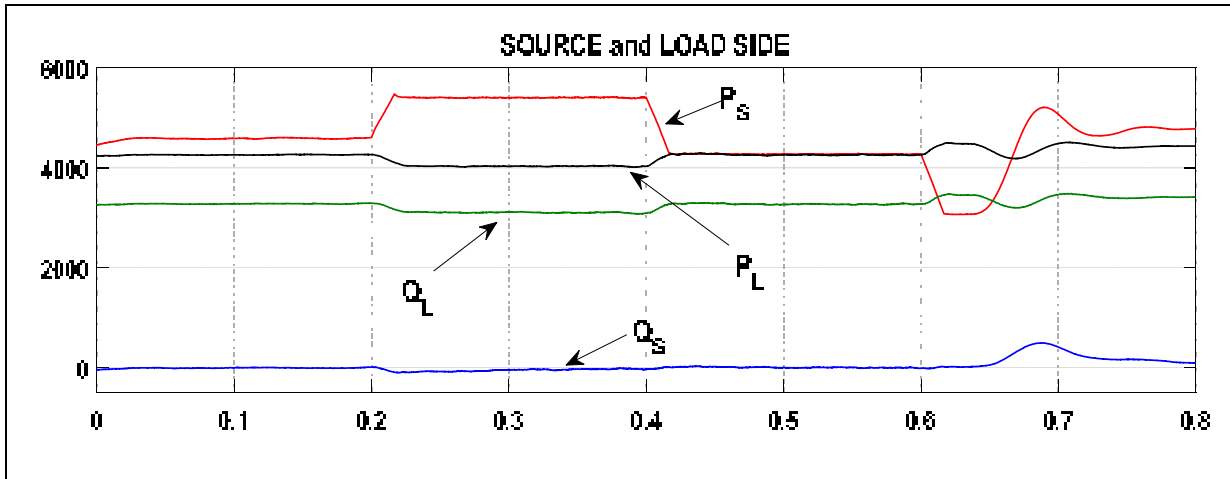


Figure 2.13 Power flow with sag and swell voltage

Table 2.5 Power parameters used during sag and swell voltage compensation

Parameters	Values
Source power	$P_s = 4.77 \text{ kW}$
	$Q_s = 92.1 \text{ Var}$
	$S_s = 4.77 \text{ kVA}$
Total load Power	$P_T = 4.43 \text{ kW}$
	$Q_T = 3.41 \text{ kVar}$
	$S_T = 5.59 \text{ kVA}$
Non Linear Load Power	$P_{N-L} = 4.04 \text{ kW}$
	$Q_{N-L} = 470 \text{ Var}$
	$S_{N-L} = 4.06 \text{ kVA}$
Linear Load Power	$P_{L-L} = 389.9 \text{ kW}$
	$Q_{N-L} = 2.94 \text{ kVar}$
	$S_{N-L} = 2.96 \text{ kVA}$
Apparent power of active filter	6.9 kVA
Passive Filter	$P_F = 13.83 \text{ W}$
	$Q_F = 3.39 \text{ kVar}$

Scenario 5: Unbalanced voltage

Figure 2.15 depicts system response in cases of unbalance in the source voltage. As can be seen, the load terminal voltage is controlled by the filter. Hence, the active power compensator can adjust to changes occurring at the load's consumption but still stop the movement of current harmonics to grid-side. As well, the compensator enables the continuation across the loads' point of common coupling of voltages that are regulated and sinusoidal. Figure 2.16 illustrates system response in cases of unbalanced voltage, where the compensator follows this variation while performing the power quality improvement.

The results shown the grid's line-to-line voltage subjected to a tough unbalance. The line voltages show distortion and unbalance that should be compensated by the passive filter to ensure a balanced and sinusoidal waveform at the load side. As described in Table 2.6, the supply voltage is unbalanced and contains, zero and negative sequence components.

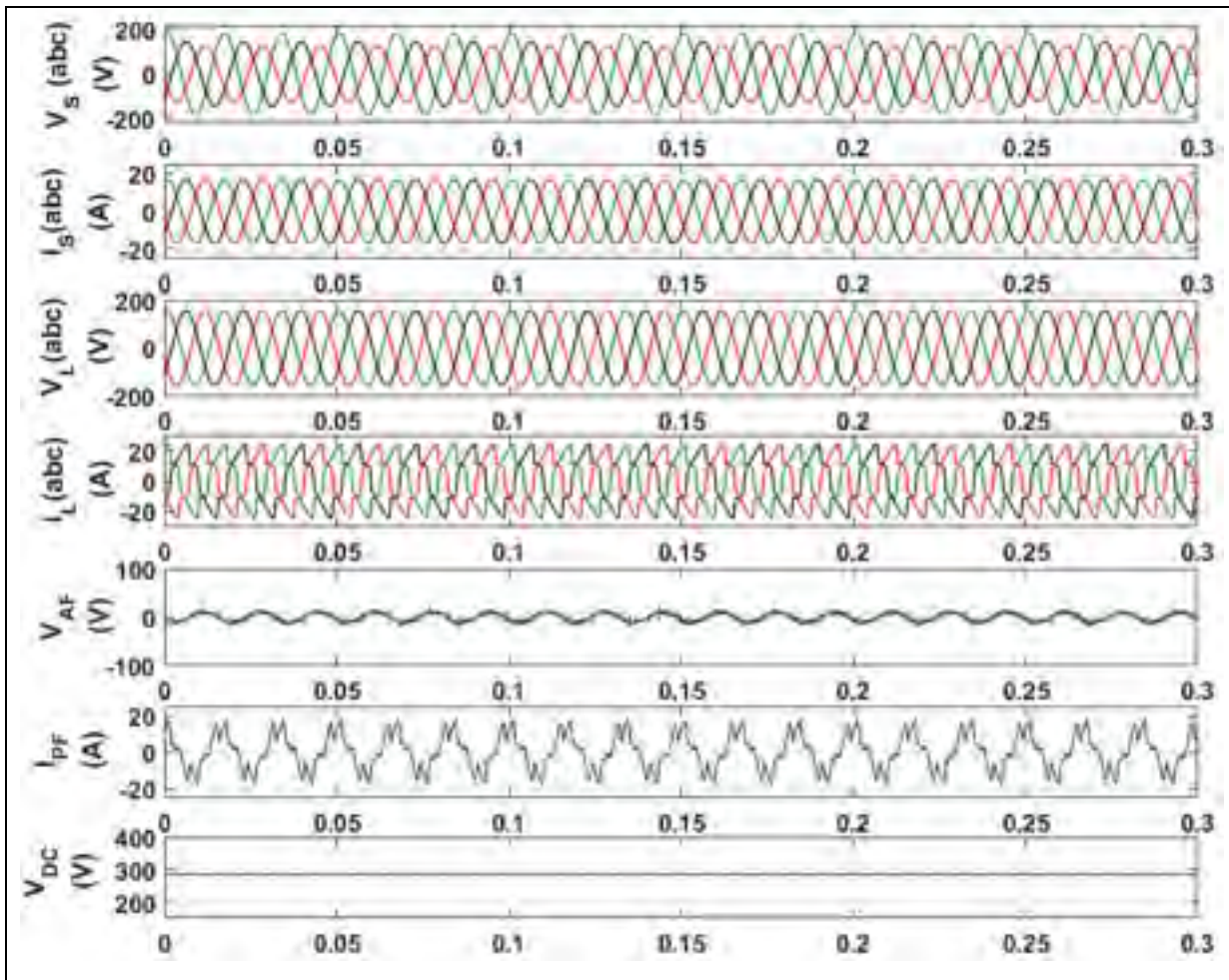


Figure 2.14 System behavior during unbalanced compensation

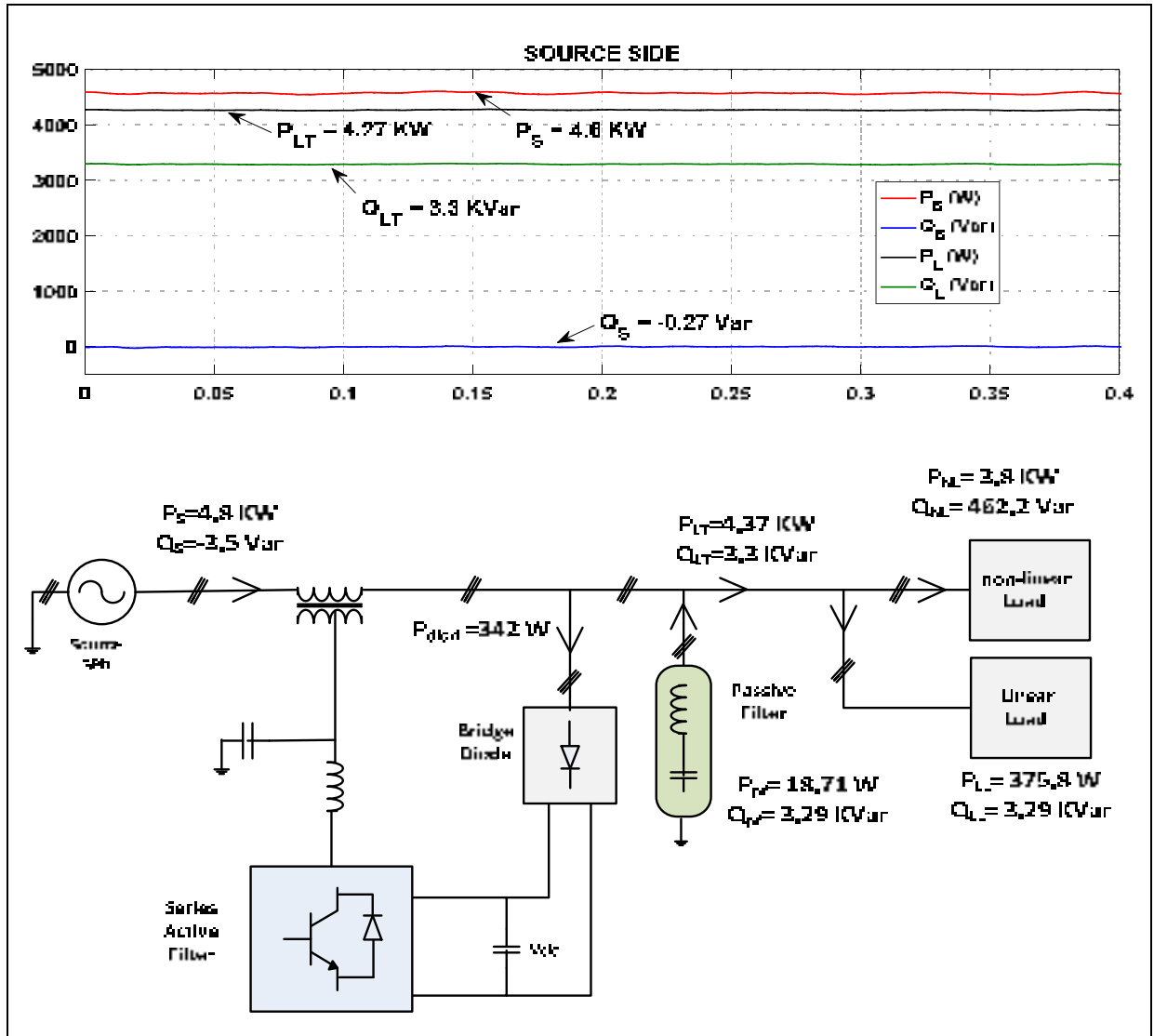


Figure 2.15 Power flow with unbalanced voltage

Table 2.6 Power parameters and THDs during unbalanced voltage

Parameters	VS (V rms)	IS (A rms)	VL (V rms)	IL (Arms)
THD (%)	0.61%	4.55%	2.88%	18.81%
Rms	160, 140, 200	18.48	120	21.18
Source power	$P_S = 4.8 \text{ kW}$			
	$Q_S = -3.5 \text{ Var}$			
	$S_S = 4.8 \text{ kVA}$			
Total load Power	$P_T = 4.37 \text{ kW}$			
	$Q_T = 3.3 \text{ kVar}$			
	$S_T = 4.47 \text{ kVA}$			
Non Linear Load Power	$P_{N-L} = 3.8 \text{ kW}$			
	$Q_{N-L} = 462.2 \text{ Var}$			
	$S_{N-L} = 3.92 \text{ kVA}$			
Linear Load Power	$P_{L-L} = 375.8 \text{ W}$			
	$Q_{N-L} = 2.83 \text{ kVar}$			
	$S_{N-L} = 2.85 \text{ kVA}$			
Apparent power of active filter	4.8 kVA			
Passive Filter	$P_F = 18.71 \text{ W}$			
	$Q_F = 3.29 \text{ kVar}$			
Power of Bridge Diode	$P_{\text{Diode}} = 342 \text{ W}$			

Remark:

When simulated the system in MATLAB during current harmonic compensation, we noted that if the capacitor of the passive filter decreased or increased, the power of bridge diode changed too. One can see in Figure 2.17 (a), that the system works with the value of the passive filter used in scenario (1). In Figure 2.17 (b), the capacitor of the passive filter increased, the

power of bridge diode received in source side decreased, where is the load side still received the same power due to the increase of the power of the passive filter.

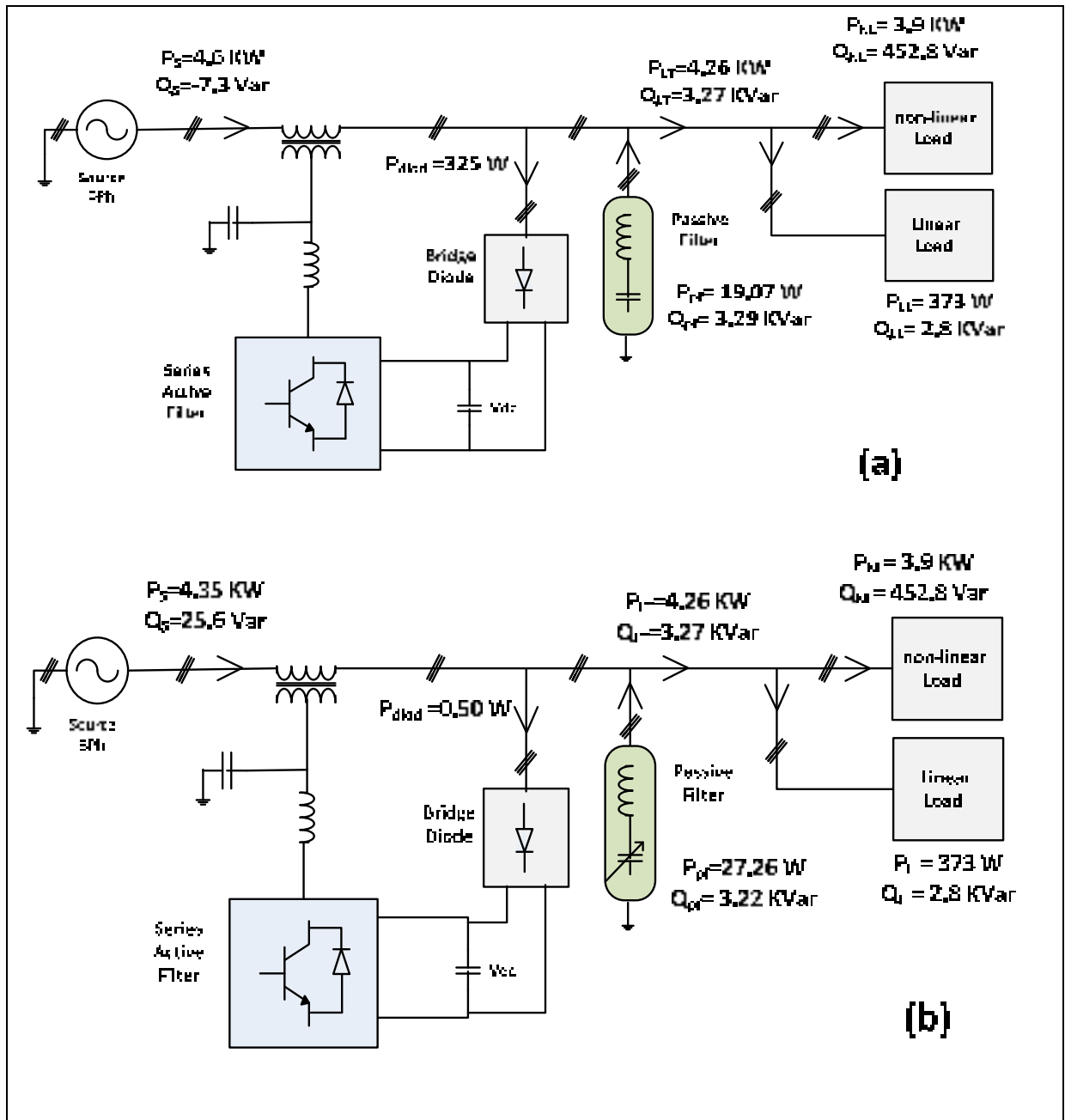


Figure 2.16 Power flow with passive filter variation

2.4.1.1 Second method to design passive filter by minimum cost of resonant filter

The cost of a resonant filter for a given harmonic rank varies with the power (var) of the filter and is minimal for a particular power (Sanae Rechka, 2002):

$$k = E g Q + M g Q^{-1} \quad (2.24)$$

where:

k : Cost (\$); Q : Filter reactive power (var); E, M : Constantes (\$/var)

E, M have the same unit, for the fundamental reactive power $h=1$, one gets:

$$V_c^2 I_{hF}^2 = V_c^2 I_F^2 = Q$$

The capacitance of the filter is subject to currents and voltages related to the fundamental frequency of the array (AC) and the harmonic frequency (of rank h) over which the filter is tuned.

The power capacity is the sum of the fundamental reactive power and the harmonic reactive power for which the filter is designed. The other harmonics in the resonant filter are negligible (Sanae Rechka, 2002).

The power capacity can be expressed as follows:

$$Q_c = V_c^2 \omega C + \frac{I_{hF}^2}{h \omega C} = Q + \frac{V_c^2 I_{hF}^2}{h g Q} \quad (2.25)$$

where:

C : is the capacitance of the filter (F);

$\omega = 2\pi f$; f is the fundamental frequency of the network (rad/s);

V_c : is the fundamental voltage across the capacitor (V);

h : is the rank of the harmonics;

I_{hF} : is the harmonic current of rank h (A);

Q : is the capacitance reactive power at the fundamental frequency (var)

It is also assumed that the inductance similarly depends on the sum of the fundamental and harmonic reactive powers:

$$Q_L = \frac{Q}{h^2} + \frac{V_C^2 I_{hF}^2}{hgQ} \quad (2.26)$$

By neglecting the cost of the resistance, the total cost of the filter is given by:

$$k = Q_C gU_C + Q_L gU_L \quad (2.27)$$

where U_C and U_L are the unit costs of capacitance and inductance respectively.

The substitution of the Q_C and Q_L values in (2.30) gives:

$$k = Qg \left(U_C + \frac{U_L}{h^2} \right) + \frac{V_C^2 I_{hF}^2}{hgQ} g(U_C + U_L) \quad (2.28)$$

$$k = E gQ + M gQ^{-1} \quad (2.29)$$

The relative power at a minimum cost is found by calculating $\frac{dk}{dQ} = 0$

$$\frac{dk}{dQ} = E - M gQ^{-2} = 0$$

$$Q_{\min} = \sqrt{\frac{M}{E}} \text{ and } K_{\min} = 2\sqrt{ME}$$

The following variables are introduced;

$$\omega_n = \frac{1}{\sqrt{LC}}; \quad f' = \frac{\omega}{\omega_n}; \quad X_n = \sqrt{\frac{L}{C}}$$

Design algorithm for resonant filters and damped filter:

Consider the simplified diagram of an electrical network with passive filters, shown in Figure 2.17, on the basis of which the design steps of a passive filter will be described.

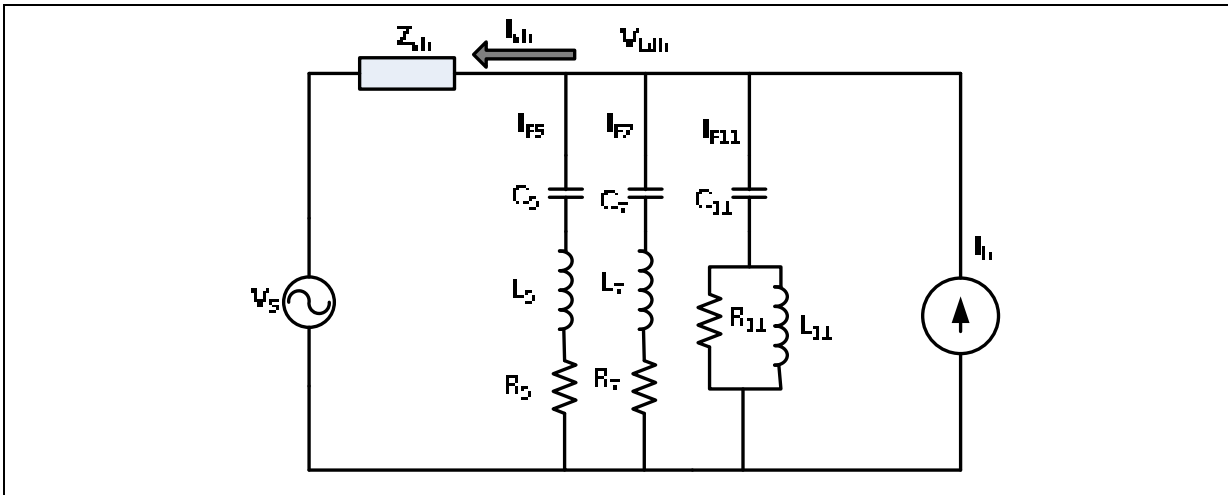


Figure 2.17 Single-phase diagram of a simplified network with filters

Step 1: Determine the total value of the required C_{tot} capacitor per phase to provide the reactive power Q .

As a first approximation, C_{tot} is determined by:

$$C_{tot} = \frac{Q}{\omega_n * V_{c1}^2} \quad (2.30)$$

V_{c1} : is the value of the fundamental voltage across the capacitor

$\omega_1 = 2\pi f$; f is the fundamental frequency (60 Hz)

Step 2: Distribute the value of C_{tot} between all the branches making up the whole filtering system.

The value of C_{tot} is distributed between the branches relating to the resonant filters tuned to the harmonic ranks 5 and 7 and the second order damped high pass filter on the harmonic rank 11 (FPH).

$$C_{tot} = C_5 + C_7 + C_{Fph} \quad (2.31)$$

The total reactive power Q of the capacitors is distributed according to the amplitude of the harmonic currents flowing through the filters and according to the procedure of reduction of the cost, described in Figure 2.17, applied to each branch, allows us to obtain:

Optimum capacity:

$$Q_{Fh} = \sqrt{\frac{M_h}{E_h}} \quad (2.32)$$

with;
$$E_h = U_C + \frac{U_L}{h^2} \quad \text{and} \quad M_h = \left(\frac{I_h^2 V_{cl}^2}{h} \right) * (U_C + U_L)$$

Note: It is assumed that the 5th harmonic current only passes through the $L_5 - C_5$ resonant filter; that the harmonic current of 7th only passes through the resonant filter $L_7 - C_7$ and that all the harmonic currents of rows greater than 11 pass through the high-pass filter $L_{ph} - C_{ph}$:

$$\begin{cases} E_h = U_C + \frac{U_L}{h^2}; \quad \text{and} \quad M_h = \left(\frac{I_h^2 V_{cl}^2}{h} \right) * (U_C + U_L) \\ Q_{Fh} = \sqrt{\frac{M_h}{E_h}}; \quad \text{and} \quad Q_{Fph} = \sum_{h=11}^{50} \sqrt{\frac{M_{ph}}{E_{ph}}} \\ C_h = \frac{Q_{Fh}}{\omega_1 * V_{clFh}^2} \end{cases} \quad (2.33)$$

and;
$$I_{ph} = \sqrt{\sum_{h=11}^{50} I_{ph}^2}$$

$$Q_{Ftot} = Q_{F5} + Q_{F7} + Q_{Fph}$$

$$C'_{tot} = C_5 + C_7 + C_{ph}$$

where:

I_5, I_7 : are respectively the effective values of the harmonic currents rows 5 and 7 passing through the tuned resonant filters $L_5 - C_5, L_7 - C_7$;

I_{ph} : is the effective value of the harmonic currents of rows greater than 11 traversing the high-pass filter;

C'_{tot} : is the total value of the capacitors to be used to obtain a minimum cost on each of the filters.

If there is no contingency on the correction of the power factor, C_5 , C_7 and C_{ph} are used as initial filter values, otherwise the total capacity is increased proportionally on each of the filters (resonant and high-passes) according to the following equations:

$$\begin{cases} C_5 = C'_{Ftot} * \frac{Q_{F5}}{Q_{Ftot}} \\ C_7 = C'_{Ftot} * \frac{Q_{F7}}{Q_{Ftot}} \\ C_{ph} = C'_{Ftot} * \frac{Q_{Fph}}{Q_{Ftot}} \end{cases} \quad (2.34)$$

where:

Q_{F5} , Q_{F7} : are the single-phase reactive power (var) of the resonant filters tuned respectively to the 5 and 7 harmonic rows;

Q_{Fph} : is the single-phase reactive power (var) of the high-pass filter;

Q_{Ftot} : is the total single-phase reactive power (var) of all filters (resonant filters + high-pass filter).

Step 3: Determine the inductance values of the resonant filters and the high-pass filter

$$L_h = \frac{1}{(2\pi f * h)^2 C_h} \quad (2.35)$$

The values of the passive filter parameters (in this case) are presented in Table 2.7, and all other values of the system are the same as those made in section 2.2.1.

Table 2.7 Parameters of the passive filter in the second method

Symbol	Definition	Value
F_5	Fifth order shunt passive filter	9.7 mH, 29.08 μ F
F_7	Seventh order passive filter	4.8 mH, 29.62 μ F
F_{11}	High-pass filter	1.9 mH, 30 μ F

2.4.2 Simulation Results

The simulated system comprised of a linear and a non-linear load is subjected to utility current harmonics and lead, lag voltage. In order to evaluate the performance of the proposed control algorithm, many scenarios are tested such as, sudden variation of different loads as balanced and unbalanced nonlinear load.

The obtained results demonstrate that the proposed control algorithm is able to protect loads from grid-initiated perturbation by monitoring the load voltage and removing compensating components. For this test, configuration shown in Figure 2.2 is implemented using Matlab/SPS by applying a fixed discrete time step of $T_s = 10\mu s$.

One can see from the obtained simulation results shown in Figures 2.18 to 2.22 that the power quality is improved and all current harmonics are compensated. Furthermore, the source voltage is perfectly balanced, which means the proposed passive filter using this configuration to be the best solution.

Scenario 1: Current harmonics compensation

The main objective of this test (scenario 1) is to demonstrate the capability of the proposed control algorithm to compensate all current harmonics in source side.

In Figure 2.18, steady state of source current (I_s) and voltage (V_s), load current (I_L) and voltage (V_L), voltage of active filter (V_{AF}), passive filter current (I_{PF}) and DC bus voltage (V_{DC}) are presented.

Figure 2.19 shows how the source current's harmonics main components can be offset immediately when the current attains a total harmonic distortion (THD) that is equal to 2.80%. However, a load's current must be considered highly polluted when it attains a THD of 19.81%. It is observed that the proposed control scheme reacts quickly, such that the PI controller is forcing the production of a precise level of voltage compensation within three cycles. The DC link voltage is well-regulated, which helps in the production of a sinusoidal current that is in phase to the relevant source voltage; it also helps in reaching the unity power factor. Table 2.8 charts the values of this scenario.

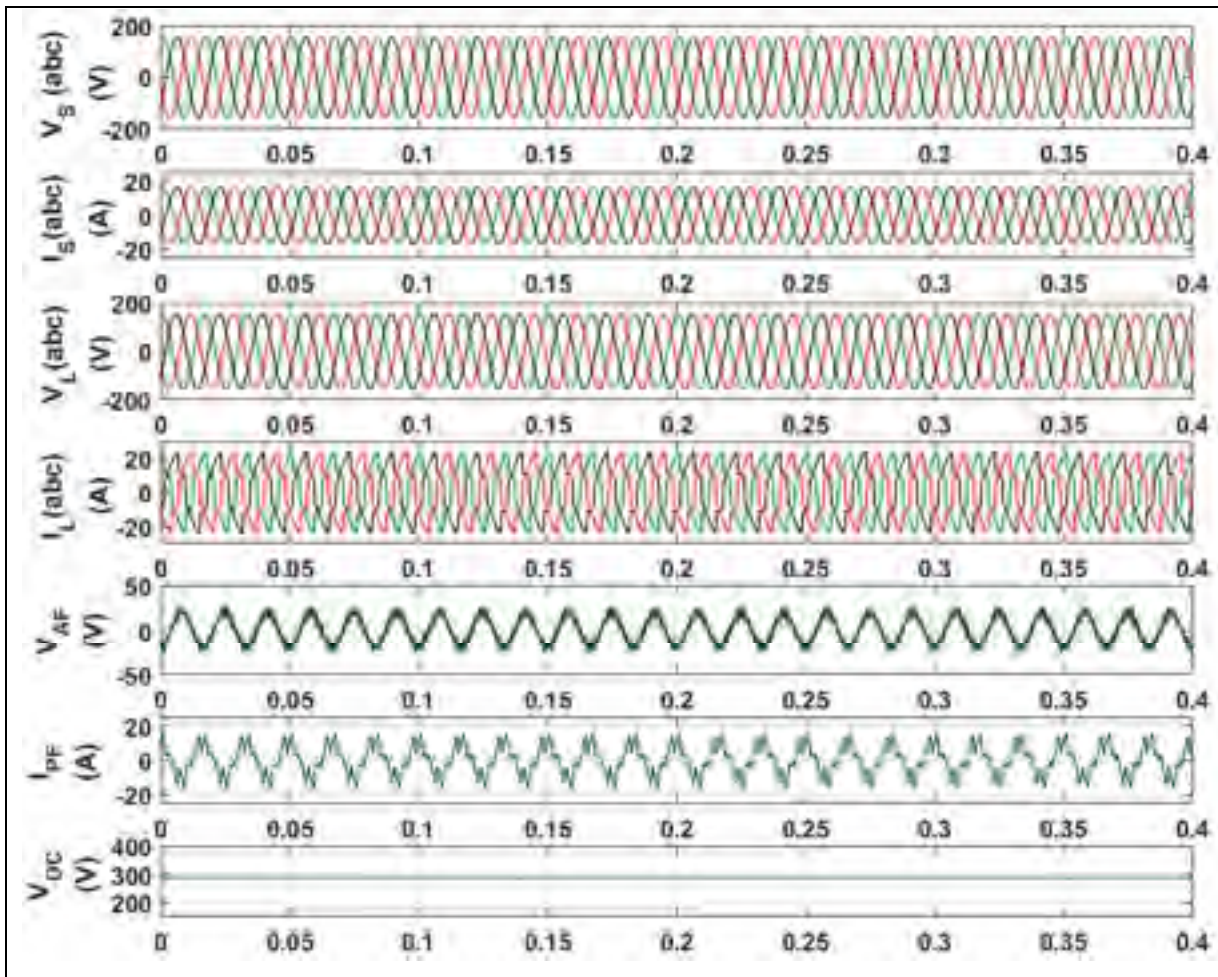


Figure 2.18 Results of the current harmonics compensation during the steady state

In cases of voltage pollution, it is the task of the compensator to maintain load terminal voltages that are suitably regulated and harmonic-free. The compensator proposed here is able to clean harmonics from the current of the grid as well as adjust the power factor, all the while keeping the THD of the load's voltage below the 5% stipulated by regulations and standards.

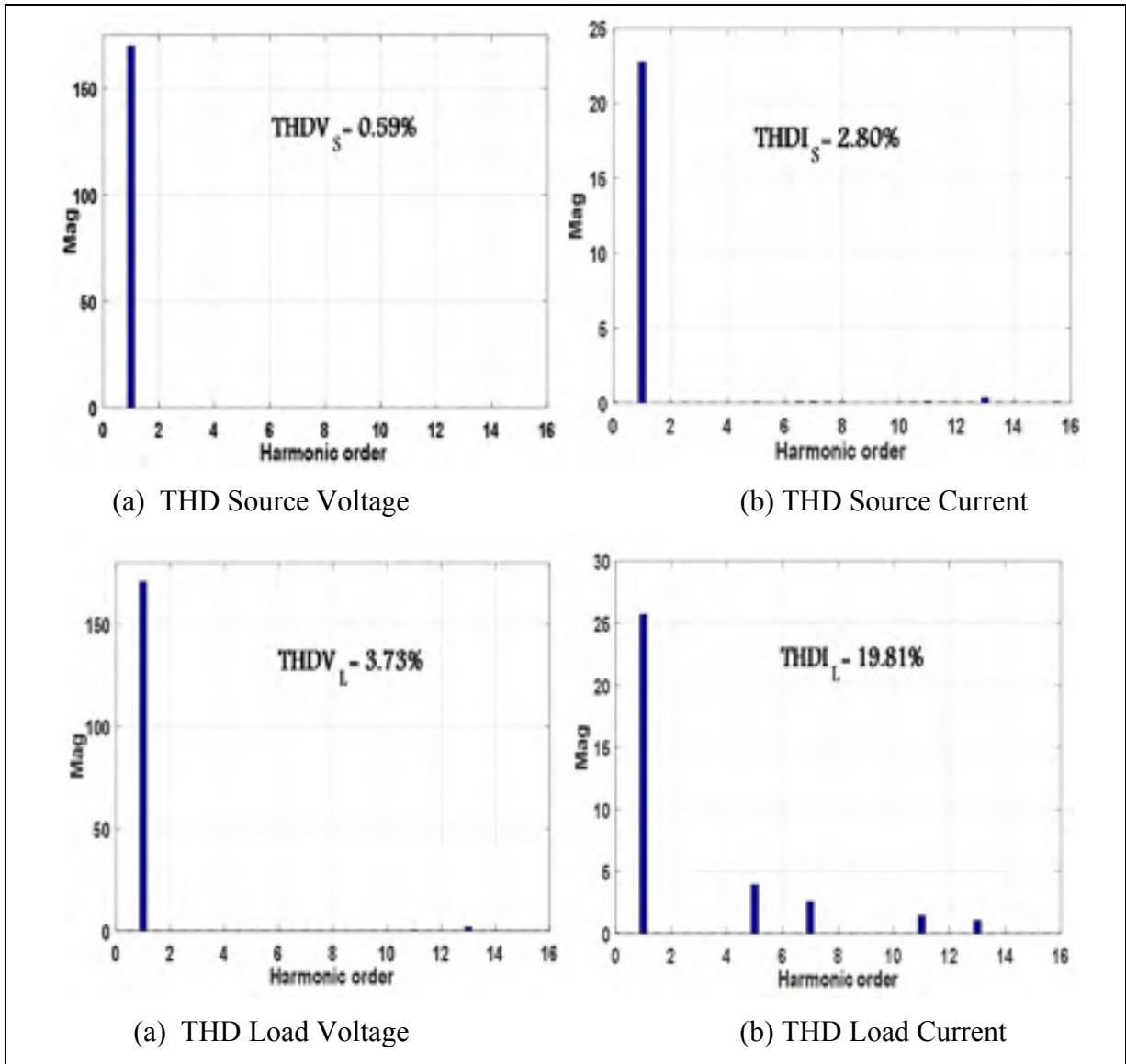


Figure 2.19 THD during current harmonics compensation

Table 2.8 Power parameters and THDs during current harmonic compensation

Parameters	V_S (V rms)	I_S (A rms)	V_L (V rms)	I_L (Arms)
THD (%)	0.59%	2.80%	3.73%	19.81%
Rms	120	23.37	120	24.82
Source power	$P_S = 4.58 \text{ kW}$			
	$Q_S = -3.4 \text{ Var}$			
	$S_S = 4.58 \text{ kVA}$			
Total load Power	$P_T = 4.26 \text{ kW}$			
	$Q_T = 3.27 \text{ kVar}$			
	$S_T = 5.37 \text{ kVA}$			
Non Linear Load Power	$P_{N-L} = 3.89 \text{ kW}$			
	$Q_{N-L} = 445.3 \text{ Var}$			
	$S_{N-L} = 3.91 \text{ kVA}$			
Linear Load Power	$P_{L-L} = 374.2 \text{ Var}$			
	$Q_{L-L} = 2.82 \text{ kVar}$			
	$S_{N-L} = 2.84 \text{ kVA}$			
Apparent power of active filter	4.56 kVA, $Q_{AF} = 517.5 \text{ Var}$			
Passive Filter	$P_F = 18.65 \text{ W}$			
	$Q_F = 2.80 \text{ kVar}$			

Scenario 2: Compensation of reactive power

The load which is highly inductive enables the drawing of a load current that represents the lead power factor for the supply voltage. Then, if the inductor is connected with resistance in parallel, the needs of the load reactive power can be satisfied through the injection of the leading quadrature current.

The passive and active filters compensate the load reactive power needs locally, which is clearly shown in Figure 2.20. Hence, the source load presents as a linear resistive load that provides active power needs only for loads in the unity power factor. On the other hand, when the capacitor is connected with resistance in series, the load reactive power needs are provided through the injection of a lagging quadrature current. Figure 2.21 illustrates how the active and passive filters can offset locally the needs of the load reactive power. As can be seen, the load source presents here like a linear resistive load that provides active power needs only for unity power factor loads.

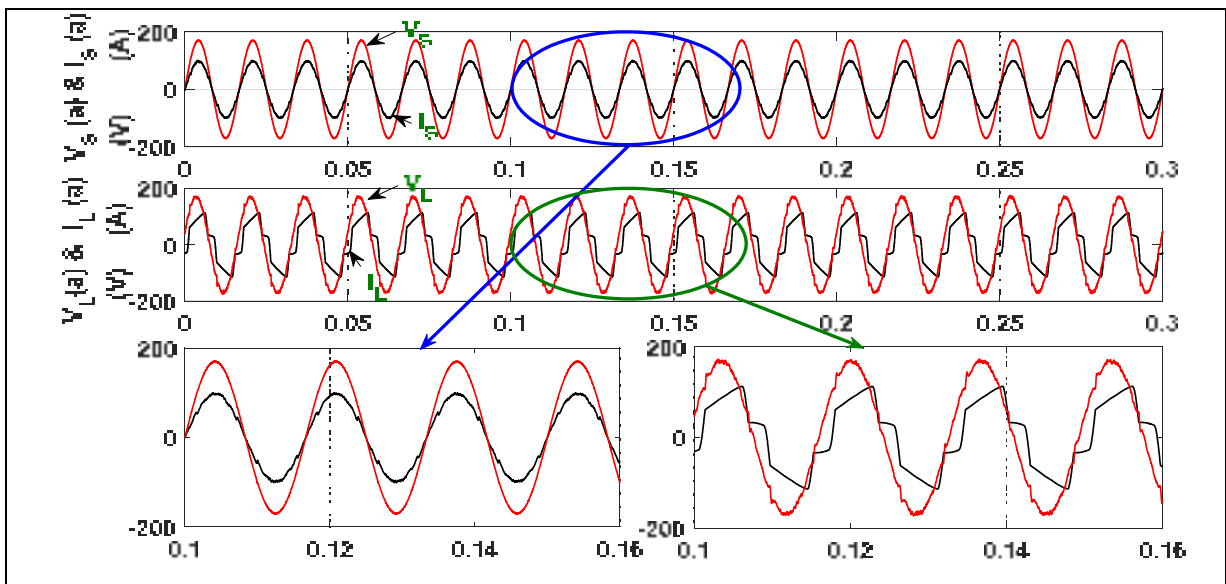


Figure 2.20 Leading voltage

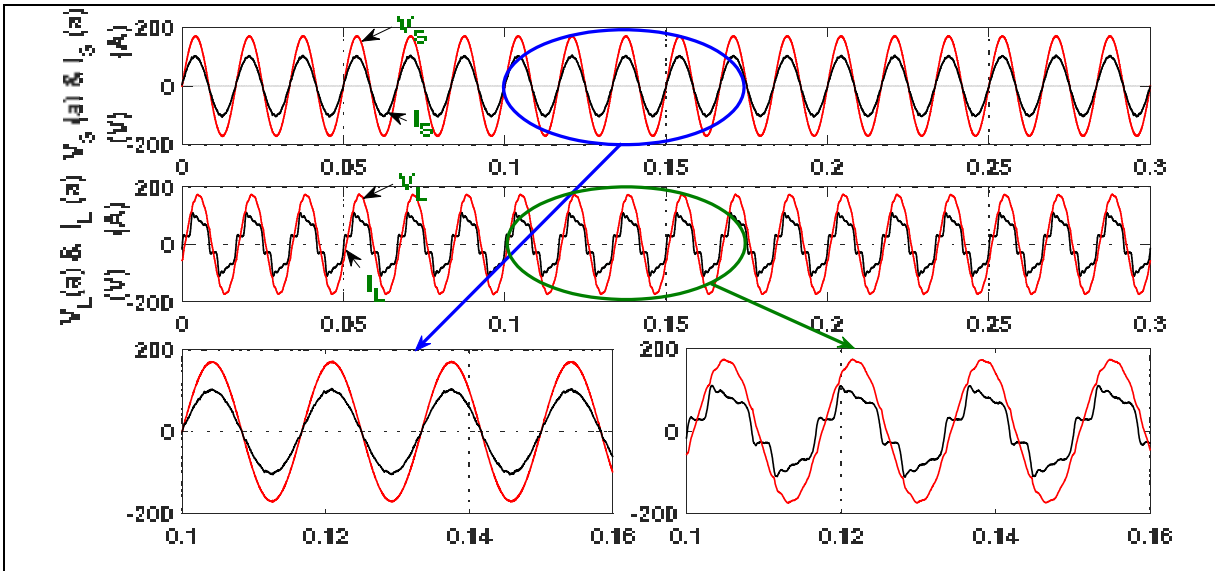


Figure 2.21 Lagging voltage

This is confirmed by the decrease of source current magnitude in comparison to actual load current magnitude. According to the vector diagrams of Figure 2.22.a, the leading compensating voltage has shifted the inductive load's voltage phase angle and the power factor is improved. While, in the diagram of Figure 2.22.b a lagging compensation voltage is applied. In this case the load's voltage is still kept constant, but the power factor has been deteriorated as a consequence. For a capacitive load the opposite result is found. As mentioned previously, one can observe that it is impossible to regulate the DC voltage and correcting the PF simultaneously. Both control strategies operate by shifting the V_{Comp} .

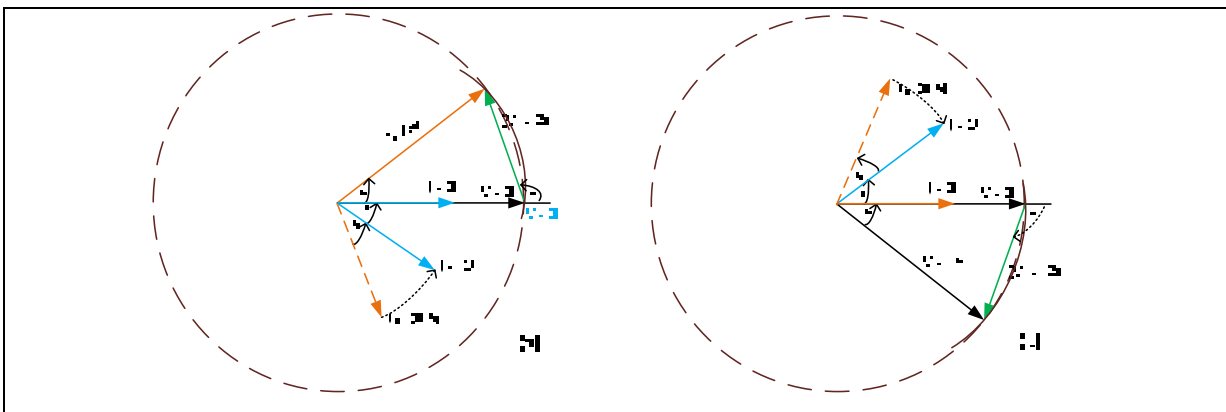


Figure 2.22 Phasor diagram (a) lagging voltage (b) leading voltage

Comparison between both methods of design of the passive filter:

During steady state, at the first method of design of the passive filter to minimize the rating of active filter is reduced THD current down to 1.95% and reactive power during lead and lag also. On the other hand, the passive filter in the second method reduces the THD current to 2.80% which means that the first method is better than the second one. Also, the first method decreased the rating of the active filter which means that the passive filter can solve all the power quality problems as shown in the figures presented in the beginning of this chapter (Figure 2.5 to Figure 2.16).

2.5 Conclusion

This chapter presented a detailed overview of the passive filter design which minimizes the rating the series active filter, and minimize the cost to minimize the passive filter, including sliding mode control strategies, key components, various configurations, and related involvements in the field. Moreover, it covered power quality issues and related problems. The operation principle of series compensation was explained theoretically and results of MATLAB/SPS simulations were given. The overall course of the study's progress continues to highlight the critical significance of tuning the converter's output passive filter for optimal operational performance. Simulation results were also presented in the chapter to underscore the impacts of the passive components used in the series active power filter.

In addition to offering a basic understanding of series active power filter (SeAF), this chapter proposed and analyzed a design of passive filter with sliding mode control approach which is intended to improve series harmonic compensation. The novel hybrid harmonic compensation method for non-linear loads decreases the dependency of the compensation to the harmonics current gain. The enhancement strategy was tested on a three-phase system. It was shown that the technique not only compensates current harmonics coming from a non-linear load, but also regulates the reactive power. The chapter closed with a presentation of related studies regarding the stability of the system. The results of these studies provide a hand tool for choosing SeAF component values and ratings.

CHAPTER 3

THREE-PHASE HYBRID SERIES ACTIVE FILTER WITHOUT BRIDGE DIODE

3.1 Introduction

This chapter presents a topology on an HSAF (hybrid series active filter) that can decrease an active filter's power ratings. In the topology, the HSAF comprises a shunt passive filter and a series active power filter, the latter which offers high impedance of current harmonics, enabling the movement of current harmonics through the passive filter. As well, the series active filter cancels or eliminates voltage harmonics while compensating reactive power. This type of passive filter is made up of a band stop filter (the notch kind) and features a filter cut-off frequency measuring 60Hz. At the same time, it offers high impedance for fundamental frequencies as well as a low impedance shunt branch for the load's current harmonics. In this way, the filter can offset any current harmonics that are moving through source.

The primary benefits of this novel filter are its relatively low cost and small rating. Additionally, this series APF is able to lessen any resonance occurring in the source impedances or shunt passive filter. In compensating harmonics, the rating for the APF equals around 29% compared to the load rating, but this would likely significantly increase if the approach is applied as a means for simultaneously compensating reactive power. The present chapter demonstrates that the APF rating is quite low in comparison with load power, if current harmonics compensation is the main goal. The series active filter can augment the passive filter in this regard. Meanwhile, the HSAF is able to retain DC bus voltage levels at stable values less than 100 volts. Overall, the HSAF proposed here boasts a DC voltage that is very low compared to traditional hybrid active filters. In fact, lower DC bus voltage is one of the main reasons why HSAF is so attractive. The chapter presents some simulation results demonstrating the HSAF's impressive performance with regard to a number of factors, including DC voltage regulation, input power factor, and the total harmonic distortion (THD) of the source current.

3.2 System Configurations

Despite not yet being part of modern power systems, series active compensators still have the greatest potential among active compensators for boosting the electric power quality of the grid. The main problem preventing the application of series compensators are their complexity and high price tag, making them currently the least popular alternative for resolving power quality issues. Despite their inherent problems, series compensators could be repositioned in the future as the technology matures.

Series compensators are generally divided into two categories: series active filters and dynamic voltage restorers, both of them being highly complex and joined to the grid through an isolation transformer. Although offering excellent isolation of the compensating system, the transformers are not only expensive, but brings with it a wide range of performance issues, including the need to be short-circuited if there is a fault in the secondary device, electrical losses, and hysteresis-related phenomena. Moreover, they are able to compensate for voltage issues, and are able to address current perturbations in the power grid.

3.2.1 Modeling of 3-Phase HSAF without Bridge Diode

With the goal of decreasing the power rating, the integration of active and passive power filters is crucial. The SPF system utilizes a minimal component count, the principle of which is to provide low-impedance higher harmonics generated by the load and high impedance at fundamental frequency. This results in efficient compensation of reactive power and harmonics, thus enhancing and improving the power factor. As the SAF gives high impedance over harmonics compensation, it forces the harmonics to flow during the SPF and thus compensates the reactive power and voltage harmonics. The SAF is controlled via the synchronous reference frame (SFR) method (Hamadi, 2007). In the following section, the topology's performance is evaluated and simulation results discussed.

In order to gauge its performance level, the proposed series hybrid power filter configuration is simulated in a MATLAB-PSB environment. The efficiency of the proposed scheme is studied through applying a set of loads consisting of current-source types of non-linear loads and voltage-source types of non-linear loads as shown in Figure 3.1. Furthermore, in order to

validate the SHPF performance, the system underwent testing for a variety of operating conditions, including steady-state, transience, voltage sag and swell, and balanced non-sinusoidal utility voltages. The results of these simulations are as follows, and they are discussed in the next sections.

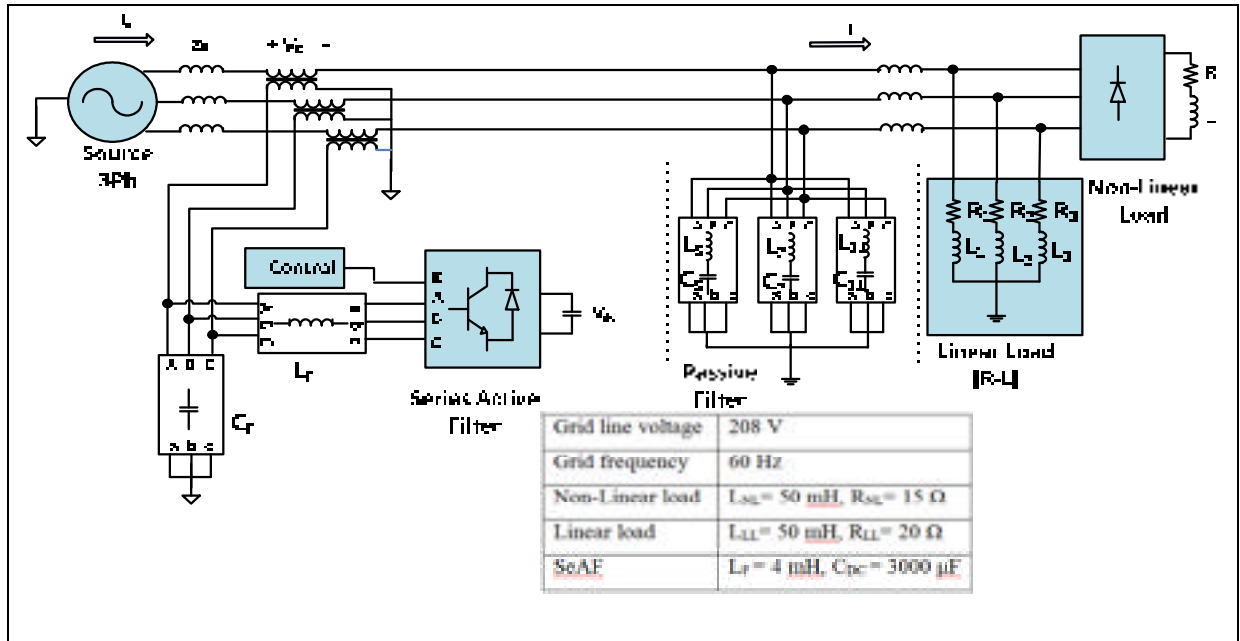


Figure 3.1 Hybrid series active filter with non-linear loads

3.2.2 Control Strategy of 3-Phase HSAF

The hybrid series active filter (HSAF) compensates load types, current/voltage harmonics, and damping of resonance and reactive power, along with serving as a collective system of series active filter (SeAF) and shunt passive filter (ShPF).

3.2.2.1 Control of HSAF Active Part

The functioning control of the series active filter is meant as a means for offsetting reactive power, source voltage distortion, and load harmonic voltages. Moreover, it is meant to support the shunt passive filter (ShPF), which offers extreme resistance to load harmonic currents and ultra-low impedance at fundamental frequencies, such that all load harmonic currents can flow into the ShPF. Controlling the compensation for source harmonic currents and voltage as well

as load harmonic voltages is contrasted in phases equal in amplitude, essentially cancelling each other out. The aim here has been boosting the filtering capacity of the shunt passive filter and thereby resolving its dynamic issues. The series active filter (SeAF) is thus rated as a portion in overall compensating kVAR power, which reduces the total cost.

Meanwhile, in the SeAPF, it is important to use a control method to create reference compensating voltages, as the reference voltage must be provided and the source harmonic component for the SsAPF revealed if the compensating voltages are to be appropriately generated (Rahmani, 2002).

As shown in Equation (3.1), the APF functions as a current-controlled voltage source that works as a type of harmonic isolator, preventing the source harmonic voltage from flowing into the load. At the same time, it also hinders the load harmonic currents from moving into the source. According to Hamadi (2007), reference compensating voltages for SeAPF, when applying the control approach, are as follows:

$$\begin{cases} V_{ca}^* = Ki_{Sah} + V_{Lah} \\ V_{cb}^* = Ki_{Sbh} + V_{Lbh} \\ V_{cc}^* = Ki_{Sch} + V_{Lch} \end{cases} \quad (3.1)$$

where i_{sah} , i_{sbh} and i_{sch} represent the source harmonic currents and V_{Lah} , V_{Lbh} and V_{Lch} represent the fundamentals required to help maintain consistent DC-side voltage, V_{dc} . We can determine source harmonic current, i_{sh} , by applying the SRF, whereby the voltage source of 3-phase will be changed into a 2-phase stationary reference frame (dq), by using Park's transformation (Hamadi, 2007), as formulated below:

$$\begin{bmatrix} V_d \\ V_q \\ V_0 \end{bmatrix} = [P] \begin{bmatrix} V_a \\ V_b \\ V_c \end{bmatrix} \quad (3.2)$$

where P is Park's transformation matrix:

$$P = \sqrt{\frac{2}{3}} \begin{bmatrix} \cos(\theta) & \cos(\theta - \frac{2\pi}{3}) & \cos(\theta + \frac{2\pi}{3}) \\ \sin(\theta) & \sin(\theta - \frac{2\pi}{3}) & \sin(\theta + \frac{2\pi}{3}) \\ \frac{1}{\sqrt{2}} & \frac{1}{\sqrt{2}} & \frac{1}{\sqrt{2}} \end{bmatrix}$$

The DC-bus controller output is then added to the active components generated by inverse transformations, as follows:

$$\begin{bmatrix} V_a \\ V_b \\ V_c \end{bmatrix} = [P^{-1}] \begin{bmatrix} V_d \\ V_q \\ V_0 \end{bmatrix} \quad (3.3)$$

where P^{-1} is the inverse of Park's transformation matrix:

$$P^{-1} = \sqrt{\frac{2}{3}} \begin{bmatrix} \cos(\theta) & -\sin(\theta) & \frac{1}{\sqrt{2}} \\ \cos(\theta - \frac{2\pi}{3}) & -\sin(\theta - \frac{2\pi}{3}) & \frac{1}{\sqrt{2}} \\ \cos(\theta + \frac{2\pi}{3}) & -\sin(\theta + \frac{2\pi}{3}) & \frac{1}{\sqrt{2}} \end{bmatrix}$$

The control scheme of the series active filter part is shown in Figure 3.2.

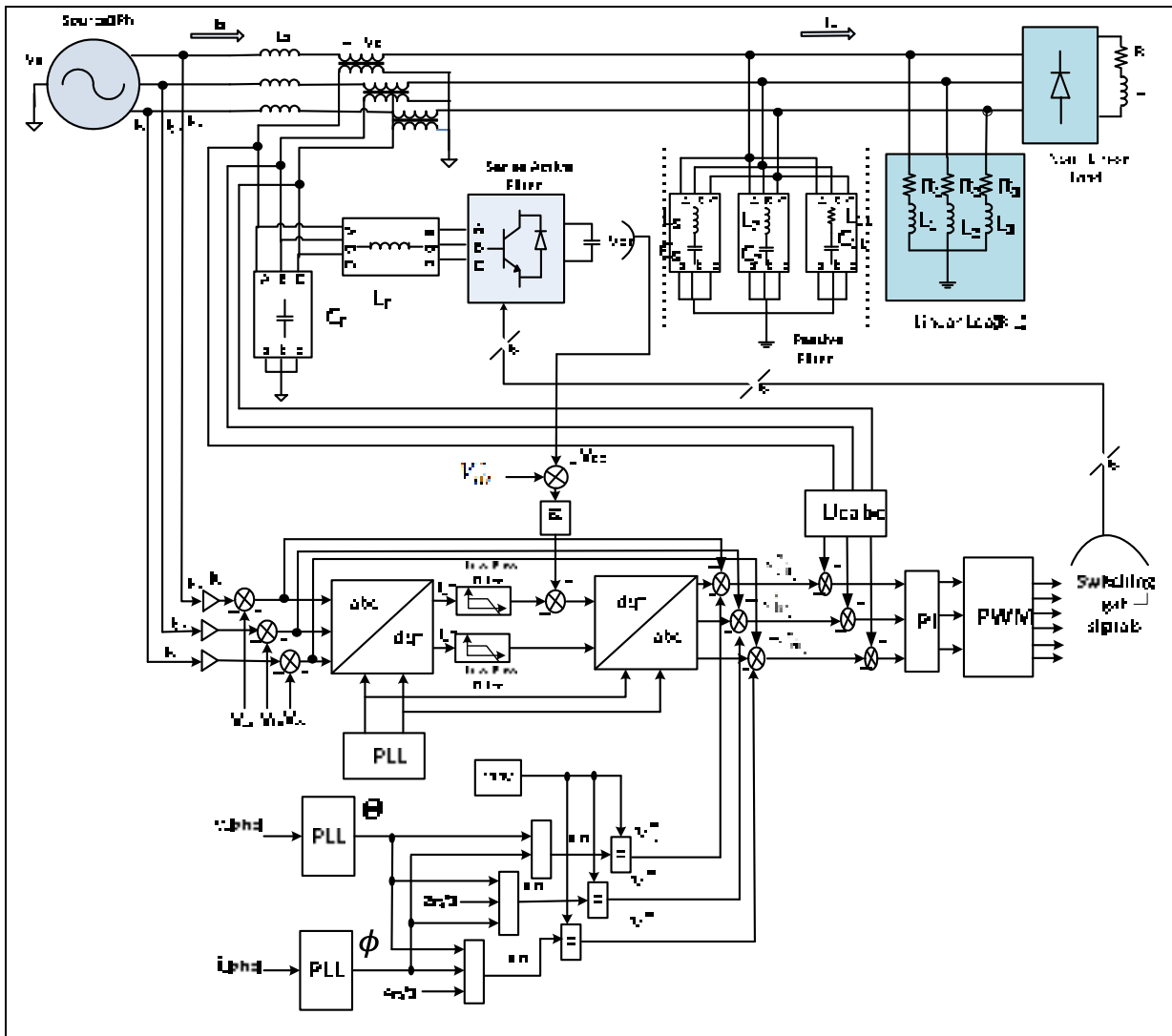


Figure 3.2 Control scheme of the active power filter

3.2.2.2 Series APF Reference Voltage Signal Generation

By applying standard mathematical formulations, the required series-injected voltage magnitude and its phase angle can be determined based on rms values. Thus, to generate time-varying, 60-Hz sinusoidal signals with estimated phase angle α_{SR} , MATLAB s-function blocks can be utilized.

By applying traditional formulations from the field of mathematics, we can find the phase angle as well as the necessary series-injected voltage magnitude in relation to rms values. Thus,

in creating 60-Hz sinusoidal signals that are time-varying and have a phase angle of around α_{sr} , MATLAB s-function blocks can be utilized.

Next, the sinusoidal and cosinusoidal signals from unity magnitude in phase-locked loop (PLL) are integrated to hold the synchronization among supply voltages and generated reference signals. These signals multiply V_{sr} by the computed series voltage magnitude to give the needed series-injected voltage signal as well as phase angle shift. Moreover, using a $\pm 120^\circ$ phase angle difference, we can calculate the two other phases' reference signals, after which we can compare three reference series-injected voltages and 3-phase series-injected voltages along with any errors in the hysteresis controller in order to determine the series inverter switches' switching signals.

3.2.3 Simulation Results

The simulated system comprised of a linear and a non-linear load is subjected to utility voltage distortions, sag and swell. The control algorithm indicated that the DVR can protect loads from grid-initiated perturbation by monitoring the load voltage and removing compensating components

3.2.3.1 Current harmonic compensation

In order to determine the proposed topology's capability for dealing with power quality problems, we can use MATLAB/SPS in the Figure 3.2 system. This can be accomplished by using a discrete time step of $T_s = 10\mu s$ to obtain reliable results such as in an experimental implementation. The simulation results shown in Figure 3.3 clearly show how the source current harmonics main portion is immediately compensated after achieving a current THD equal to 1.55%; however, the current ends up being extremely polluted with a THD measuring 18.57%, as shown in Figure 3.5. As can be seen, the converter is forced by the PI regulator into following the reference, which then creates the appropriate compensating voltage. As a means of attaining unity power factor, nonlinear loads are forced by the compensator-created voltage into manifesting a sinusoidal current which is in phase to corresponding source

voltages. In this configuration, passive filters are crucial for stopping current harmonics from moving through the grid.

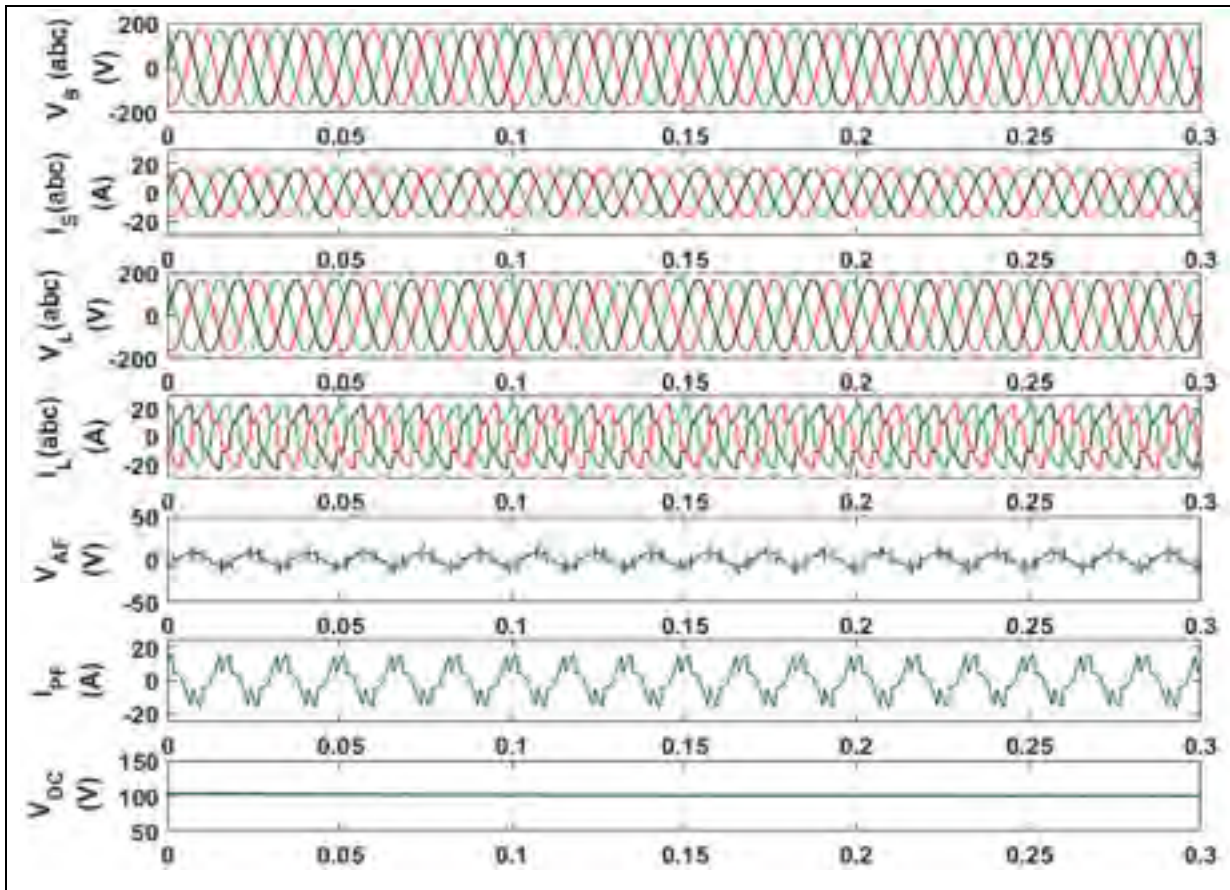


Figure 3.3 Steady state simulation results of the active power filter control scheme

Figure 3.4 illustrates how the load's reactive power is offset by the compensator, thus allowing the source to supply active parts only. The diagram shows the measured average 3-phase active (P) and reactive (Q) powers related to 3-phase currents and voltages in one or two cycles and determines their average values. Although the compensator can control power flow through leading or lagging of the current, it does not hinder the active power flow.

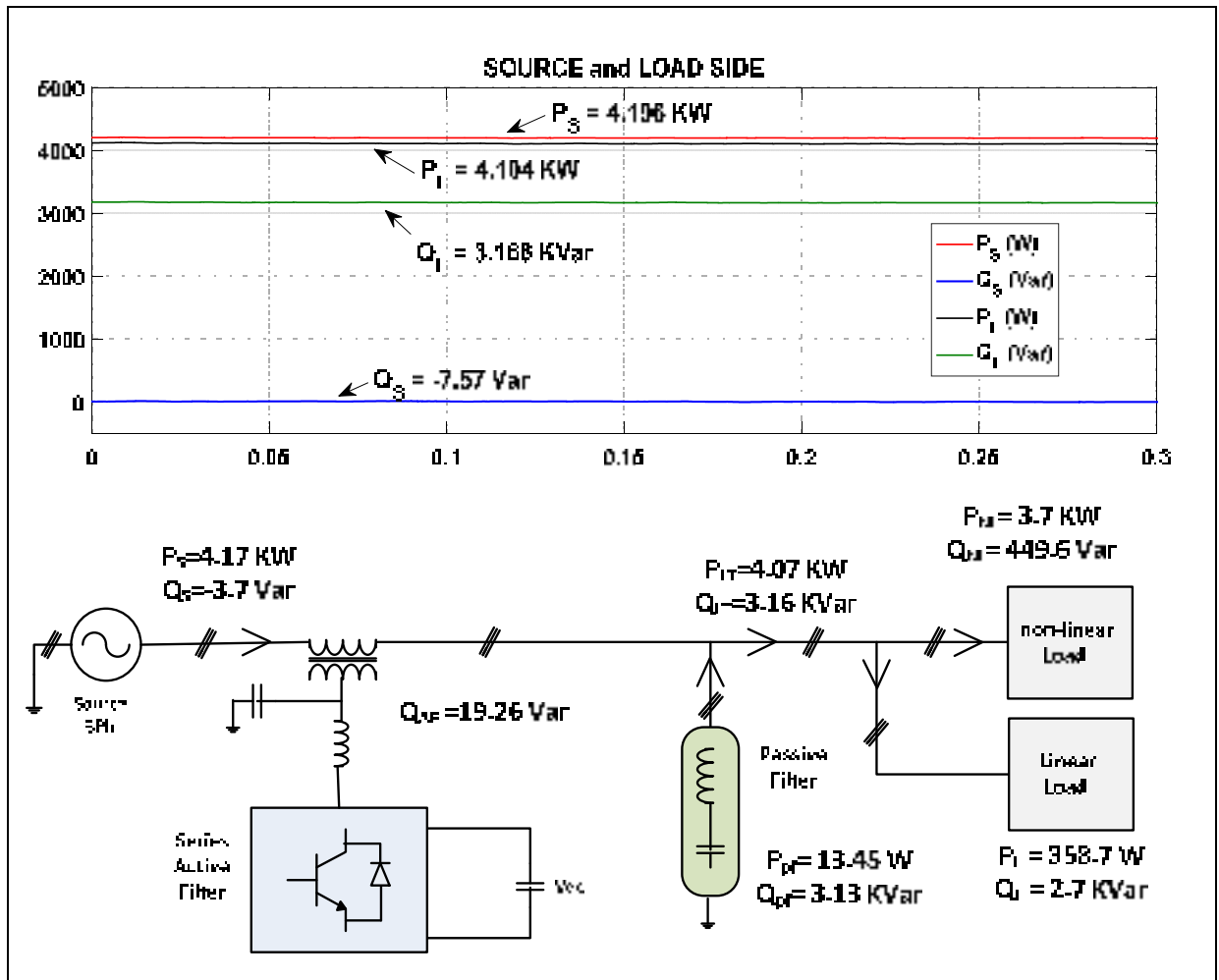


Figure 3.4 Power flow with the steady state

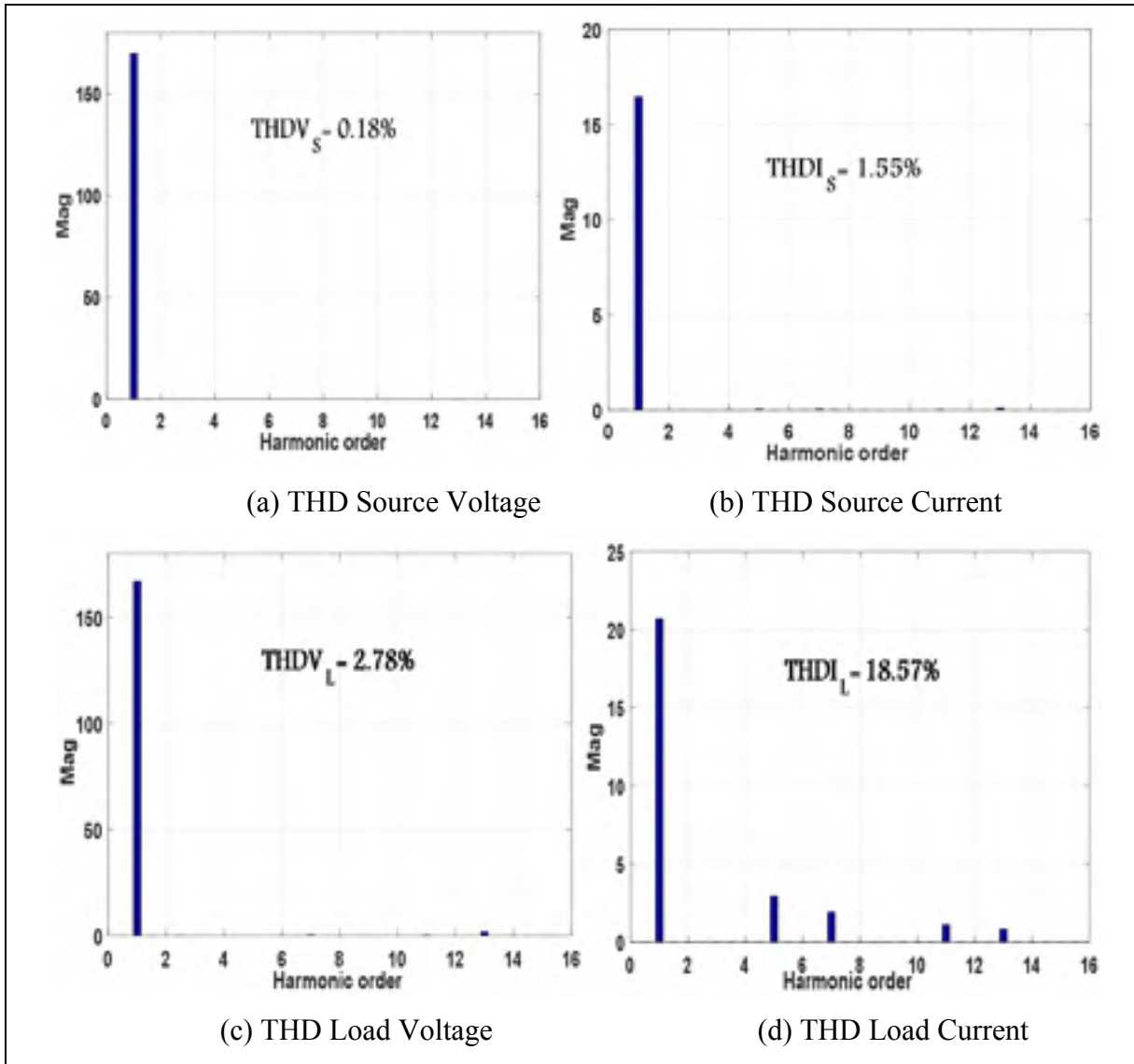


Figure 3.5 THD during current harmonics compensation

Table 3.1 Power parameters and THD's during steady state

Parameters	V_S (V rms)	I_S (A rms)	V_L (V rms)	I_L (Arms)
THD (%)	0.18%	1.55%	2.78%	18.57%
Rms	169.8	16.47	166.9	20.71
Source power	$P_S = 4.17$ kW			
	$Q_S = -3.7$ Var			
	$S_S = 4.17$ kVA			
Total load Power	$P_T = 4.07$ kW			
	$Q_T = 3.16$ kVar			
	$S_T = 5.15$ kVA			
Non Linear Load Power	$P_{N-L} = 3.7$ kW			
	$Q_{N-L} = 449.6$ Var			
	$S_{N-L} = 3.73$ kVA			
Linear Load Power	$P_{L-L} = 358.7$ Var			
	$Q_{L-L} = 2.7$ kVar			
	$S_{N-L} = 2.72$ kVA			
Apparent power of active filter	$S_{AF} = 4.17$ kVA, $Q_{AF} = 19.26$ Var			
Passive Filter	$P_F = 13.45$ W			
	$Q_F = 3.13$ kVar			

3.2.3.2 Load variation

Generally, as nonlinear loads tend to be time-varying, we should look at HSAF performance with regard to nonlinear load variations. Figure 3.6 illustrates how the system reacts when the step increases to 100% for load current at a ratio of $t=0.166s$. As can be seen, unity power factor has been maintained by the system throughout the load condition change phase, showing the HSAF's good performance. The response of the system during a load variation is demonstrated in Figure 3.7, where the compensator follows this variation while performing the power quality improvement.

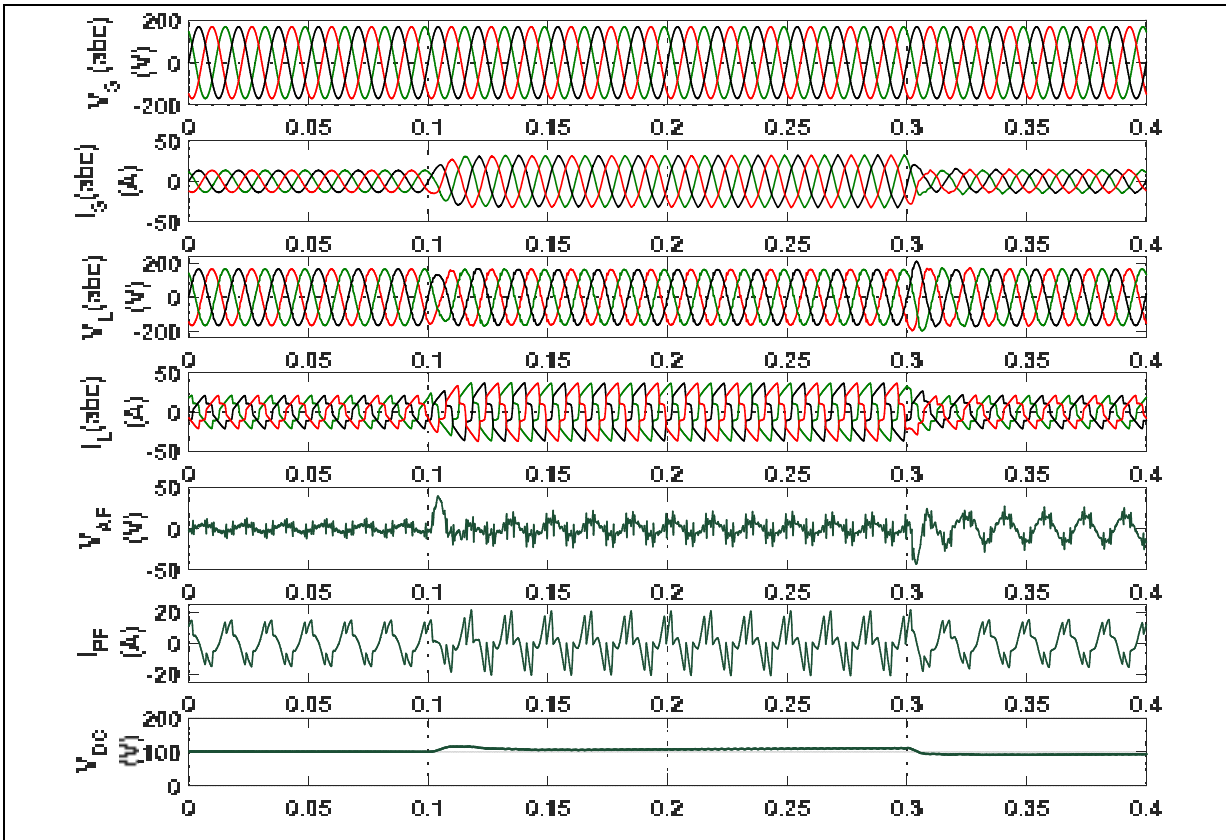


Figure 3.6 Simulation results of the system during the load variation

3.2.3.3 Unbalanced voltage

Figure 3.7 depicts system response to unbalances in the source voltage. As can be seen, the load terminal voltages are controlled by the filter. Hence, the active power compensator can adapt to changes of load consumption without allowing current harmonics to access grid-side, all while holding well-controlled sinusoidal voltage at the loads' point of common coupling. The results are shown the grid's line-to-line voltage subjected to a tough unbalance. The line voltages show distortion and unbalance that should be compensated by the passive filter to ensure a balanced and sinusoidal waveform at the load side.

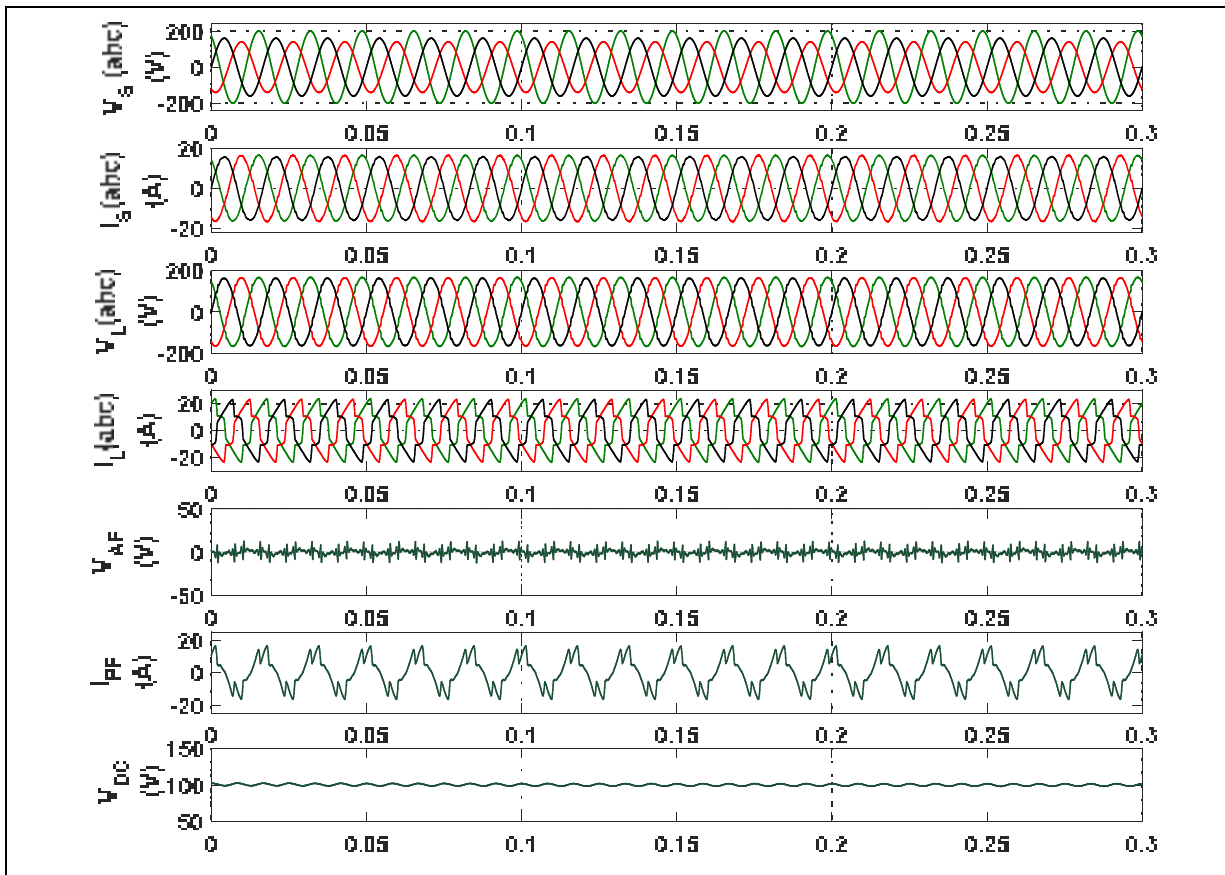


Figure 3.7 Results of the system during a source voltage unbalance

3.2.3.4 Sag and swell voltage

Figure 3.8 shown simulations using the SHPF method employing the fixed power angle concept. As can be seen, prior to 0.1s, steady state offsets load reactive power with a passive filter. By 0.1s, however, there is a notable 30% swell in the system lasting 0.1sec to 0.3sec. Then, from $t=0.3\text{sec}$ to $t=0.5\text{sec}$, there is a reversion to steady-state, after which emerges a 30% sag in the system (this sag lasts until time $t=0.5\text{sec}$).

As illustrated in Figure 3.8, the SHPF without bridge diode has no benefit if the voltage experiences swells and sags, as the compensator can neither inject nor absorb the necessary active power for continuing a constant load voltage amplitude. One can see that the sags and swells applied for all the system. That means the HSPF without bridge diode does not solve the sag and swell voltage.

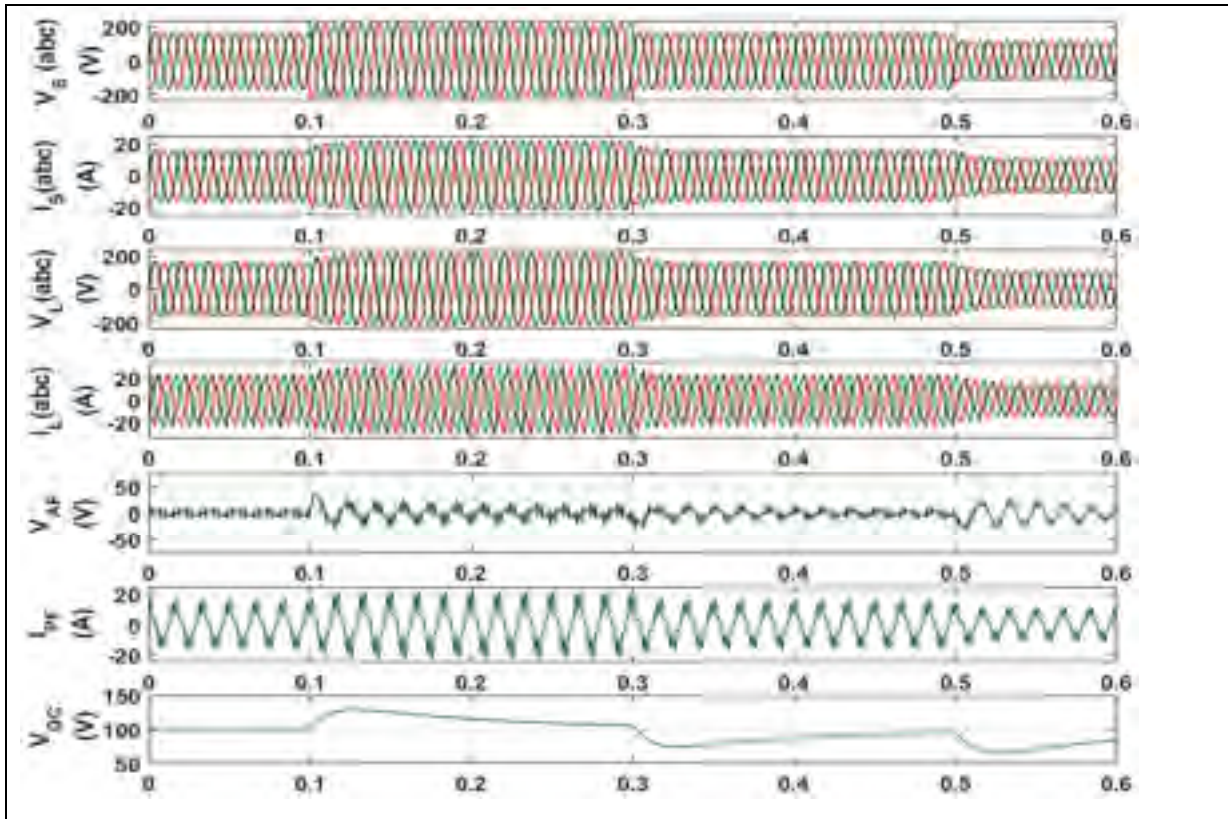


Figure 3.8 Results of the system during sag/swell source voltage

3.3 Conclusion

This chapter presented a series hybrid filter without bridge diode, including control strategies, key components, various configurations, and related involvements in the field. As well, a detailed literature review on series active compensation was provided, covering power quality issues and related problems. The operation principle of series compensation was explained theoretically and the results of the MATLAB/SPS simulation were given. The overall course of the study's progress continues to highlight the critical significance of tuning the converter's output passive filter for optimal operational performance. Simulation results were also presented in the chapter to underscore the impacts of the passive components used in the series active power filter.

In addition to offering a basic understanding of series active power filter (SeAF), this chapter proposed and analysed nonlinear control approach which is intended to improve power quality compensation. The novel hybrid harmonic compensation method for non-linear loads decreases the dependency of the compensation to the harmonics current gain. The technique does not only compensate current harmonics coming from a non-linear load, but also regulates the reactive power and unbalanced voltage. However this technique is not able to solve sag/swell voltage. The chapter closed with a presentation of related studies regarding the stability of the system. The results of these studies provide a hand tool for choosing SeAF component values and ratings.

CHAPTER 4

THREE-PHASE HYBRID SERIES ACTIVE FILTER INTEGRATING RENEWABLE ENERGY CONNECTED TO THE GRID

4.1 Introduction

This chapter outlines and analyzes an effective solution to improve power quality of a 3-phase system with PV solar with and without grid. This 3-phase series compensator is studied to improve the 3-phase power quality in low-voltage distribution systems. The presented series active power filter, which is similar to the last chapters and has been adapted for the 3-phase system, can effectively correct the power factor while cleaning the grid current harmonics. The presented system also has the ability to eradicate the load-side voltage issues and create a stable supply that is relatively free of disturbance.

In the first part of the chapter, we discuss and assess the proposed detection approach to create series hybrid active filters with PV solar configuration. This type of configuration can be connected to the grid without the necessity for the DC bus. The presented control strategy has been presented in the chapter 3, this topology compensates current distortions at the source utility as well as voltage harmonics. The swift and accurate response afforded by this strategy makes the system more reliable while cleaning the load current and correcting the power factor.

In the second section of the chapter, we demonstrate the proposed detection approach for grid ON-OFF to creating series hybrid active filters with PV solar configuration. This type of configuration can be connected to the grid without the necessity of DC bus. The proposed topology is able not only to compensate current harmonics at the source but also to mitigate voltage distortion at the PCC when the grid is turned off. As well, a control scheme will be the same as presented in the chapter 3. The second part of the chapter also describes the operation of the proposed topology. Additionally, the modeling and controller design are presented and validated using simulations for different load and supply conditions.

4.2 Solar Photovoltaic (PV) System

Solar photovoltaic arrays convert sunlight into electricity through the use of PV cells. Solar PV array output depends on a variety of environmental factors, including solar radiance and cell temperature (Villalva, Gazoli and Filho, 2009). In PV systems, complementary ESs, e.g., battery energy storage system, power converters, and loads (Rezkallah, 2016) are necessary for the following reasons:

- to ensure a constant power supply to the loads by compensating the inconstancy of the power provided by PV;
- to track the maximum power point (MPPT);
- to control power flow;
- to regulate the AC voltage and the system frequency at the PCC.

A diagram of the solar PV energy conversion system constituted by a post regulated dc-dc converter, battery storage and inverter is depicted in Figure 4.1. On the DC side, a boost converter is used to extract the maximum power available from the solar panels. The battery storage system is connected between the boost converter and the inverter, its function is to balance the energy and ensure load autonomy (Ndtoungou, 2014). The inverter control the AC power transferred to the load, mainly coming from the solar panels, and regulate the AC output voltage.

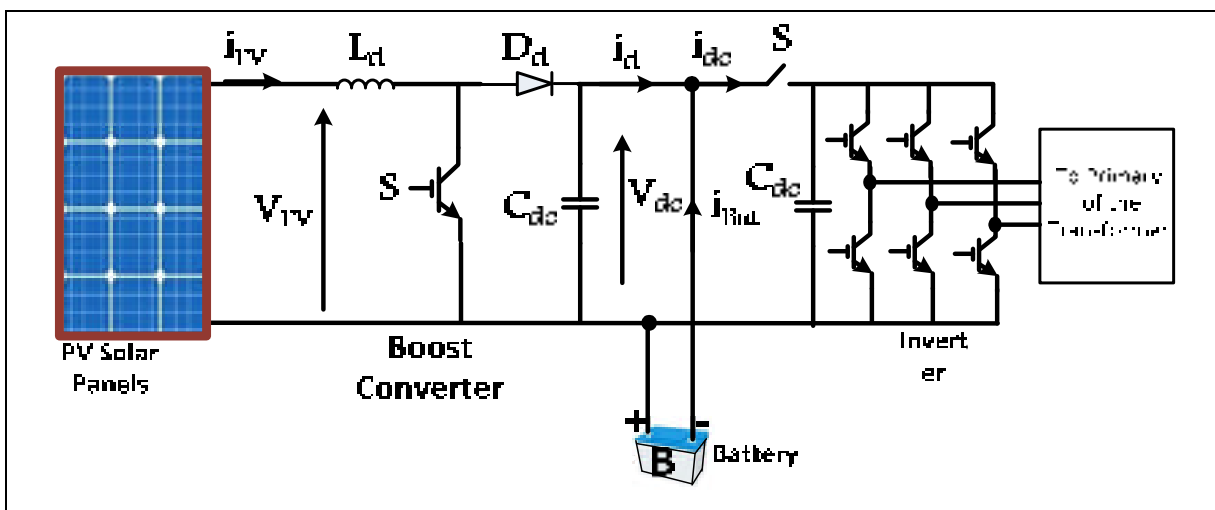


Figure 4.1 Scheme of the PV solar panels based energy supply system

4.2.1 Boost converter modeling

The boost converter topology is shown in figure 4.2. The modeling technique is based on modes of operation. The first mode exists when the switch S is ON and the second mode, when the switch S is OFF.

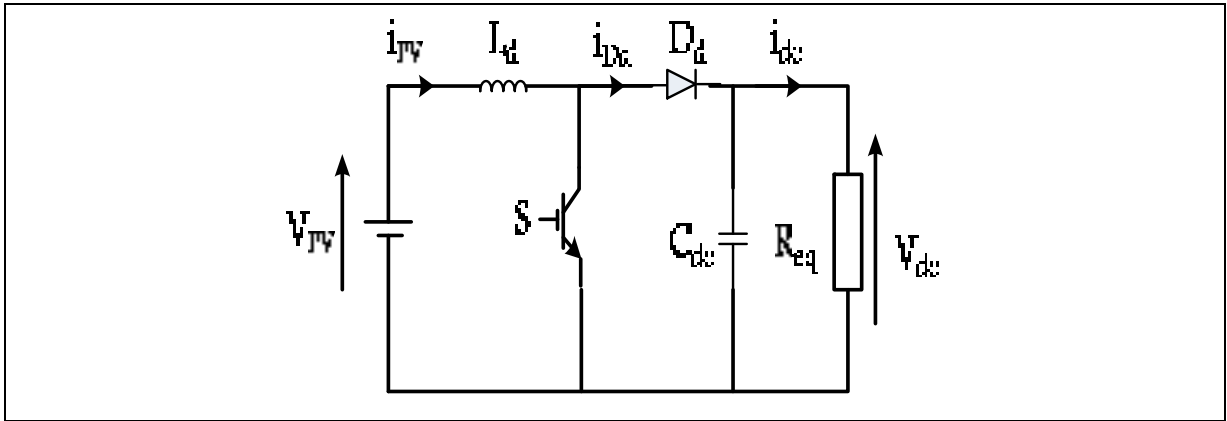


Figure 4.2 Post regulator boost converter

where i_{PV} , i_{Dd} , i_{dc} , denote the input boost converter, the diode and the load equivalent currents; V_{PV} ; v_{dc} denote respectively the PV solar panel and the boost converter voltages; L_d , D_d , R_{eq} are the input inductance, the diode and the equivalent resistance of the Boost converter.

Global system of equations representing both modes is as follows:

$$A = A_1d + A_2(1-d); \quad (4.1)$$

$$B = B_1d + B_2(1-d)$$

$$\begin{bmatrix} \frac{di_{PV}}{dt} \\ \frac{dV_{dc}}{dt} \end{bmatrix} = \begin{bmatrix} 0 & -\frac{(1-d)}{L_d} \\ \frac{(1-d)}{C_{dc}} & -\frac{1}{R_{eq}C_{dc}} \end{bmatrix} \begin{bmatrix} i_{PV} \\ V_{dc} \end{bmatrix} + \begin{bmatrix} 1 \\ 0 \end{bmatrix} \frac{1}{L_d} V_{PV} \quad (4.2)$$

$$A = \begin{bmatrix} 0 & -\frac{(1-d)}{L_d} \\ \frac{(1-d)}{C_{dc}} & -\frac{1}{R_{eq}C_{dc}} \end{bmatrix}, B = \begin{bmatrix} 1 \\ 0 \end{bmatrix} \quad (4.3)$$

An equivalent input u is defined as follows:

$$u = L_d \frac{di_{PV}}{dt} = V_{PV} - (1-d)V_{dc} \tag{4.4}$$

The control law is defined as follows:

$$d = 1 + \frac{u - V_{PV}}{V_{dc}} \tag{4.5}$$

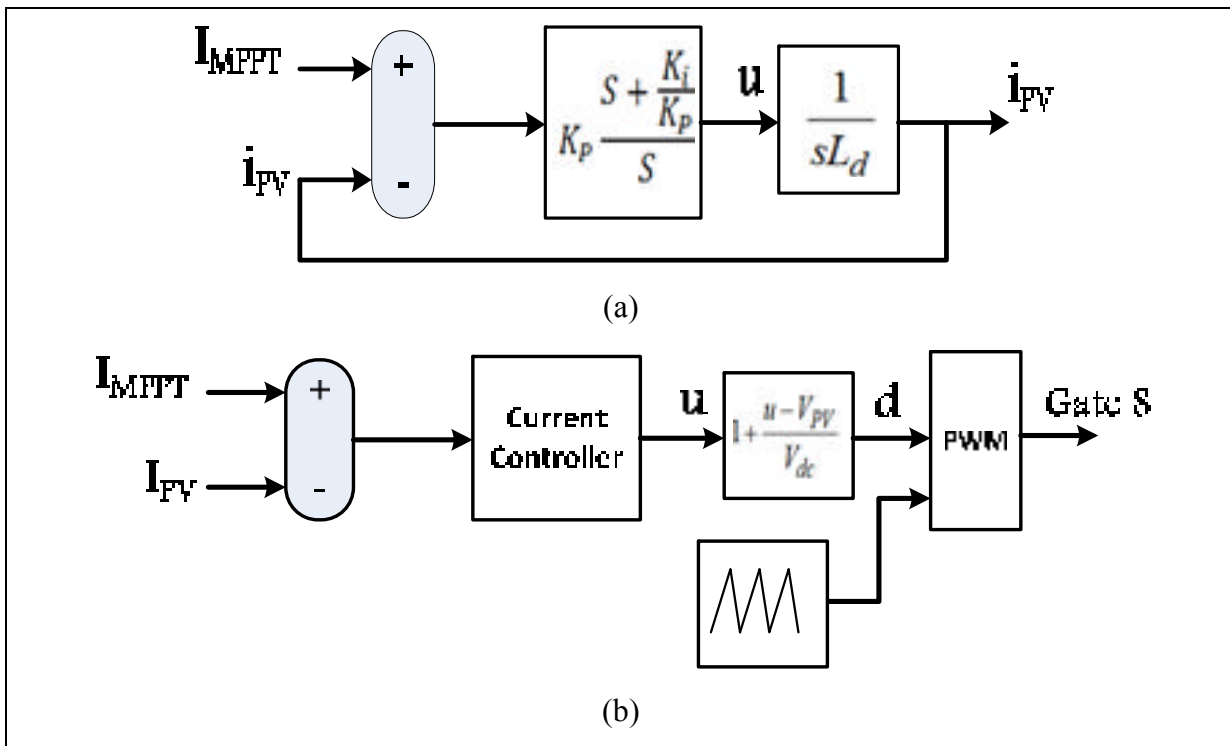


Figure 4.3 (a) Current control loop of the boost converter, (b) Control scheme of the boost converter

The closed loop used in PI controller of the regulation of the current is given by:

$$G_{0i} = \frac{i_{PV}}{I_{MPPT}} = \frac{K_i}{L_d} \frac{\frac{K_p}{K_i} S + 1}{S^2 + \frac{K_p}{L_d} S + \frac{K_i}{L_d}} = \frac{K_i}{L_d} \frac{\frac{K_p}{K_i} S + 1}{S^2 + 2\xi\omega_0 S + \omega_0^2} \quad (4.6)$$

where, K_p and K_i are the parameters of the PI controller and I_{MPPT} is the optimal solar panel current corresponding to the maximum power. By choosing the overshoot $D_1 = 0.05$, and the damping ratio becomes:

$$\xi = \frac{-\ln(0.05)}{\sqrt{\pi^2 + \ln^2(0.05)}} = 0.6901$$

Then the natural frequency is:

$$\omega_0 = \frac{0.9257}{T_r} e^{1.6341\xi} = \frac{\omega_s}{10} = \frac{2 * \pi * 4000}{10} = 2513.3 \text{ rad / s}$$

where ω_s is the carrier frequency. By identification, one can obtain: $\begin{cases} K_p = 2\xi\omega_0 L_d \\ K_i = L_d \omega_0^2 \end{cases}$

4.2.2 PV solar design

Taking the efficiency of the inverter equal to 95%, W_{Load} is the daily energy needs and W_{dc} is the energy needed at the input of the inverter calculated as follows (Ndtoungou, 2014):

$$W_{dc} = \frac{W_{Load}}{0.95} = \frac{21640}{0.95} = 22.778 \text{ KWh} \quad (4.7)$$

Taking the efficiency of the DC/DC converter equal to 95%, then the average energy of the solar panel WSP is calculated as:

$$W_{PV} = \frac{W_{dc}}{0.95} = \frac{22778}{0.95} = 23.977 \text{ KWh} \quad (4.8)$$

The peak solar panel power is given by:

$$P_c(W) = \frac{W_{PV}}{N * C_p} = \frac{23977}{5 * 0.85} = 9403W \quad (4.9)$$

where N is the number of hours, C_p is the loss coefficient (assumed to be 0.85).

The peak load current is expressed as follows:

$$I_{L1ms} = \frac{9403}{3 * 120} = 26.12A \rightarrow I_{L1ms} = 26.12\sqrt{2} = 36.93A \quad (4.10)$$

The insolation in Montreal is varying from 3.3 to 4.2kWh/m². The mean value is:

$$3.75 \text{ kWh/m}^2 = 3.75\text{h} * 1000 \text{ W/m}^2$$

The demand peak power is the required power divided by the number of the hours and the coefficient C_p. The solar panel potential and the insolation in Canada are taken from the environment of Canada. The solar panel characteristics are given in Table 4.1.

4.2.3 Solar panels arrangement

$$N_{PVS} = \frac{\text{total solar DC voltage panel}}{\text{optimal voltage for one solar panel}} = \frac{200V}{30V} = 6.76 \approx 7 \text{ Panels} \quad (4.11)$$

7 panels connected in series are required

$$N_{PPS} = \frac{\text{total optimal current}}{\text{optimal current for one solar panel}} = \frac{9403/200}{8.1} = 5.8 \quad (4.12)$$

$\approx 6 \text{ Panels}$

6 panels connected in parallel are required

42 solar panels organised 4 strings of 7 modules covering an area of 1.5*42=63 m².

4.2.4 Energy storage system design

For this purpose, lead acid type of battery is chosen because of its low cost. The battery available on the market has nominal voltage 48V with nominal capacity C_n=400 Ah. The total capacity size of the battery is chosen for 2 days of autonomy (N_d=2days), the total energy (E_B) stored in the battery for the installation is calculated as follows:

$$E_B = N_d * W_{dc} = 2 * 22779 = 45.558 kWh \quad (4.13)$$

The battery capacity (in A.h) required is calculated as follows:

$$C_{Bat} = \frac{E_B}{\text{DC bus voltage}} = \frac{45558 \text{Wh}}{425 \text{V}} = 107.19 \text{ Ah} \quad (4.14)$$

Considering 30% the efficiency losses (noted as C_1) in the battery and a 30% of security margin (noted as C_S):

$$C_1 = C_{Bat} * 0.3 = 107.13 * 0.3 = 32.16 \text{ Ah} \quad (4.15)$$

$$C_S = (C_{Bat} + C_1) * 0.3 = (107.13 + 32.16) * 0.3 = 41.787 \text{ Ah} \quad (4.16)$$

Table 4.1 Solar panel characteristics

Name	Value
Maximum power	243W
Open circuit Voltage	Voc = 37.1V
Short circuit current	Isc = 8.8A
Optimal voltage	Vmp = 30V
Optimal current	Imp = 8.1A
Area	1.5m ²

The total capacity of the battery is:

$$C_{tot} = C_{Bat} + C_1 + C_S = 181.07 \text{ Ah} \quad (4.17)$$

The number of parallel (N_{BatP}) and series (N_{BatSe}) batteries cells are calculated as follows:

$$N_{BatP} = \frac{C_{tot}}{C_n} = \frac{181.07}{400} = 0.45 \approx 1 \text{ battery in parallel} \quad (4.18)$$

$$N_{BatSe} = \frac{400}{48} = 8.3 \approx 9 \text{ battery in series} \quad (4.19)$$

The total capacity of the battery may be calculated using the equation given below:

$$\begin{aligned} V_{Bat_max} &= (48 + 8\% * 48) * 9 = 466.56 V \\ V_{Bat_min} &= (48 - 8\% * 48) * 9 = 397.44 V \end{aligned} \quad (4.20)$$

$$\begin{aligned} C_B &= \frac{(KWh * 3600 * 1000)}{0.5 * (V_{Bat_max}^2 - V_{Bat_min}^2)} = \frac{(45.558 * 3600 * 1000)}{0.5 * (466.56^2 - 397.44^2)} \\ &= 5492.6F \end{aligned} \quad (4.21)$$

4.2.5 Maximum Power Point Tracking (MPPT) Algorithm

The MPPT algorithm is based on the calculation of actual and previous values of panel's output power (dP). At each iteration, the MPPT algorithm calculates the dP. The processes will end when the difference dP is switching between positive and negative values, as described in Figure 4.5. Figure 4.4 shows the characteristics of the solar $P=f(v)$ and $I=f(v)$ for various irradiation levels. The current-voltage and power voltage for different values of insolation, $G = 600, 800$ and 1000 W/m^2 .

Figure 4.5 shows how the algorithm reaches the maximum power point identified by, it also shows the direction of moving PV current to reach the MPPT corresponding to the maximum power available on the PV which serves as a Set Point to the DC/DC converter controller.

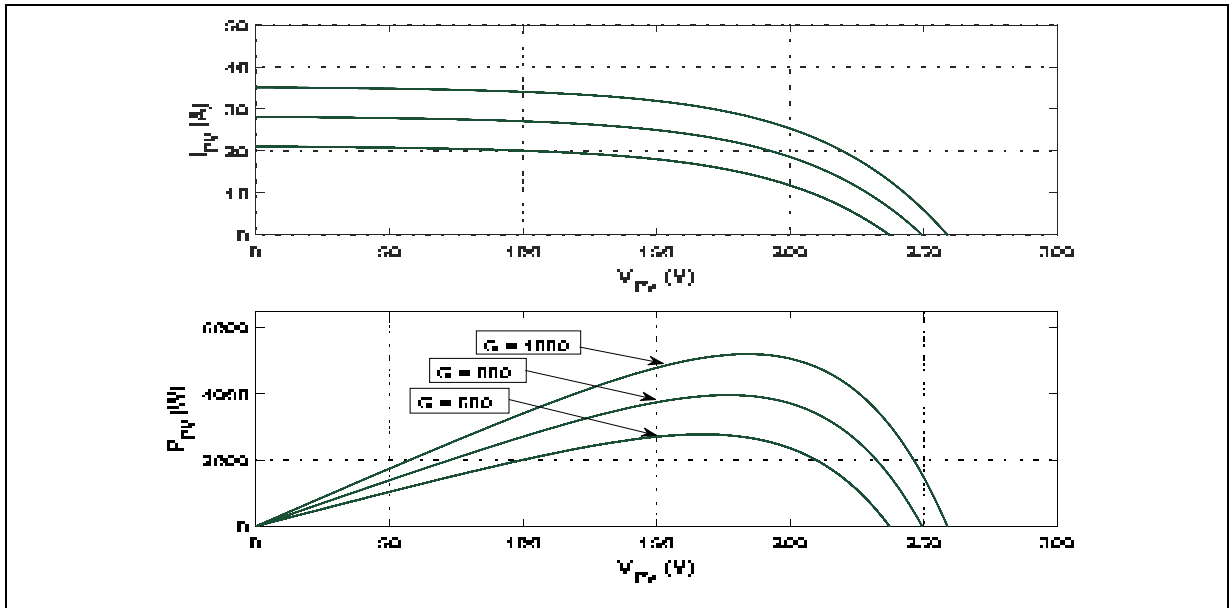


Figure 4.4 Characteristics of the PV solar

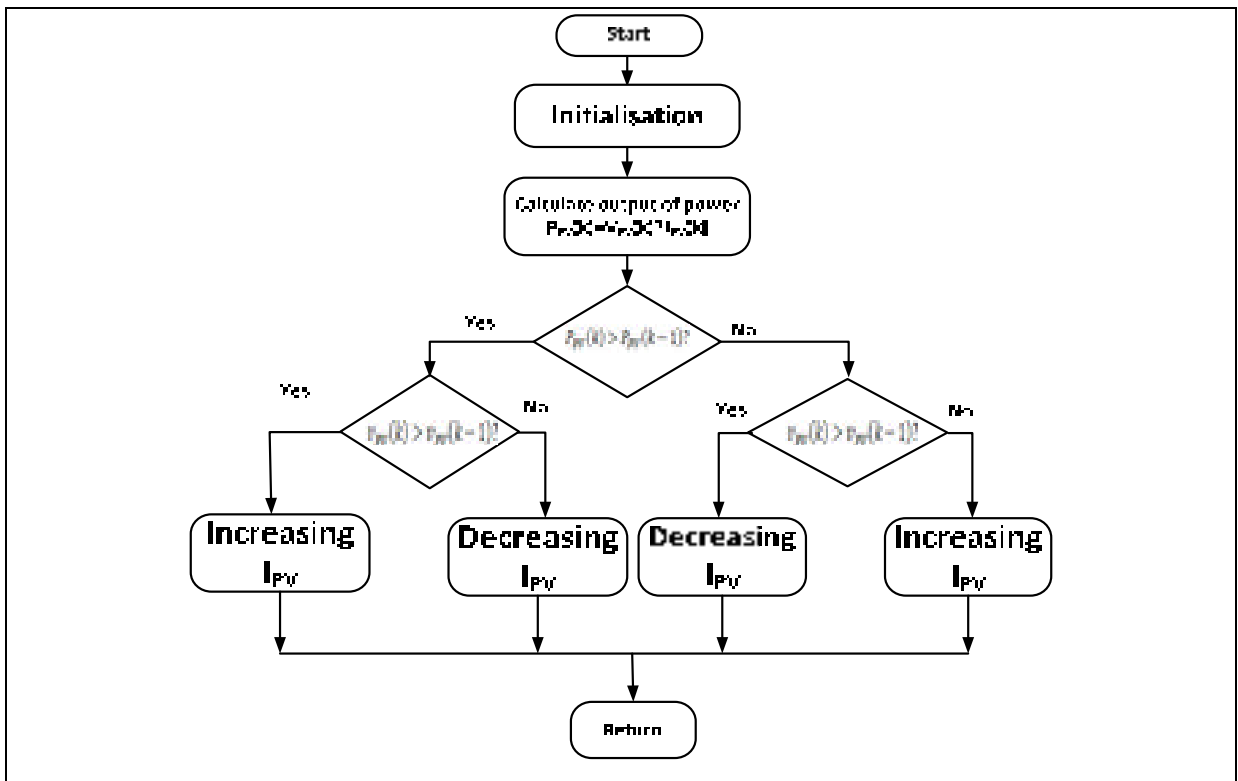


Figure 4.5 Perturb and observe MPPT algorithm

4.3 System Configurations

As depicted in Figure 4.2, the proposed scheme in this chapter features a PV-based series hybrid active filter comprising a passive filter and a PV-connected series active power filter, as well as non-linear and linear loads to the grid. The SAF is able to guard the load against any supply voltage fluctuations while introducing in-series compensation voltage to the supply voltage via coupling transformer, making it a type of controlled VSI. The PV array that is connected to the DC-DC boost converter feeds the SAF the needed DC bus voltage.

4.3.1 Modeling of 3-Phase HSAF with PV solar

The design of the PV-SHAPF enables the energy created in the PV array to power the compensator, if the PV system produces too much energy for load demand. Any extra energy can then be allotted for storage in a battery bank and later applied for regulating load voltage during times when solar irradiation might be unavailable (e.g., at night). The proposed system can be employed for offsetting any distortions in current, voltage or reactive power. In this mode of operation, voltage swell and sag are compensated through the use of a series injection transformer which has been configured in series together with PCC. Continuous compensation is provided by the PV/battery that is joined to the DC-DC boost converter, forming a DC link.

The control will be the same as that used in Chapter 3 for the active filter part. Indeed, the main value in creating a DC bus voltage from VSI-based hybrid filter compensation can be found in the power that is immediately accessible by the active filter. In this way, the voltage of the DC-link capacitor is applicable for reference valuation, as variations in load conditions act to disrupt the power balance among load and source, which is then offset through the DC-link capacitor.

In order to gauge its performance level, the proposed series hybrid power filter configuration with PV solar array is simulated in a MATLAB-PSB environment. The efficiency of the proposed scheme is studied through applying a set of loads consisting of current-source types of non-linear loads and voltage-source types of non-linear loads. Furthermore, in order to validate the SHPF performance, the system underwent testing for a variety of operating

conditions, including steady-state, transience, voltage sag and swell, and balanced non-sinusoidal utility voltages. The results of this simulation are given in the Figures 4.8 to 4.11.

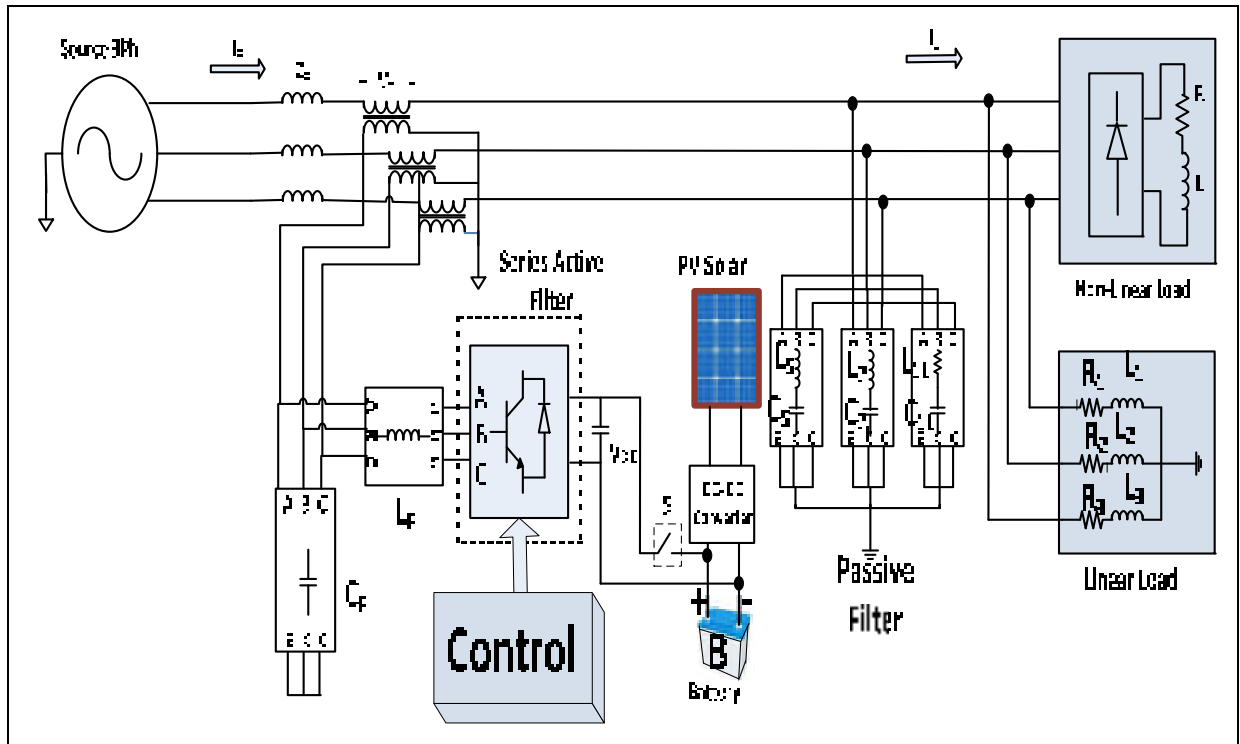


Figure 4.6 Hybrid series active filter with PV solar

4.3.2 Control Strategy of 3-Phase HSAF

The hybrid series active filter (HSAF) compensates load types, current/voltage harmonics, and damping of resonance and reactive power, along with serving as a collective system of series active filter (SeAF) and passive filter (PF).

The topology of the control will be the same as the one presented in chapter 3. Moreover, the passive filter used in this part is the same as the first method presented in chapter 2. During the steady state, the DC regulation with itself, but when the grid turns off, the switch S turns on to connect the PV system to the DC bus voltage in order to apply voltage to the load and regulate the DC voltage at the same time.

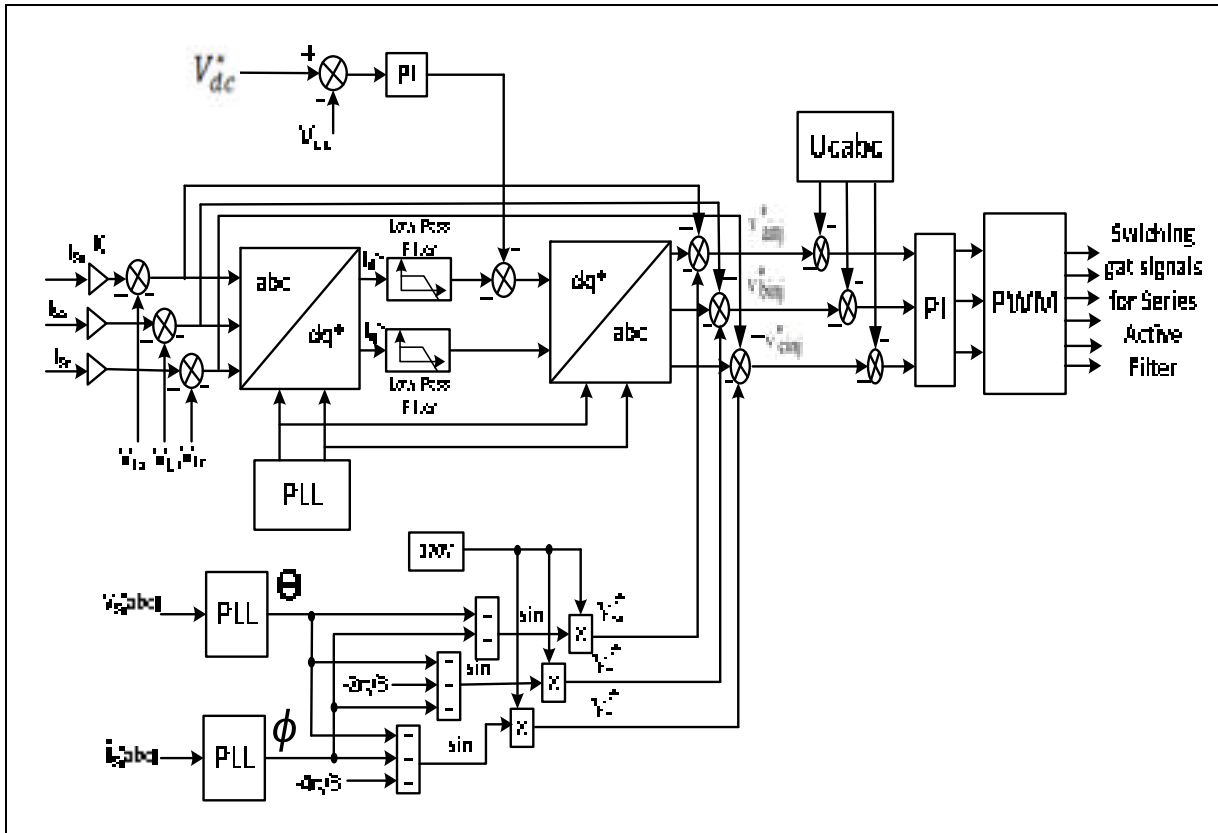


Figure 4.7 Control scheme of the active power filter

4.3.3 Simulation results

The simulated system comprised of a linear and a non-linear load is subjected to utility voltage distortions, sag and swell. The control algorithm indicated that the DVR can protect loads from grid-initiated perturbation by monitoring the load voltage and removing compensating components

4.3.3.1 Current harmonic compensation

In order to determine the proposed topology's capabilities for dealing with power quality-related problems, we can use MATLAB/SPS in the Figure 4.7 system. This can be accomplished by using a discrete time step of $T_s = 10\mu s$ to obtain reliable results such as in an experimental implementation. The simulation result shown in Figure 4.8 clearly show how the source current harmonics main portion is immediately compensated after achieving a current THD equal to 1.92%; however, the current ends up being extremely polluted by a THD

measuring at 19.20%. As a means of attaining unity power factor, nonlinear loads are forced by the compensator-created voltage into manifesting a sinusoidal current which is in phase to corresponding source voltages. In this configuration, passive filters are crucial for stopping current harmonics from moving through the grid.

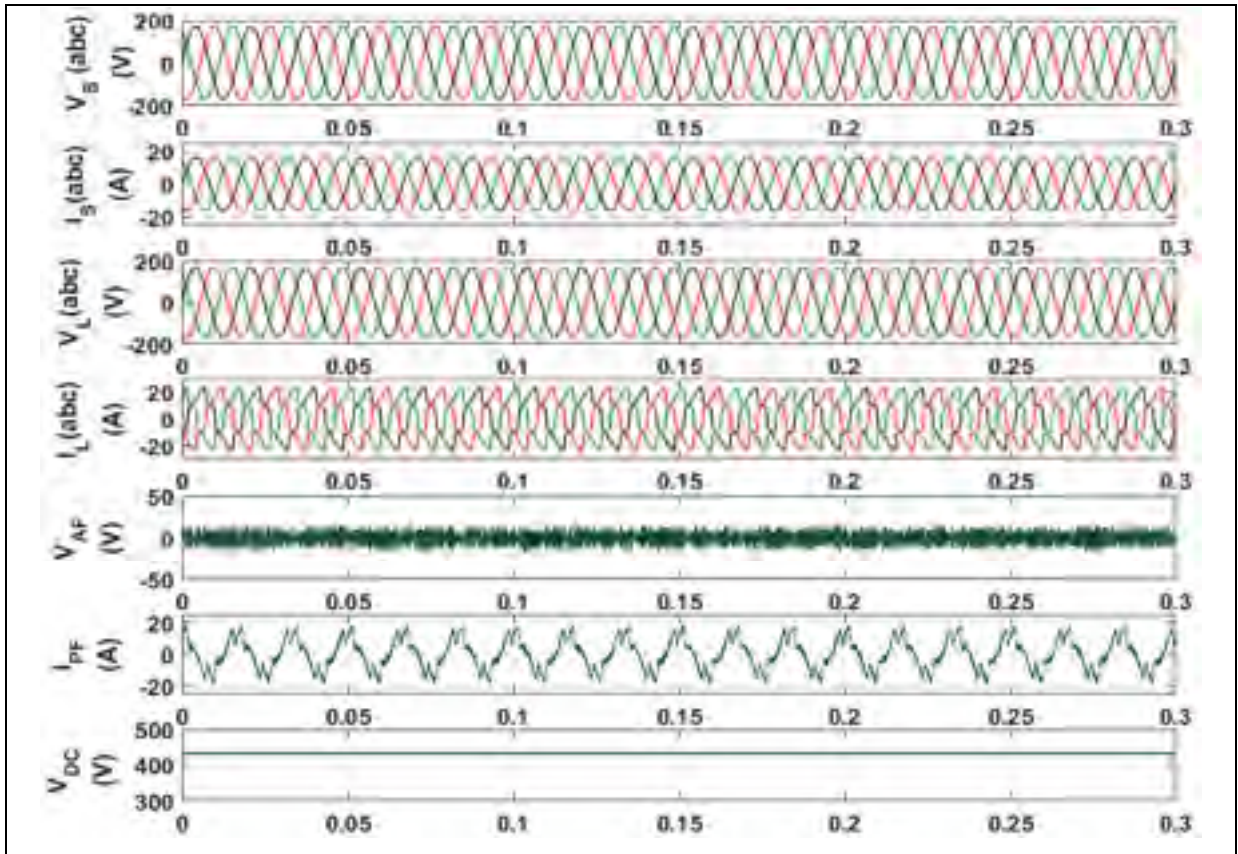


Figure 4.8 Simulation results of the system in steady state

Figure 4.9 illustrates how the load's reactive power is offset by the compensator, thus allowing the source to supply active parts only. The diagram shows the measured average 3-phase active (P) and reactive (Q) powers related to 3-phase currents and voltages in one or two cycles and determines their average values. Although the compensator can control power flow through leading or lagging of the current, it does not hinder the active power flow.

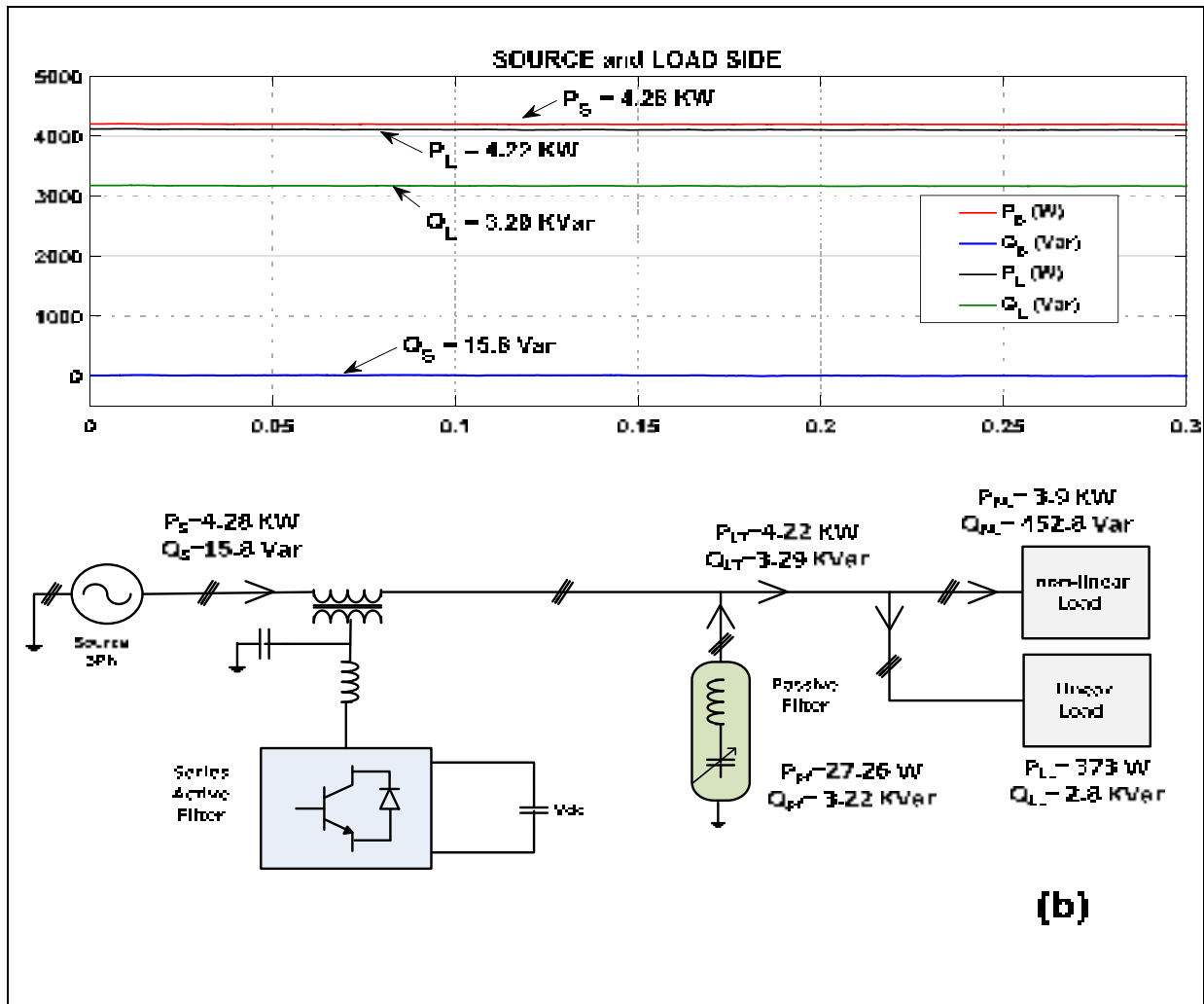


Figure 4.9 Power flow with the steady state

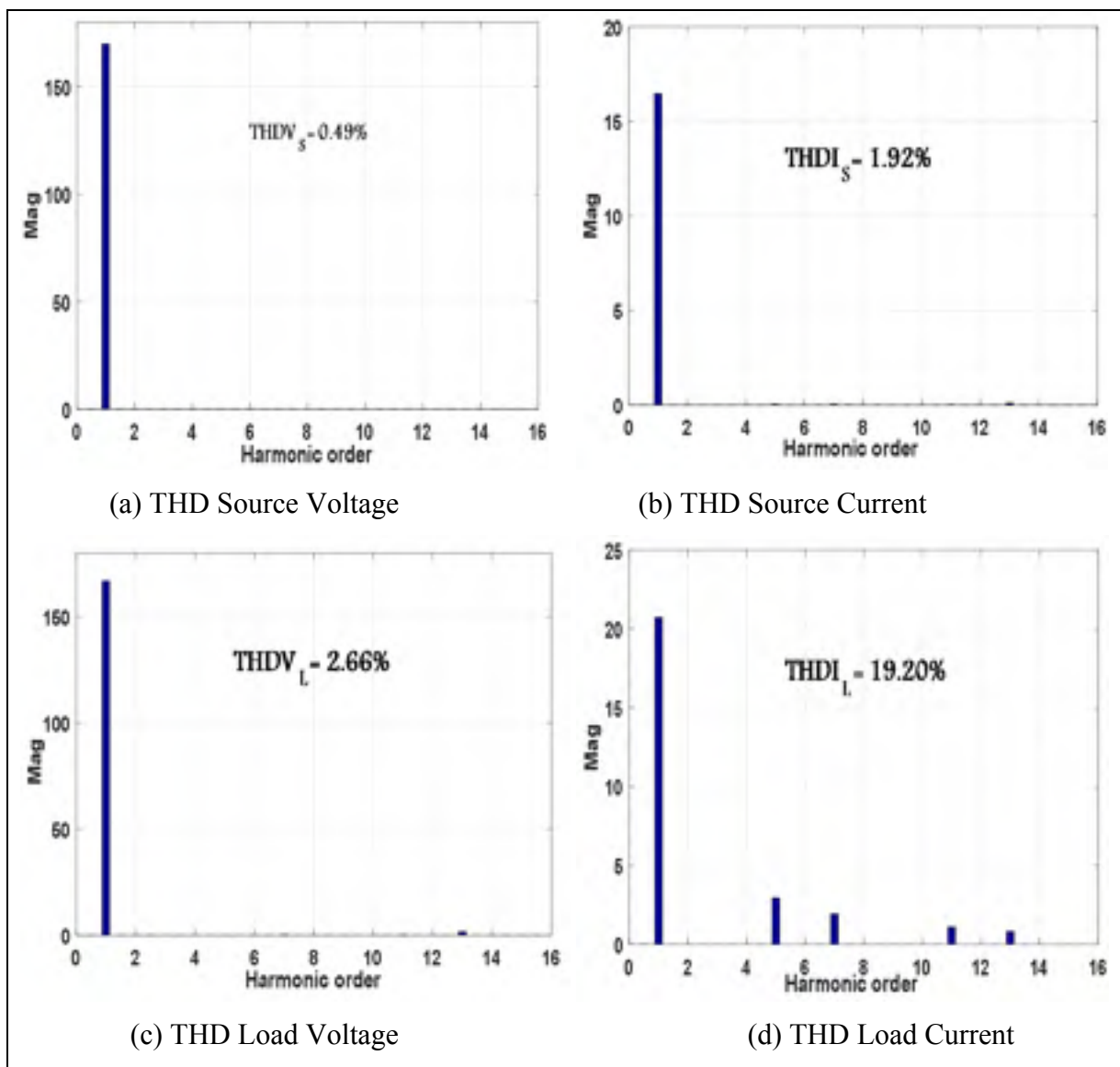


Figure 4.10 THD during current harmonics compensation

Table 4.2 Power parameters and THD's during steady state

Parameters	V_S (V rms)	I_S (A rms)	V_L (V rms)	I_L (Arms)
THD (%)	0.49%	1.92%	2.66%	19.20%
Rms	169.8	16.47	166.9	20.71
Source power	$P_S = 4.28 \text{ kW}$			
	$Q_S = 15.8 \text{ Var}$			
	$S_S = 4.28 \text{ kVA}$			
Total load power	$P_T = 4.22 \text{ kW}$			
	$Q_T = 3.29 \text{ kVar}$			
	$S_T = 5.38 \text{ kVA}$			
Non-Linear Load power	$P_{NLL} = 3.9 \text{ kW}$			
	$Q_{NLL} = 452.8 \text{ Var}$			
	$S_{NLL} = 3.93 \text{ kVA}$			
Linear Load power	$P_{LL} = 373 \text{ W}$			
	$Q_{LL} = 2.8 \text{ kVar}$			
	$S_{LL} = 2.81 \text{ kVA}$			
Apparent power of active filter	4.28 kVA			
Passive Filter	$P_F = 27.26 \text{ W}$			
	$Q_F = 3.22 \text{ kVar}$			

4.3.3.2 Grid ON/OFF

As nonlinear loads tend to be time-varying, it is important to look at the HSAF performance during grid ON/OFF times. Figure 4.11 depicts system response in a step for grid ON/OFF. At $t=0.1\text{s}$ the grid is turned off and then turned on again at $t=0.2\text{s}$. During this time the load still received power because the battery charge supplies the injection voltage by the DC bus voltage. Throughout the alterations in the source conditions, unity power factor is maintained by the system, indicating HSAF's good performance during rapid variations of load current.

One can see in Figure 4.11 that when the grid turns off the load side still receive power. On the other hand, when the grid turns on the system takes 0.07s to come back to steady state.

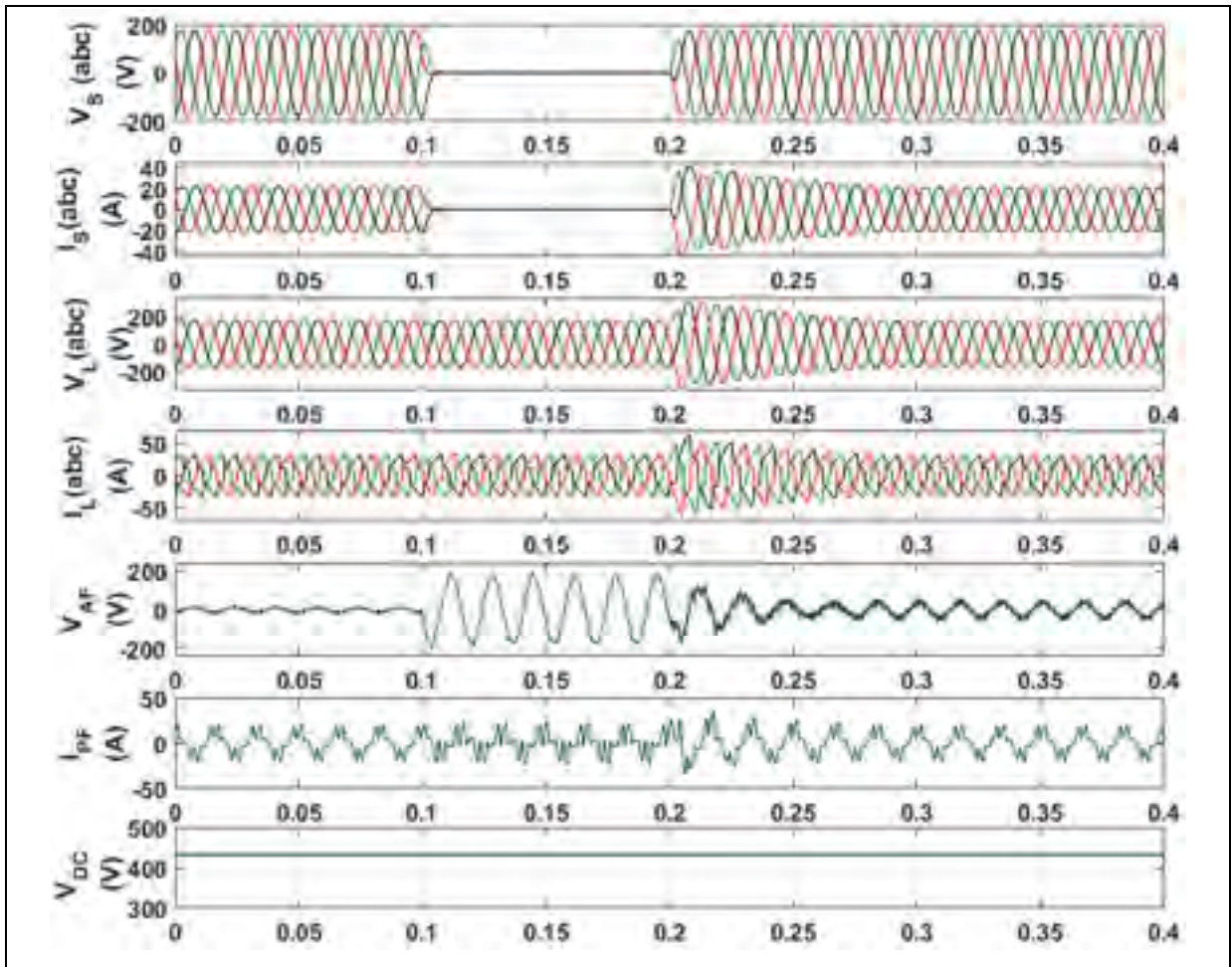


Figure 4.11 Shows the simulation results during grid ON/OFF

4.4 Conclusion

This chapter demonstrated the efficacy of using PV solar with series hybrid power filter for harmonics reductions while improving the efficiency of the electrical system and not resorting to active power consumption. A hybrid series power filter could thus prove to be a viable alternative to UPQCs for compensating current-related problems. To that end, the control algorithm used in the series active filter is crucial.

In the first section of the chapter, we presented and analyzed renewable energy through series hybrid power filter to charge the batteries which are able to regulate the DC voltage. This approach worked by adjusting the power factor and compensating current harmonics created by non-linear loads.

The proposed HSPF is useful for dealing with problems related to power quality in both commercial and residential structures. A control algorithm was used to remove current and voltage and harmonics, along with swells, sags and unbalance. The results of the simulations performed on a typical non-linear load point to the robust capability of the compensator and controller to deal with reactive power and harmonic currents, as a constant, reliable and sustainable power supply was resumed at the PCC of the load. The simulations also showed the compensator's ability to respond effectively to alterations pertaining to load power and source voltage, and to eliminate source harmonic currents and unbalances. The simulations also showed the behavior of the compensator during grid on/off.

CONCLUSION

The aim of this thesis was to find and analyze an appropriate strategy in order to improve the quality of distribution and low-level power in systems using hybrid series active power filters (HSeAFs). The thesis investigated the topology, control, of series compensators for industrial applications and used a smart power electronic compensator to enhance the static and dynamic behavior of electrical network hampered by a high percentage of fluctuating renewable energy sources. Throughout the chapters, new methods were presented, discussed, analyzed via offline simulations.

The stated scope of the thesis covered, 3-phase SHAF for power quality compensation and the integration the renewable energy for uninterruptible power supply. The most important contributions of this work are highlighted and summarized below.

The compilation of a thorough literature review of published research studies pertaining to power quality compensation using series active filters; In the review, the literature topics were briefly introduced, while several different kinds of non-linear loads based on the power quality compensation objective were discussed and analyzed. As well, a brief overview of conventional harmonic compensation techniques (e.g., passive compensators) was provided, along with details on active power filtering principles. Power quality information, such as key concepts and theoretical backgrounds, was also provided.

Extended reviews on the feasibility of the series hybrid active power compensator to mitigate issues and enhance power quality problems. The presented a detailed overview of the passive filter design for minimum rating of the series active filter and minimum cost to minimize the passive filter compensator history. Additionally, this part proposed and analyzed a design of passive filter with sliding mode control approach which is intended to improve series harmonic compensation. The enhancement strategy was tested on a three-phase system. The results of these studies provide a hand tool for choosing SeAF component values and ratings.

The presented a series hybrid filter without Diode Bridge detailed including nonlinear control strategies for power quality compensation. Moreover, the operation principle of series compensation was explained theoretically and the results of the MATLAB/SPS simulation were given. Simulation results were also presented in the chapter to underscore the impacts of the passive components used in the series active power filter.

The demonstrated the efficacy by covering the application of the PV solar through three phase series hybrid power filter method, and presentated the simulation results, which validated the proposed grid on/off operation scheme. The configuration proposed of the HSPF integrates a PV solar and the battery in the DC side of the active filter to be acted during grid OFF operation in order to maintain uninterruptible power supply to the load.

In total, this thesis introduced a novel topology and control strategies for hybrid series active power filters that not only improve power quality but also reduce overall costs. The thesis also points to the importance of properly adapting controllers and using available resources to resolve issues and achieve greater benefits. The present research work and validated results provide a clear progress in power quality enhancement using series active power compensators and contribute to the development of smart technologies.

RECOMMENDATIONS

The research study in this thesis introduced, discussed, analyzed and tested the design and implementation of a hybrid series power filter, with the end goal of improving the quality of power at the distribution level. This section suggests some ways to extend the research and points to possible directions for future related work.

Recommendations to Extend Present Research

- The work in this thesis uses 3-phase system configurations. The concepts developed here (SeAF, HSeAF) can be used in this system, but if the aim is to enhance power quality, adjustments are required due to the way in which compensating voltage is created through active filters. In 3-phase system, the control method is for all configurations that can compensate source current harmonics and reactive power, and regulate load voltage, while neutral wire for the 3-phase system has an impact on the controller algorithm.
- The present work focuses on a HSPF configuration, so the main components of the series active filter that help to produce a series compensating voltage are the output RLC filters. In designing a passive filter, the switching frequency and DC voltage are crucial parameters. A potential solution for reducing the damping resistor is the active damping technique, but this would require further investigation regarding its efficacy in series compensation.
- As mentioned throughout this work, power factor correction and DC voltage regulation are important limitations that must be taken into account in series active power filters. In this thesis, passive filter design and DC regulation are discussed in detail (Chapter 2) as a means to transfer power and make the series compensator function better. An extension of this work would be to carry out a systematic comparative study in order to evaluate these approaches with regards to, for instance, the need for a DC voltage to make the VSI function like a controlled voltage source. Connecting an auxiliary source would help with the power transfer while at the same time ensuring constant DC bus voltage. This could lead to highlighting the connection of renewable sources and how they can regulate the DC voltage, which might be of interest toward the integration of renewable energy sources. The findings could also serve

as a guide for making non-predictive energy sources into energy storage components that act as a UPS during grid problems such as sags and swells.

Future Works

Among the most promising of emerging renewable power sources are photovoltaics (PVs) and wind energy. Solar PV is considered one of the cleanest of the sustainable energy options, but it is also highly unpredictable. This thesis work showed that renewable energy sources could be used as an auxiliary DC source in a THSeAF, with a series compensator interfacing these energies to the grid while enhancing the system's power quality. The compensator could then regulate the distributed generation (DG) power to either partially or fully supply the loads connected to the PCC as well as manage power transfers between grid and load.

Series active power filters can store active power in a battery pack connected to the DC bus and supply it to users during different types of grid interruptions. The battery usually stores renewable energy as back-up. Given their current level of use (and, arguably, underuse) renewable energy sources should not only be supplying electric power but also being utilized towards power quality enhancement (voltage and current) in order to increase the reliability of smart grids. The THSeAF presented in this work offers one such option.

As it is imperative to study the behavior of the compensator during transient and faulty conditions, future work should involve the testing of different types of scenarios that can happen either at the grid or load side. These can be analyzed for single- and 3-phase systems. The real and potential impact of the compensator in each scenario as well as its effect impact on system operation also needs further investigation.

LIST OF BIBLIOGRAPHICAL REFERENCES

- A. Hamadi, S. Rahmani, and K. AI-Haddad, "A Novel Hybrid Series Active Filter for Power Quality Compensation," IEEE Power Electronics Specialists Conference, PESC 2007, p.1099-1104, June 2007.
- Ab. Hamadi, K. AI-Haddad and R. Rahmani, "Series active filter to mitigate power quality for medium size industrial loads (multi Pulses Transformer and modem AC drive)", IEEE international Symposium on ind. Electronics, vol.2, pp.1510 - 1515, July 2006.
- Ab. Hamadi, S. Rahmani and K. AI-Haddad. 2009. «A New Hybrid Series Active Filter Configuration to Compensate Voltage Sag, Swell, Voltage and Current Harmonics and Reactive Power». Industrial Electronics, IEEE Power Electronics Specialists Conference, PESC 2007, p.286-291, July 2009.
- Ajaei, F. B., S. Afsharnia, A. Kahrobaeian et S. Farhangi. 2011. « A Fast and Effective Control Scheme for the Dynamic Voltage Restorer ». Power Delivery, IEEE Transactions on, vol. 26, no 4, p. 2398-2406.
- Akagi, H. 2005. « Active Harmonic Filters ». Proceedings of the IEEE, vol. 93, no 12, p. 2128-2141.
- Akagi, H., et K. Isozaki. 2012a. « A Hybrid Active Filter for a Three-Phase 12-Pulse Diode Rectifier Used as the Front End of a Medium-Voltage Motor Drive ». IEEE Transaction on Power Delivery, vol. 27, no 1, p. 69-77.
- Akagi, H., et R. Kondo. 2010. « A Transformerless Hybrid Active Filter Using a Three-Level Pulsewidth Modulation (PWM) Converter for a Medium-Voltage Motor Drive ». Power Electronics, IEEE Transactions on, vol. 25, no 6, p. 1365-1374.
- Akagi, H., Y. Tsukamoto et A. Nabae. 1990. « Analysis and design of an active power filter using quad-series voltage source PWM converters ». IEEE Transactions on Industry Applications, vol. 26, no 1, p. 93-98.
- Alireza Javadi. 2016. « Design and implementation of Hybrid Series Compensators for Smart Grid Applications» École de Technologie Supérieure, Université du Québec. PHD Thesis, P. 328.
- Analytical Expressions for DG Allocation in Primary Distribution Networks Duong Quoc Hung, Nadarajah Mithulananthan, Member, IEEE, and R. C. Bansal, Senior Member, IEEE, IEEE transactions on energy conversion, vol. 25, no. 3, september 2010.

- Auguste Ndtougou, Abdelnamid Hamadi, Salem Rahmani and Kamal Al-Haddad. 2014 «Standalone Solar Photovoltaic Energy System Analysis and Design». International Journal of Engineering Education Vol. 30, No. 5, pp. 1324–1336.
- Babaei, E., et M. F. Kangarlu. 2011. « Voltage quality improvement by a dynamic voltage restorer based on a direct three-phase converter with fictitious DC link ». Generation, Transmission & Distribution, IET, vol. 5, no 8, p. 814-823.
- Barbosa, P. G., J. A. Santisteban et E. H. Watanabe. 1998. « Shunt-series active power filter for rectifiers AC and DC sides ». Electric Power Applications, IEE Proceedings -, vol. 145, no 6, p. 577-584.
- Basu, M., S. P. Das et G. K. Dubey. 2008. « Investigation on the performance of UPQC-Q for voltage sag mitigation and power quality improvement at a critical load point ». Generation, Transmission & Distribution, IET, vol. 2, no 3, p. 414-423.
- Brenna, M., R. Faranda et E. Tironi. 2009. « A New Proposal for Power Quality and Custom Power Improvement: OPEN UPQC ». Power Delivery, IEEE Transactions on, vol. 24, no 4, p. 2107-2116.
- Choi, S. S., B. H. Li et D. M. Vilathgamuwa. 2000. « Dynamic voltage restoration with minimum energy injection ». Power Systems, IEEE Transactions on, vol. 15, no 1, p. 51-57.
- Choi, S. S., B. H. Li et D. M. Vilathgamuwa. 2000. « Dynamic voltage restoration with minimum energy injection ». Power Systems, IEEE Transactions on, vol. 15, no 1, p. 51-57.
- Dan Simon “Biogeography – Based Optimization” IEEE Trans. Comp.Vol.12.No.6, December 2008.
- Debasish Mahapatra and Rakesh Kumar Sahu, Under, Pravat Kumar ray "Comparative Study Between Active and Hybrid Power Filters for Power Quality Enhancement–", Department of Electrical Engineering, National Institute of technology, Rourkela, Odisha, India-769008, p.54, May-2013.
- Dixon, J. W., G. Venegas et L. A. Moran. 1997. « A series active power filter based on a sinusoidal current-controlled voltage-source inverter ». Industrial Electronics, IEEE Transactions on, vol. 44, no 5, p. 612-620.
- Emanuel, Alexander Eigeles. 2004. « Summary of IEEE standard 1459: Definitions for the measurement of electric power quantities under sinusoidal, nonsinusoidal, balanced, or unbalanced conditions ». IEEE Transactions on Industry Applications, vol. 40, no 3, p. 869-876.

- F. Z. Peng, H. Akagi, and A. Nabae, "A new approach to harmonic compensation in power systems—A combined system of shunt passive and series active filters," *IEEE Trans. Ind. Applicat.*, Vol. 26, No. 6, pp. 983–990, 1990.
- F.Z. Peng and J.S. Lai, "Generalised instantaneous reactive power theory for three-phase power systems", *IEE Trans on Instrumentation and Measurement*, Vol. 45, No. 1, pp. 293-297, 1996.
- Fujita, H., et H. Akagi. 1998. « The unified power quality conditioner: the integration of series and shunt-active filters ». *IEEE Transactions on Power Electronics*, vol. 13, no 2, p. 315-322.
- Ganguly, S. 2014. « Impact of Unified Power-Quality Conditioner Allocation on Line Loading, Losses, and Voltage Stability of Radial Distribution Systems ». *Power Delivery, IEEE Transactions on*, vol. 29, no 4, p. 1859-1867.
- Gyugyi, Laszlo. 1979. « Reactive Power Generation and Control by Thyristor Circuits ». *IEEE Transactions on Industry Applications*, vol. IA-15, no 5, p. 521-532.
- Hamadi, A., S. Rahmani et K. Al-Haddad. 2010. « A Hybrid Passive Filter Configuration for VAR Control and Harmonic Compensation ». *Industrial Electronics, IEEE Transactions on*, vol. 57, no 7, p. 2419-2434.
- Han, B., B. Bae, S. Baek et G. Jang. 2006. « New configuration of UPQC for mediumvoltage application ». *Power Delivery, IEEE Transactions on*, vol. 21, no 3, p. 1438- 1444.
- Huayun, Yang, et Ren Shiyan. 2008. « A Practical Series-Shunt Hybrid Active Power Filter Based on Fundamental Magnetic Potential Self-Balance ». *Power Delivery, IEEE Transactions on*, vol. 23, no 4, p. 2089-2096.
- IEEE Guide for Application and Specification of Harmonic Filters. 2003. « ». *IEEE Std 1531-2003*, p. 0_1-60.
- IEEE Guide for Application of Power Electronics for Power Quality Improvement on Distribution Systems Rated 1 kV Through 38 kV. 2012. « ». *IEEE Std 1409-2012*, p. 1-90.
- Javadi, A., et K. Al-Haddad. 3-5 Oct. 2011. « Unfunctionality of the instantaneous p-q theory for the control of series active filters ». In *2011 IEEE Electrical Power and Energy Conference (EPEC)*. p. 386-391.
- Javadi, A., H. Fortin Blanchette et K. Al-Haddad. 2012a. « An advanced control algorithm for Series hybrid active filter adopting UPQC behavior ». In *IECON 2012 - 38th Annual Conference on IEEE Ind. Electron. Society. (Montreal, Canada, 25-28 Oct. 2012)*, p. 5318-5323. IEEE.

- Khadkikar, V. 2012. « Enhancing Electric Power Quality Using UPQC: A Comprehensive Overview ». *Power Electronics, IEEE Transactions on*, vol. 27, no 5, p. 2284-2297.
- Khadkikar, V., et A. Chandra. 2008. « A New Control Philosophy for a Unified Power Quality Conditioner (UPQC) to Coordinate Load-Reactive Power Demand Between Shunt and Series Inverters ». *Power Delivery, IEEE Transactions on*, vol. 23, no 4, p. 2522-2534.
- Khadkikar, V., et A. Chandra. 2009. « A Novel Structure for Three-Phase Four-Wire Distribution System Utilizing Unified Power Quality Conditioner (UPQC) ». *Industry Applications, IEEE Transactions on*, vol. 45, no 5, p. 1897-1902.
- Khadkikar, V., et A. Chandra. 2011. « UPQC-S: A Novel Concept of Simultaneous Voltage Sag/Swell and Load Reactive Power Compensations Utilizing Series Inverter of UPQC ». *Power Electronics, IEEE Transactions on*, vol. 26, no 9, p. 2414-2425.
- Khadkikar, Vinod. 2008. « Power Quality Enhancement at Distribution Level Utilizing the Unified Power Quality Conditioner (UPQC) ». *École de Technologie Supérieure, Université du Québec. PHD Thesis*, P. 325.
- M Vijayakumar and S Vijayan, "Photovoltaic based three-phase four-wire series hybrid active power filter for power quality improvement", Department of Electrical and Electronics Engineering, K. S. R. College of Engineering, Tiruchengode 637 215, India, pp 358-370, August 2014.
- Miloud Rezkallah. 2016. «Design and control of standalone and hybrid standalone power generation systems». *École de Technologie Supérieure, Université du Québec. PHD Thesis*, P. 324.
- Mohammadi, H. R., A. Y. Varjani et H. Mokhtari. 2009. « Multiconverter Unified Power-Quality Conditioning System: MC-UPQC ». *IEEE Transactions on*, vol. 24, no 3, p. 1679-1686.
- Mohammadi, H. R., A. Y. Varjani et H. Mokhtari. 2009. « Multiconverter Unified Power-Quality Conditioning System: MC-UPQC ». *IEEE Transactions on*, vol. 24, no 3, p. 1679-1686.
- Nassar Mendalek, Kamal Al-Haddad, Farhat Fnaiech and Louis A. Dessaint 2002. «Sliding Mode Control of 3-Phase Shunt Active Filter in the d-q ». *École de Technologie Supérieure, Université du Québec. IEEE 33rd Annual IEEE Power Electronics Specialists Conference. Proceedings*. P. 369-375. IEEE.
- Nguyen Xuan, Tung, G. Fujita et K. Horikoshi. 2010. « An adapted control strategy for dynamic voltage restorer to work as series active power filter ». In *Power Electronics Conference (IPEC), 2010 International. (21-24 June 2010)*, p. 2283-2287.

- Nielsen, J. G., et F. Blaabjerg. 2005. « A detailed comparison of system topologies for dynamic voltage restorers ». *Industry Applications, IEEE Transactions on*, vol. 41, no 5, p. 1272-1280.
- Peng, F. Z., H. Akagi et A. Nabae. 1990. « A new approach to harmonic compensation in power systems-a combined system of shunt passive and series active filters ». *Industry Applications, IEEE Transactions on*, vol. 26, no 6, p. 983-990.
- Quoc-Nam, Trinh, et Lee Hong-Hee. 2014. « Improvement of unified power quality conditioner performance with enhanced resonant control strategy ». *Generation, Transmission & Distribution, IET*, vol. 8, no 12, p. 2114-2123.
- S. Rahmani, K. Al-Haddad and F. Fnaiech, “A Series Hybrid Power Filter To Compensate Harmonic Currents and Voltages”, *IEEE Industrial Electronics Conference IECON 2002*, Seville, Spain November 5 to 8 2002, pp. 644-649.
- Salmero, P., et S. P. Litra. 2010. « A Control Strategy for Hybrid Power Filter to Compensate Four-Wires Three-Phase Systems ». *IEEE Trans. Power Electron.*, vol. 25, no 7, p. 1923-1931.
- Singh, B., K. Al-Haddad et A. Chandra. 1998. « A new control approach to three-phase active filter for harmonics and reactive power compensation ». *Power Systems, IEEE Transactions on*, vol. 13, no 1, p. 133-138.
- Singh, B., K. Al-Haddad et A. Chandra. 1999. « A review of active filters for power quality improvement ». *IEEE Transactions on Industrial Electronics*, vol. 46, no 5, p. 960- 971.
- Sng, Eng Kian Kenneth, S. S. Choi et D. M. Vilathgamuwa. 2004. « Analysis of series compensation and DC-link voltage controls of a transformerless self-charging dynamic voltage restorer ». *IEEE Trans. Power Delivery*, vol. 19, no 3, p. 1511-1518.
- Villalva, M. G., J. R. Gazoli et E. R. Filho. 2009. « Comprehensive Approach to Modeling and Simulation of Photovoltaic Arrays ». *Power Electronics, IEEE Transactions on*, vol. 24, no 5, p. 1198-1208.
- Wang, Zhaoan, Qun Wang, Weizheng Yao et Jinjun Liu. 2001. « A series active power filter adopting hybrid control approach ». *IEEE Transactions on Power Electronics*, vol. 16, no 3, p. 301-310.
- Yun Wei, Li, F. Blaabjerg, D. M. Vilathgamuwa et Loh Poh Chiang. 2007a. « Design and Comparison of High Performance Stationary-Frame Controllers for DVR Implementation ». *Power Electronics, IEEE Transactions on*, vol. 22, no 2, p. 602-612.

Yun Wei, Li, Loh Poh Chiang, F. Blaabjerg et D. M. Vilathgamuwa. 2007c. « Investigation and Improvement of Transient Response of DVR at Medium Voltage Level ». *Industry Applications, IEEE Transactions on*, vol. 43, no 5, p. 1309-1319.